UNITED STATES DEPARTMENT OF COMMERCE
DANIEL C. ROPER, Secretary
NATIONAL BUREAU OF STANDARDS
Lyman J. Briggs, Director

✦

Journal of Research

of the

National Bureau of Standards

✦

Volume 19, Number 2
August 1937

UNITED STATES
GOVERNMENT PRINTING OFFICE
WASHINGTON : 1937

For sale by the Superintendent of Documents, Washington, D. C. - - - - Price 25 cents
$2.50 per year on subscription

The prices of the separate Research Papers appearing in this JOURNAL are given on the front cover page. If 100 or more copies of any separate are ordered, a discount of 25 percent is allowed. Those who desire copies of separate Research Papers should send their orders and remittances without delay to the Superintendent of Documents, U. S. Government Printing Office, Washington, D. C. This will aid him to determine the number of copies to be printed for sale. Research Papers are not printed from electrotypes, and usually no more reprints can be had when the first and only printing is exhausted.

U. S. DEPARTMENT OF COMMERCE NATIONAL BUREAU OF STANDARDS

RESEARCH PAPER RP1016

Part of Journal of Research of the National Bureau of Standards, Volume 19, August 1937

SUDDEN DISTURBANCES OF THE IONOSPHERE

By John Howard Dellinger

ABSTRACT

The phenomenon described in this paper is the occurrence of a very sudden change in ionization of a portion of the ionosphere. It manifests itself by the complete fading out of high-frequency radio transmission for a period of a few minutes to an hour or more and by perturbations of terrestrial magnetism and earth currents. The effect was discovered in 1935, and it was found to occur simultaneously everywhere throughout the illuminated half of the globe but not in the night half. The results of a world-wide investigation of the phenomenon, which followed this discovery, are presented in this paper.

The radio and magnetic effects have been shown to be of a distinct type, quite different from previously known vagaries in these fields. They are of maximum intensity in that region of the earth where the sun's radiation is perpendicular.

Many of the occurrences are simultaneous with great eruptions on the sun. Such eruptions emit vast quantities of ultraviolet light. These radiations are sometimes of such frequencies as to cause intense ionization of part of the ionosphere below the *E* layer. This sudden ionization causes the radio and other perturbations. Their characteristics are explained. Study of this effect is leading to new understanding of the nature of the ionosphere, the processes of radio-wave transmission, the mechanisms of terrestrial magnetism, and the phenomena occurring in the sun.

CONTENTS

	Page
I. Introduction	112
II. Data	113
III. Characteristics of the radio-transmission effects	125
1. Geographic simultaneity	125
2. Suddenness	126
3. Degree of intensity change	126
4. Frequencies affected	127
5. Geographic distribution	128
IV. Characteristics of the terrestrial magnetic and earth-current effects	129
1. Limitation to illuminated hemisphere	129
2. Simultaneity with radio fadeouts	129
3. Geographic distribution	130
4. Comparison with magnetic storms	130
V. Solar phenomena associated with sudden ionosphere disturbances	131
1. Exactness of simultaneity	131
2. Proportionate number of simultaneous occurrences	131
3. Character of eruptions	132
4. Location of eruptions on sun	132
5. Recurrence tendency	133
6. Relation to sunspots	134
VI. Discussion and explanation	135
1. Seat of the disturbances deduced from radio effects	135
2. Magnetic effects	137
3. Solar source	138
VII. Bibliography	140

I. INTRODUCTION

This paper presents the conclusions and data up to the end of 1936 of an investigation, started about the middle of 1935, of a hitherto unknown phenomenon. The phenomenon is the occurrence of a sudden intense increase in the ionization of a part of the earth's upper atmosphere, with resultant transient disturbances in such phenomena as radio-wave transmission, terrestrial magnetism, and earth currents. The radio effect is of serious practical import, as it manifests itself principally as a sudden disappearance of radio signals received on high frequencies, the period of silence ranging from a few minutes to an hour or more. The whole phenomenon is of scientific interest particularly because it appears to have its origin in sudden bursts of radiation from the sun, and it is opening the way to increased understanding of the sun, the ionosphere, radio transmission, terrestrial magnetism, and related phenomena.

In October 1935 the author reported [1] the occurrence of radio fadeouts on March 20, May 12, July 6, and August 30 of that year. He pointed out that they occurred throughout the illuminated half of the globe but not the dark half, advanced the hypothesis that they depend on some solar emanation lasting only a few minutes, and suggested observations by workers in other sciences with a view to learning of the possible occurrence of effects in terrestrial magnetism, earth currents, solar radiation, etc., simultaneous with radio fadeouts. The suggestion met with widespread interest, and the author has had the collaboration of numerous individuals and organizations in this investigation.

Evidence followed rapidly that the postulated simultaneous effects do occur. The astronomers at Mt. Wilson Observatory of the Carnegie Institution of Washington were asked to examine their spectrohelioscopic data for the dates in question, and in November 1935, R. S. Richardson of that Observatory informed the author that on July 6 and August 30 bright eruptions had been observed on the sun within a few minutes of the times of the radio fadeouts, and on the other two dates no observations had been made at the times of the fadeouts. These results were announced by Dr. Richardson and the author at the end of 1935.

The magnetograms of the Cheltenham, Md., Observatory of the U. S. Coast and Geodetic Survey were examined by the author for the times of all the fadeouts then known, and for several of them small abrupt pulses were found, beginning at a time within 2 minutes of the radio-fadeout time. Also, H. H. Beverage, of RCA Communications, Inc., reported to the author the occurrence of a large, sharp pulse on an earth-current recorder within a few minutes of the time of several of the radio fadeouts.

From these beginnings has grown an extensive research upon these interrelated phenomena. Through the kindness of many cordial cooperators the author is able to present a summary of data on the known occurrences. Acknowledgments of the work of these cooperators are given on p. 140. Systematic recording of the phenomena has been carried on by the National Bureau of Standards, and complete reports have been furnished by a few other groups, but many of the reports from scattered places are sporadic and partial. Data are relatively meager for the

[1] See first two citations in section VII, Bibliography.

Asiatic and Pacific regions. It is believed that the results are of sufficient value to provide encouragement for more widespread and systematic observations and for more intensive exploration of the several fields of inquiry opened up by this work.

Preliminary reports of the results, and explanation in terms of ionosphere effects, were given by the author in papers presented at the Washington meeting of the American Section, International Scientific Radio Union, May 1, 1936, and at the Cleveland Convention of the Institute of Radio Engineers, May 11, 1936. A number of brief papers have been published by the author and others, giving some of the results and preliminary conclusions (see section VII, Bibliography).

This paper presents a compressed summary of the known facts regarding 118 sudden disturbances of the ionosphere, many of which were accompanied by solar eruptions, many of which were manifested by perturbations of terrestrial magnetism and earth currents, and each of which was manifested by the wiping out of hundreds or thousands of radio transmissions.

II. DATA

In this section a summary of the available data is presented. In sections III, IV, and V the facts regarding particular aspects of the data are presented and discussed. In section VI is given a discussion and explanation of the entire phenomenon.

The data considered in this paper are given in very condensed form in table 1 and are essentially for the years 1935 and 1936. One earlier occurrence is included, that of Nov. 28, 1934, as it was clearly the same phenomenon. There is little reliable information on earlier occurrences of this type. Some records indicate occurrences which may or may not be the same phenomenon. Thus, the logs of radio operating companies show radio traffic interruptions on many occasions in 1934 and earlier, but there is very little information at hand to judge whether they were of the type due to the sudden ionosphere disturbances here studied or to others of the various radio wave vagaries mentioned at the beginning of section III, page 125. Information on a number of such traffic interruptions occurring in 1928 is given in an article by T. L. Eckersley.[2] From the data given in that paper, the failure of radio transmission on October 10, 1928, from 1100 to 1200 GMT, may have been a case of the phenomenon here studied. Likewise, from data reported to the author of the present paper, the failure of radio transmission from 1305 to 1400 GMT on May 11, 1934, may also have been a case.

Similarly, there is some information on a few early occurrences of sudden terrestrial magnetic pulses simultaneous with visible solar eruptions, occasionally reported by astronomers many years ago. Some instances are given in an article by G. E. Hale,[3] and interesting ones were observed on August 3 and 5, 1872, by C. A. Young, as described in his book.[4] These occurrences may have been of the type associated with the sudden ionosphere disturbances here studied.

[2] *An investigation of short waves*, J. Inst. Elec. Engrs. (London) **67**, 992 (1929).
[3] *The spectrohelioscope and its work, pt. 3, Solar eruptions and their apparent terrestrial effects.* Astrophys. J. **73**, 379 (1931).
[4] The Sun (1884).

TABLE 1.—*Data on radio fadeouts and other manifestations of sudden ionosphere disturbances*

Date	Time, GMT	Reported observed in	Reported locations of transmitting stations	Reported solar and magnetic effects, etc.
1934				
Nov. 28	1710 to 1740	Georgia	Eastern United States of America.	Solar eruption, beginning about 1710. Ter mag pulse, 1707 to 1730. Earth-current pulse, 1710 to 1740.
	1710 to 1745	New York	South America	
	1710 to 1730	District of Columbia	District of Columbia [1]	
1935				
Jan. 25	0335 to 0535	California	Asia, Philippines, Java	
Mar. 20	0150 to 0200	Philippines	California	
	0148 to 0200	California	Asia, Philippines, Java	
May 12	1157 to 1215	France	Numerous	Ter mag pulse, 1157.
	1156 to 1214	New Jersey	England	
	1200 to 1215	New York	Europe, South America	
July 6	1409 to 1437	do	England, United States of America, South America.	Solar eruption, 1358 to 1418. Ter mag pulse, 1407 to 1412. Earth current pulse, 1400 to 1411.
	1408 to 1430	France	North and South America, Asia.	
Aug. 30	2320 to 2325 to 2335	California	Asia, Philippines, Java, Western United States of America.	Solar eruption 2312 to after 2330.
	2300 to 2329	Philippines	California	
Sept. 13	1630 to 1640 to 1650	California	United States of America, Manila, Shanghai, Tokyo.	Solar eruption, 1635 to 1641. Ter mag pulse, 1630.
Sept. 27	1250 to 1350	New York	Europe, South America	Solar eruption, from before 1200 to after 1230. Ter mag pulse, 1230.
	1245 to 1315	England	Numerous	
Sept. 29	2055 to 2120 to 0150	California	Tokyo, Shanghai, Hawaii, New York.	
	2050 to 2110	District of Columbia	Massachusetts	
Oct. 24	1100 to 1200	New York	Numerous	Earth-current pulse, 1130 to 1215.
Nov. 18	1755 to 1815	Puerto Rico	United States of America.	
	1757 to 1800	District of Columbia	Ohio	
Nov. 29	1405 to 1415	New York	South America	Solar eruption, from before 1431 to 1445.
	1405 to 1415	Brazil	All stations	
Nov. 30	1721 to 1730 to 1815	District of Columbia	Ohio, Massachusetts	Solar eruption, 1751 to 1830.
Nov. 30	1850 to 1908 to 1930	do	do	
	1900 to 1925 to 1935	Hawaii	California	
Dec. 16	2209 to 2230	District of Columbia	Massachusetts	Solar eruption, 2210 to 2238.
	2223 to 2225	Hawaii	California	
Dec. 17	1615 to 1630	New York	South America	Solar eruption, beginning before 1609. Ter mag pulse, 1610 to 1630.
	1630 to 1700	New Jersey	England	
	1610 to 1618 to 1630	District of Columbia	Massachusetts, Ohio	
	1620 to 1630 to 1655	Texas	Numerous amateur stations.	
Dec. 18	0450 to 0615	California	Asia, Philippines, Java	
Dec. 23	1730 to 1826 to 2000	District of Columbia	Ohio, Massachusetts, District of Columbia. [1]	Solar eruption, from before 1757 to after 1805.
	1730 to 2000	California	Asia, Philippines, Java	
	1730 to 1930	New York	Europe, South America	
	1740 to 1930	Georgia	Eastern United States of America.	
	1745	Puerto Rico	United States of America	

[1] Disappearance or weakening of sky-waves reflected vertically from ionosphere.

TABLE 1.—*Data on radio fadeouts and other manifestations of sudden ionosphere disturbances*—Continued

Date	Time, GMT	Reported observed in	Reported locations of transmitting stations	Reported solar and magnetic effects, etc.
1936				
Feb. 6	1520 to 1545 to 2040	District of Columbia	Ohio, District of Columbia.[1]	Ter mag pulse, 1520. Low-freq atm increase, 1520 to 1600.
	1520 to 1550 to 1645	Georgia	Eastern United States of America.	
	1515 to 1530 to 1700	New York	South America, Europe	
	1520 to 1620	England	Numerous	
Feb. 8	0130 to 0310	Philippines	China, Guam, Hawaii	
	0130 to 0230	Japan	California, Brazil, Syria	
	0205 to 0300	California	Asia, Philippines, Java	
	0200 to 0315	Malaya	Asia	
	0200 to 0325	Siam	do	
	0210 to 0330	French Indo-China	Asia, Philippines, Java	
Feb. 8	1315 to 1402	Puerto Rico	United States of America	Solar eruption, 1330 to after 1400. Ter mag pulse, about 1328. Low-freq atm increase, 1325.
	1325 to 1500	England	Numerous	
	1326 to 1350 to 1420	District of Columbia	Ohio, Massachusetts	
	1323 to 1358	New York	Europe, South America	
Feb. 14	1515 to 1550 to 1730	District of Columbia	Ohio, Massachusetts, California, Illinois, Texas. District of Columbia.[1]	
	1516 to 1540 to 1700	New York	Europe, North and South America.	
	1518 to 1542	New Jersey	England	
	1518 to 1600	Michigan	United States of America	
	1517 to 1545	Missouri	do	
	1515 to 1550	Texas	do	
	1520 to 1540	Pennsylvania	do	
	1516 to 1536 to 1546	Arkansas	do	
	1519 to 1545 to 1600	Holland	Dutch Indies, Europe, North and South America.	
	1518 to 1542	England	South Africa, Egypt, India, Europe, North and South America, Australia.	
Feb. 14	1513 to 1545	Spain	Europe, North and South America.	
	1516 to 1545	France	Africa, North and South America, Japan, China.	Solar eruption, 1530 to 1600. Ter mag pulse, 1515 to 1600. Low-freq atm increase, 1526.
	1519 to 1550	Germany	North and South America.	
	1520 to 1545	Africa	France	
	1515 to 1540	Syria	do	
	1515 to 1605	Argentina	Numerous	
	1520 to 1545	Quebec, Canada	United States of America and Canada.	
	1515 to 1635	Panama, Canal Zone	North and South America.	
	1515 to 1545 to 1730	Puerto Rico	United States of America	
	1518 to 1542	Florida	Puerto Rico	
	1518 to 1548	California	United States of America	
	1518 to 1540	Louisiana	do	
	1517 to 1550	Illinois	do	
	1515 to 1533	Idaho	do	
	1515 to 1545	Nebraska	do	
	1520 to 1546	Ohio	do	
	1515 to 1600	Georgia	do	
	1515 to 1545	Massachusetts	do	
	1515 to 1540	Oklahoma	do	
	1517 to 1536	Virginia	do	
Feb. 16	1550 to 1613 to 1627	District of Columbia	Ohio, Massachusetts, District of Columbia.[1]	Solar eruption, from before 1630 to after 1700. Low-freq atm increase, 1545 to 1700.
	1600 to 1630	Rhode Island	New England States	
	1545	France	Numerous	
Mar. 4	1956 to 2010	California	Asia, Philippines, Java, United States of America.	Ter mag pulse, 1955 to 2005. Slight earth-current pulse, 1956.
	1956 to 2007 to 2020	District of Columbia	Ohio, Massachusetts, District of Columbia.[1]	

[1] Disappearance or weakening of sky-waves reflected vertically from ionosphere.

TABLE 1.—*Data on radio fadeouts and other manifestations of sudden ionosphere disturbances*—Continued

Date	Time, GMT	Reported observed in	Reported locations of transmitting stations	Reported solar and magnetic effects, etc.
1936 Mar. 10	0540 to 0600	Japan	India, Syria, China, Siam, Java.	
Mar. 23	1545 to 1553 to 1603	District of Columbia	Ohio, Massachusetts, District of Columbia [1]	Solar eruption, 1530 to 1607. Ter mag pulse, 1545. Low-freq atm increase, 1545 to 1650.
Apr. 1	0930 to 0950	England	Numerous	Solar eruption, 0926 to 1040.
	0938	France	do	
April 1	1200 to 1220	England	do	
	1218 to 1223 to 1229	District of Columbia	Ohio, Massachusetts	
Apr. 2	0405 to 0417 to 0640	Malaya	Java, Malaya	
	0400 to 0420	Japan	California, Philippines, Asia.	
	0400 to 0415	California	Asia, Philippines, Java	
	0400 to 0420	Argentine	Japan	
Apr. 6	1356 to 1403 to 1418	District of Columbia	Ohio, Massachusetts, District of Columbia [1]	Ter mag pulse, 1355 to 1402. Low-freq atm increase, 1357 to 1448.
	1353 to 1418	New York	Numerous	
	1353 to 1359	New Jersey	England	
	1355 to 1405	Holland	South America, Portugal, Hungary.	
	1355 to 1405	England	North and South America, Africa, Japan.	
Apr. 7	0230 to 0430	Japan	Europe	Solar eruption, starting before 0231.
Apr. 8	0920 to 0945	Holland	Austria, Hungary	Solar eruption, 0810 to 1000. Ter mag pulse, 0912 to 0925.
April 8	1450 to 1520	District of Columbia	Ohio, Massachusetts, District of Columbia. [1]	Ter mag pulse, 1450.
	1450 to 1520	Texas	United States of America	
	1450 to 1520	Arizona	do	
April 8	1646 to 1726 to 1815	District of Columbia	Ohio, Massachusetts, District of Columbia. [1]	Solar eruption, 1645 to 1703. Ter mag pulse, 1645 to 1705. Earth-current pulse, 1645 to 1700. Low-freq atm increase, 1650 to 1745.
	1650 to 1700	France	United States of America, South America.	
	1645 to 1657 to 1720	New York	England, South America, United States of America.	
	1650 to 1658 to 1704	New Jersey	England	
	1645 to 1708	Holland	Japan, Europe, North and South America.	
	1650 to 1706 to 1725	Georgia	United States of America	
	1648 to 1705	California	Asia, Philippines, Java, United States of America.	
	1645 to 1657 to 1720	England	New York, South America, Africa.	
	1630 to 1655 to 1705	Quebec	England, Australia	
	1630 to 1655 to 1705	British Columbia	Quebec, Australia	
	1650 to 1710	Spain	South America	
	1645 to 1740	Peru	Peru [1]	
	1703 to 1738	Oklahoma	Numerous	
	1650 to 1712	Texas	do	
	1650 to 1703 to 1720	Florida	do	
	1645 to 1655 to 1715	Tennessee	do	
	1640 to 1720	Illinois	do	
	1648 to 1704 to 1720	Indiana	do	
	1658 to 1705 to 1730	Iowa	do	
	1658 to 1704 to 1725	Nebraska	do	
	1655 to 1718	Missouri	do	
Apr. 9	1320 to 1400	District of Columbia	Ohio, Massachusetts	Solar eruption, from before 1330 to 1430. Low-freq atm increase, 1310 to 1440.
	1320 to 1330 to 1430	New York	Europe	
	1325 to 1335 to 1345	Holland	Europe, North and South America.	
	1340 to 1348	England	Numerous	
Apr. 25	1427 to 1500	District of Columbia	Ohio, Massachusetts	Solar eruption, 1428 to 1445.

[1] Disappearance or weakening of sky-waves reflected vertically from ionosphere.

TABLE 1.—*Data on radio fadeouts and other manifestations of sudden ionosphere disturbances*—Continued

Date	Time, GMT	Reported observed in	Reported locations of transmitting stations	Reported solar and magnetic effects, etc.
1936 April 25	1653 to 1735	District of Columbia.	Ohio, Massachusetts, District of Columbia.[1]	Solar eruption, 1650 to 1724. Ter mag pulse, 1650 to 1700. Low-freq atm increase, 1658 to 1755.
Apr. 30	0940 to 1100	Japan	Europe	
	1000 to 1100	France	Japan	
	1000 to 1100	Germany	do	
	1000 to 1110	England	do	
May 8	2020 to 2029 to 2037	District of Columbia.	Ohio, Massachusetts	Ter mag pulse, 2020 to 2035. Earth-current pulse, 2020.
May 14	1755 to 1759	New York	Europe, United States of America.	
	1750 to 1800 to 1817	District of Columbia.	Ohio.	
May 15	0550 to 0730	Japan	Philippines, Asia, Europe.	Solar eruption, from before 0704 to 0830.
	0550 to 0620	Philippines	Japan	
	0600 to 0620	France	do	
May 25	1233 to 1240 to 1256	District of Columbia.	Ohio, Massachusetts, District of Columbia.[1]	Ter mag pulse, 1233 to 1250. Earth-current pulse, 1233 to 1234 to 1236. Low-freq atm increase, 1228 to 1330.
	1232 to 1243 to 1257	New York	Numerous	
	1238	Florida	United States of America	
	1235 to 1300	Holland	Canada, Japan, Java	
	1232 to 1245	France	United States of America, South America, Japan	
	1237 to 1245	England	Europe, South America, Japan.	
May 26	1130 to 1135	New York	Numerous	Solar eruption, 1115 to 1203. Low-freq atm increase, 1128 to 1158.
	1130 to 1134	District of Columbia.	Ohio	
	1132 to 1139	Holland	Hungary	
	1131	France	Numerous	
	1130 to 1145	England	do	
May 27	0335 to 0430	Holland	Japan, Java	
	0355 to 0410	California	Asia, Philippines, Java	
	0350 to 0415	Japan	California, Philippines, Asia, Europe.	
May 27	2345 to 2430	do	North and South America.	
	2345 to 2430	Argentina	Japan	
	2345 to 2430	California	do	
May 28	0345 to 0415	do	Asia, Philippines, Java	
	0340 to 0420	Holland	Japan, Java	
	0330 to 0420	Japan	China, Philippines, California.	
May 28	0730 to 0745	Philippines	Hawaii	Solar eruption, 0715 to 0800. Ter mag pulse, 0725 to 0738. Low-freq atm increase, 0726 to 0800.
	0728 to 0743	California	Asia, Philippines, Java	
	0730 to 0800	Holland	Japan, Austria, Java	
	0728 to 0730	France	Numerous	
	0720 to 0745	Japan	Europe, Philippines	
May 28	1403 to 1416 to 1430	District of Columbia.	Ohio, Massachusetts	Low-freq atm increase, 1400 to 1450.
	1400 to 1409 to 1445	New York	Europe, South America, California.	
	1402 to 1430	Holland	North and South America, Europe.	
	1405	France	Numerous	
May 28	1759 to 1840 to 2000	District of Columbia.	Ohio, Massachusetts, Texas, Nebraska, Oklahoma.	Ter mag pulse, 1800 to 1850. Earth-current pulse, 1758 to 1807. Low-freq atm increase 1758 to 1907.
	1800 to 1808 to 1817	New York	Europe, North and South America.	
	1800 to 1823	Oklahoma	Numerous	
	1800 to 1823	Texas	do	
	1800 to 1823	Nebraska	do	
	1758 to 1815	North Dakota	do	
	1800 to 1815	Illinois	do	
	1800 to 1815 to 1830	British Columbia	do	
	1759 to 1820 to 1830	Ohio	do	
	1800 to 1818 to 1828	Arkansas	do	
	1800 to 1818 to 1828	Kansas	do	
	1800 to 2000	South Carolina	do	

[1] Disappearance or weakening of sky-waves reflected vertically from ionosphere.

TABLE 1.—*Data on radio fadeouts and other manifestations of sudden ionosphere disturbances*—Continued

Date	Time, GMT	Reported observed in	Reported locations of transmitting stations	Reported solar and magnetic effects, etc.
1936				
May 28—Contd.	1758 to 1815	Missouri	Numerous	
	1800 to 1816	England	do	
	1800	France	do	
	1755 to 1825	Japan	California, Europe	
	1800 to 1813 to 1840	Holland	New York, Argentina	
May 29	1020 to 1030	do	Java, Sweden, Austria	Low-freq atm increase, 1015 to 1115.
	1020 to 1035	Japan	Europe	
	1025 to 1035	England	Numerous	
	1023	France	do	
	1020 to 1027	New York	do	
May 30	1730 to 1800	Florida	do	Ter mag pulse, 1728 to 1750.
June 3	0045 to 0130	Japan	California, Philippines, Europe, North and South America, Asia.	
	0045 to 0130	California	Japan	
	0045 to 0130	Buenos Aires	do	
	0045 to 0130	Philippines	do	
	0100 to 0110	S. S. General Pershing, long. 154°52' W.	Numerous	
June 3	1635 to 1655 to 1712	District of Columbia	Ohio, Massachusetts	Solar eruption, 1629 to 1700. Ter mag pulse, 1635 to 1700. Low-freq atm increase, 1635 to 1718.
	1636 to 1640 to 1720	New York	Europe, North and South America.	
	1637 to 1650	Illinois	Numerous	
	1630	Missouri	do	
	1630 to 1645 to 1700	Pennsylvania	do	
	1640 to 1700	Holland	United States of America, Japan, Java.	
	1633 to 1650	France	Numerous	
	1635 to 1650	England	do	
June 3	1830 to 1835	New York	Europe, South America	Ter mag pulse, 1825.
	1823 to 1841	District of Columbia	Ohio, District of Columbia.[1]	
June 4	0440 to 0500	Japan	California, South America, Asia.	
	0442 to 0455	California	Asia, Philippines, Java	
	0440 to 0505	Holland	Java	
June 4	1154 to 1200 to 1210	District of Columbia	Ohio, District of Columbia.[1]	Ter mag pulse, 1153 to 1206. Low-freq atm increase, 1152.
	1151 to 1206 to 1300	New York	Europe, North and South America.	
	1155 to 1210	France	Numerous	
	1153 to 1209	Holland	Japan, South America, Europe.	
	1155 to 1205	England	Numerous	
June 5	0235 to 0250	California	Asia, Philippines, Java	
	0236 to 0250	Japan	California, South America, Phillippines.	
June 9	0131 to 0150	do	Asia	
	0130 to 0155	California	Asia, Philippines, Java	
June 9	1424 to 1451 to 1512	District of Columbia	Ohio, Massachusetts	Solar eruption, 1424 to 1432. Low-freq atm increase, 1425 to 1500.
	1422 to 1441 to 1530	New York	Numerous	
	1425	France	do	
	1425 to 1440 to 1515	England	Europe, North and South America.	
	1426 to 1440 to 1500	Holland	United States of America, Java, Europe.	
June 9	1750 to 1845	do	North and South America.	Solar eruption, from before 1755 to after 1805. Ter mag pulse, 1750 to 1805.
June 9	1859 to 1923 to 2023	District of Columbia	Ohio, Massachusetts, District of Columbia[1]	Ter mag pulse, 1900. Low-freq atm increase, 1900.
	1900 to 1930	Missouri	Numerous	
	1900 to 2030	Ohio	do	
	1906	Illinois	do	
	1900 to 1915	New York	Europe, North and South America.	
	1900 to 1920	England	North and South America.	

[1] Disappearance or weakening of sky-waves reflected vertically from ionosphere.

TABLE 1.—*Data on radio fadeouts and other manifestations of sudden ionosphere disturbances*—Continued

Date	Time, GMT	Reported observed in	Reported locations of transmitting stations	Reported solar and magnetic effects, etc.
1936				
June 10	2056 to 2136 to 2159	District of Columbia	Ohio, Massachusetts, District of Columbia.[1]	
	2105 to 2115 to 2150	Oregon	Numerous	
	2050	Nebraska	do	
	2056 to 2120	Illinois	do	Ter mag pulse, 2055.
	2058 to 2103 to 2107	Hawaii	California	
	2058 to 2103 to 2107	California	Hawaii	
	2053 to 2200	do	Asia, Philippines, Java	
	2051 to 2146	New York	Numerous	
	2045 to 2129	Guatemala	do	
June 11	0625 to 0710	California	Asia, Philippines, Java	
	0620 to 0700	Holland	Japan, Java	
	0625 to 0700	Japan	California, South America, Europe, Asia.	Low-freq atm increase 0620 to 0724.
	0625 to 0700	Argentina	Japan	
	0630 to 0640	England	Japan, India	
	0625	France	Numerous	
June 11	1230 to 1250	Holland	North and South America, Norway, Java.	
	1228 to 1240	England	Asia, North and South America.	Low-freq atm increase, 1225 to 1330.
	1230 to 1243 to 1300	District of Columbia	Ohio, Massachusetts	
	1230	France	Numerous	
June 16	1330 to 1400	Holland	North and South America, Europe.	
	1330 to 1335 to 1400	District of Columbia	Ohio, Massachusetts	Solar eruption, 1327 to 1348.
	1330 to 1349	New York	England, Spain	
	1330 to 1337	England	Numerous	
June 16	1713 to 1718 to 1733	District of Columbia	Ohio, Massachusetts	Low-freq atm increase, 1715.
	1715 to 1728 to 1745	New York	South America, California.	
June 16	1803 to 1808 to 1820	do	do	Solar eruption, 1801 to 1809. Ter mag pulse 1800. Low-freq atm increase, 1802.
	1800 to 1807	District of Columbia	Ohio	
June 17	0723 to 0740	Japan	South America, Asia, Europe, Philippines.	Solar eruption, 0727 to 0610. Low-freq atm increase, 0718.
	0720	France	Numerous	
June 17	0908 to 0925	Japan	India, Holland, Norway	
	0908 to 0925	Holland	Japan	
	0908 to 0925	India	do	
June 17	1248 to 1254 to 1316	District of Columbia	Ohio, Massachusetts	
	1248 to 1254	England	India, Italy	
	1246 to 1256	New York	Numerous	
June 19	0907 to 0910 to 1000	Holland	Belgian Congo	
	0910 to 0920	England	India, Egypt, North and South America.	Solar eruption, 0900 to 1100. Low-freq atm increase, 0905.
	0910	France	Numerous	
	0910 to 0930	Japan	Europe, India	
June 19	1633 to 1638	District of Columbia	Ohio	Solar eruption, 1629 to 1637. Ter mag pulse, 1630.
	1610 to 1630	France	Numerous	
June 19	1730 to 1815	Massachusetts	do	Solar eruption, 1736 to 1800.
	1733 to 1737	District of Columbia	Ohio	
June 19	1936 to 1955 to 2115	do	do	Solar eruption, 1938 to 1957.
	1940 to 2000	Idaho	Numerous	
	1937 to 1945 to 2005	New Jersey	England	
June 25	1030 to 1135	Holland	Hungary, Norway	Solar eruption, 1051 to 1140. Low-freq atm increase, 1025.
	1045	France	Numerous	
	1050 to 1100	England	do	
June 25	1115 to 1125	do	do	Solar eruption, 1110 to 1130.
	1113 to 1135	District of Columbia	Ohio	

[1] Disappearance or weakening of sky-waves reflected vertically from ionosphere.

TABLE 1.—*Data on radio fadeouts and other manifestations of sudden ionosphere disturbances*—Continued

Date	Time, GMT	Reported observed in	Reported locations of transmitting stations	Reported solar and magnetic effects, etc.
1936				
July 1	0130 to 0150	Japan	North and South America, Philippines, Java, China.	
	0133 to 0150	California	Japan	
	0135 to 0155	China	do	
July 15	1327 to 1331	New York	South America, Europe	Solar eruption, from before 1330 to 1340. Ter mag pulse, 1325 to 1330. Low-freq atm increase, 1328 to 1413.
	1330	France	Numerous	
	1328 to 1342	England	do	
	1322 to 1332	District of Columbia	Ohio	
July 30	1337 to 1347	New York	Numerous	Low-freq atm increase, 1332 to 1432.
	1340	France	do	
	1342 to 1346 to 1400	District of Columbia	Ohio	
July 31	0015 to 0035	Japan	Europe, North and South America, Asia.	Solar eruption, 0011 to 0030.
	0016 to 0025	England	Numerous	
	0015 to 0020 to 0030	California	do	
Aug. 4	1727 to 1733 to 1746	District of Columbia	Ohio, Massachusetts	Solar eruption, 1719 to 1723. Ter mag pulse, 1725.
Aug. 5	1609 to 1615 to 1630	New York	West Indies, South America, Europe.	Solar eruption, 1603 to 1630. Ter mag pulse, 1605.
	1606 to 1617 to 1621	District of Columbia	Ohio, District of Columbia.[1]	
Aug. 8	1725 to 1729 to 2000	do	do.[1]	Solar eruption, 1716 to 1834.
	1726 to 1730 to 1830	New York	South America	
Aug. 23	1130 to 1210	England	Numerous	Ter mag pulse, 1140.
Aug. 25	1829 to 1851 to 1930	District of Columbia	Massachusetts	Solar eruption, from before 1858 to 1922. Ter mag pulse, 1825 to 1930. Earth-current pulse, 1825 to 1910. Low-freq atm increase, 1831.
	1830 to 1850 to 1955	New York	Europe, North and South America.	
	1917 to 1945	New Jersey	Bermuda	
	1830 to 1905	Ontario, Canada	Numerous	
	1835 to 1850 to 1920	France	North and South America.	
	1828 to 1854 to 1925	California	Numerous	
	1835 to 1908	Japan	North and South America.	
	1840 to 1855	England	United States of America	
	1839 to 1855 to 1920	Holland	North and South America.	
	1800 to 2000	South America	do	
	1800 to 2000	British Columbia, Canada.	Canada	
Aug. 26	0000 to 0020	Japan	Europe, Asia, California.	Solar eruption, 2357 to 0001.
Aug. 28	0930 to 1020	Italy	Numerous	Solar eruption, 0920 to 1030. Ter mag pulse, 0920. Low-freq atm increase, 0923 to 1022.
	0930	France	do	
	0930 to 0955 to 1020	Holland	Japan, Java	
	0930 to 0955 to 1015	England	Numerous	
	0929 to 0945	Japan	Europe	
Sept. 4	0147 to 0202 to 0230	California	Asia, Philippines, Java	Solar eruption, 0140 to 0256.
	0145 to 0215	Java	Numerous	
	0145 to 0200	Philippines	do	
	0150 to 0200	Argentina	Japan	
	0146 to 0208	Siam	Numerous	
	0145 to 0210	England	Japan, Australia	
	0145 to 0215	Japan	Asia, Java, Europe, North and South America.	
Sept. 4	1238 to 1244 to 1252	District of Columbia	Ohio, Massachusetts, District of Columbia.[1]	
	1238 to 1250	England	Numerous	
Sept. 4	1713 to 1732 to 1740	District of Columbia	Ohio, Massachusetts	Ter mag pulse, 1714 to 1721. Earth-current pulse, 1714.
	1715 to 1720 to 1750	New York	North and South America.	
	1714 to 1723 to 1740	California	United States of America.	

[1] Disappearance or weakening of sky-waves reflected vertically from ionosphere.

TABLE 1.—*Data on radio fadeouts and other manifestations of sudden ionosphere disturbances*—Continued

Date	Time, GMT	Reported observed in	Reported locations of transmitting stations	Reported solar and magnetic effects, etc.
1936				
Sept. 5	0902 to 0912 to 0932	Holland	Japan, Java	Ter mag pulse, 0900. Low-freq atm increase, 0859.
	0902 to 0915 to 0930	England	Numerous	
	0905	France	do	
	0902 to 0930	Japan	Europe	
Oct. 9	1424 to 1440 to 1517	District of Columbia	Ohio, Massachusetts	Solar eruption, from before 1454 to after 1503. Low-freq atm increase, 1417 to 1554.
	1422 to 1542	New York	Numerous	
	1435	France	do	
	1430 to 1450	England	do	
Oct. 13	0342 to 0355	Japan	Asia, Europe	Solar eruption, 0250 to 0430.
Oct. 16	1733 to 1752 to 1820	District of Columbia	Ohio, Massachusetts, District of Columbia.[1]	Ter mag pulse, 1730.
	1735 to 1750 to 1815	New York	Europe, North and South America.	
	1740 to 1750	California	Numerous	
	1736 to 1754 to 1834	Panama, Canal Zone	North America	
	1736 to 1754 to 1834	Florida	do	
	1720 to 1820	Japan	Europe	
Oct. 21	1535 to 1545 to 1600	District of Columbia	United States of America, Panama, Spain.	Solar eruption, 1600. Ter mag pulse, 1535 to 1550. Earth-current pulse, 1535. Low-freq atm increase, 1535 to 1645.
	1538 to 1550 to 1615	New York	England, North and South America.	
	1536 to 1550 to 1555	California	District of Columbia, Panama, West Indies.	
	1536 to 1550 to 1555	Panama, Canal Zone	District of Columbia, California, West Indies.	
	1538 to 1550	England	Numerous	
Nov. 4	1701 to 1715 to 1720	District of Columbia	Ohio	Solar eruption, beginning 1657.
Nov. 6	1610 to 1638 to 1700	do	Ohio, Massachusetts, District of Columbia.[1]	Solar eruption, from before 1624 to 1650. Ter mag pulse, 1610 to 1645. Earth-current pulse, 1606 to 1616 to 1636. Low-freq atm increase, 1612 to 1658.
	1611 to 1630 to 1655	New York	North and South America, Europe.	
	1609 to 1702	Peru	Peru [1]	
	1614 to 1630 to 1645	California	United States of America, Philippines, China, Japan.	
	1610 to 1625 to 1640	Massachusetts	Numerous	
	1610 to 1625 to 1640	Pennsylvania	do	
	1615 to 1650	Illinois	do	
	1615	Japan	North and South America.	
	1612 to 1626 to 1630	Germany	do	
	1615 to 1625	England	Numerous	
	1613 to 1620	Holland	do	
	1612 to 1645	France	North and South America.	
Nov. 7	0344 to 0410	Japan	Asia, North and South America.	
	0345 to 0415	Philippines	Numerous	
	0347 to 0358	California	Japan	
Nov. 7	1450 to 1523 to 1624	District of Columbia	Ohio, Massachusetts, District of Columbia.[1]	Solar eruption, from before 1537 to 1600. Low-freq atm increase, 1451 to 1550.
	1452 to 1459 to 1620	New York	North and South America, Europe.	
	1450 to 1505	England	Numerous	
	1450 to 1530 to 1620	Holland	South America, Japan	
	1450 to 1530	France	South America	
Nov. 8	1819 to 1827 to 1834	District of Columbia	Ohio, Massachusetts, District of Columbia.[1]	Solar eruption, 1819 to 1827. Ter mag pulse, 1815 to 1825.
	1812 to 1834	California	Japan	
Nov. 16	1500 to 1545	New York	North and South America, Europe.	Solar eruption, from before 1530 to after 1700. Low-freq atm increase, 1450 to 1605.
	1457 to 1530	District of Columbia	Ohio, Massachusetts, District of Columbia.[1]	

[1] Disappearance or weakening of sky-waves reflected vertically from ionosphere.

TABLE 1.—*Data on radio fadeouts and other manifestations of sudden ionosphere disturbances*—Continued

Date	Time, GMT	Reported observed in	Reported locations of transmitting stations	Reported solar and magnetic effects, etc.
1936				
Nov. 24	1710 to 1749 to 1820	District of Columbia	Ohio, Massachusetts, District of Columbia,[1] Panama, Puerto Rico, California.	
	1720 to 1735 to 1800	Holland	North and South America.	
	1712 to 1744 to 1810	New York	North and South America, Europe.	
Nov. 24	1915 to 1930	Argentina	Holland	Solar eruption, 1908 to after 1944. Ter mag pulse, 1914 to 1940.
	1913 to 1945 to 2010	District of Columbia	Ohio, Massachusetts, California, District of Columbia,[1] Panama, West Indies.	
	1915 to 1948	West Indies	Numerous	
	1915 to 1940	England	do	
	1914 to 1945 to 2015	California	New York, Washington, Philippines.	
	1914 to 1935 to 2010	New York	North and South America, Europe.	
	1845 to 1945	British Columbia, Canada.	Quebec	
	1920 to 1940 to 2000	Holland	South America	
	1915 to 2000	France	do	
Nov. 26	0900 to 0930	England	Numerous	Low-freq atm increase, 0857 to 1000.
	0900 to 0920 to 0940	Holland	do	
	0901 to 0925	France	do	
Nov. 26	1749 to 1835 to 1859	District of Columbia	Ohio, Massachusetts, District of Columbia,[1] Panama, West Indies, California.	Solar eruption, 1749 to 1828. Ter mag pulse, 1750.
	1750 to 1825 to 1840	British Columbia, Canada.	Canada	
	1755 to 1820	England	Numerous	
	1753 to 1810 to 1900	New York	North and South America, Europe.	
	1755 to 1815	France	North and South America.	
Nov. 27	1651 to 1659 to 1713	District of Columbia	Ohio, District of Columbia.[1]	Solar eruption, 1650 to 1658. Ter mag pulse, 1650. Earth-current pulse, 1650. Low-freq atm increase, 1658.
	1650 to 1724	New York	Numerous	
	1651 to 1654	Peru	Peru [1]	
	1656 to 1715	France	South America	
Nov. 28	1500 to 1520	District of Columbia	Ohio	Low-freq atm increase, 1507 to 1537.
	1510 to 1545	France	South America	
Nov. 29	1547 to 1602 to 1640	District of Columbia	Ohio, District of Columbia.[1]	Solar eruption, from before 1555 to after 1637.
	1546 to 1631	New York	Numerous	
Nov. 30	1235 to 1315	England	do	Low-freq atm increase, 1230 to 1400.
	1240 to 1300	France	South America	
Dec. 3	1215 to 1330	Holland	North and South America, Europe.	Solar eruption, from before 1146 to after 1245. Low-freq atm increase, 1200 to 1302.
	1205 to 1245	France	South America, Japan	
	1205 to 1242	England	Numerous	
	1200 to 1320	New York	do	
Dec. 9	1337 to 1517	do	do	Low-freq atm increase, 1300.
	1320 to 1700	Holland	South America	
	1315 to 1330	France	do	
	1310 to 1355	England	do	
Dec. 21	1817 to 1822 to 1828	District of Columbia	Ohio	Ter mag pulse, 1815.
	1825 to 1829	California	Oregon, Washington California.	
Dec. 22	1305 to 1315	France	Numerous	
	1303	Holland	do	
Dec. 24	2202 to 2220	California	Western United States of America, Japan, China, Philippines.	Solar eruption, 2200 to 2215.

[1] Disappearance or weakening of sky-waves reflected vertically from ionosphere.

TABLE 1.—*Data on radio fadeouts and other manifestations of sudden ionosphere disturbances*—Continued

Date	Time, GMT	Reported observed in	Reported locations of transmitting stations	Reported solar and magnetic effects, etc.
1936 Dec. 24	2348 to 2400	California	Western United States of America, Japan, China, Philippines.	Solar eruption, 2349 to 2358. Ter mag pulse, 2348.
Dec. 26	1932 to 1958 to 2019	District of Columbia	Ohio, Massachusetts	
	1944 to 1954 to 2015	New York	Numerous	
	1939 to 2016	California	United States of America, Japan, China, Philippines.	
Dec. 28	1055 to 1100	England	Numerous	Low-freq atm increase, 1103 to 1145.
	1100	Holland	do	
	1100 to 1110	France	do	
Dec. 29	0820 to 0835	do	Africa, Asia	
	0820	Holland	Java	
	0848 to 0910	England	Numerous	
Dec. 30	0852 to 0908	France	Africa, Asia	Low-freq atm increase, 0848 to 0920.
Dec. 30	1031 to 1045	England	Numerous	Solar eruption, from before 0944 to 1056. Low freq atm increase, 1030.
Dec. 30	1100 to 1120	do	do	Solar eruption, from before 1053 to 1217. Low-freq atm increase, 1053.

Table 1 summarizes the data from all sources. It is regretted that only a summary can be given; the complete details are so voluminous that it is not practicable to tell the whole story of each of the occurrences. The complete details would occupy hundreds of pages. Thus, in the case of numerous publications listed in section VII, the entire article is devoted to observations at a single place of a single one of these occurrences. Table 1 includes some information based on published articles. Most of the data, however, were derived from observations made at the National Bureau of Standards and from reports sent by other observers to the author. Acknowledgements of this assistance are given at the end of this paper.

Even though they represent very extensive observations, the data we have do not give comprehensive information on the occurrences. In some cases we have knowledge of the disturbance from only two places of observation (and effects reported from only one place are included in two or three cases, where radio waves were received over numerous paths and the effects were extremely intense and clearly authentic). It would be desirable that we have for each occurrence information from numerous points all over the world, on the effects which occurred in radio transmission, terrestrial magnetism, and earth currents. In no case have we such complete information, and in many cases we also lack certainty as to whether a solar eruption occurred at the time. The incomplete character of our knowledge should be remembered in interpreting the data.

This investigation has dealt primarily with the radio aspects of the sudden ionosphere disturbances, as the form of table 1 indicates. The table gives, for each receiving location reporting a radio fadeout, the average time of the fadeout of high-frequency radio waves for

each of the locations of transmitting stations whose emissions were affected. For the terrestrial magnetic and earth-current pulses, the effects upon atmospherics, and solar eruptions, only the times of occurrence are given. All times given in this paper are in GMT, i. e., Greenwich Mean Time. Eastern Standard Time is 5 hours less than GMT.

In the second column of table 1, the first time given on each line is the time of beginning of the radio fadeout. Where three times are given, the second is the time when the radio signals began to come in again and the third is the time when the intensities had risen to normal. Where two times are given, the second is in most cases the time when the radio signals had risen to approximately normal.

On account of the necessity of compressing the data into a table of reasonable length, the times given are in most cases averages. The individual times of beginning of the radio fadeout or other effect agree, however, in almost all cases within 2 or 3 minutes. For the radio fadeouts, the times of ending differed greatly. The times given are averages. (See section III regarding the differences at different frequencies.)

The data on the radio fadeouts are based on: (a) Experiences of operators receiving radio signals; (b) graphical records from field-intensity recorders; and (c) observations of echo signal pulses from the ionosphere. All the radio fadeouts which occurred at Washington, including practically all observable in the American hemisphere, after August 1935, were recorded on automatic field-intensity recorders maintained by the National Bureau of Standards at Meadows, Md., near Washington, D. C. These recorders made continuous records of the field intensities of certain high-frequency transmitting stations.

Typical fadeouts as recorded graphically are shown in figures 1 to 8. Note the sudden drop of intensity and the subsequent gradual rise. As observed by a radio operator, a radio fadeout is simply the sudden disappearance of the signal from a distant high-frequency transmitting station. In most instances the intensity of the received signal was reduced to zero, but in some it merely sank to an intensity so low as to be unreadable. Whenever echo signal pulses were being transmitted at the time of the fadeout in a given locality, the ionosphere echoes weakened or disappeared. This is also illustrated in the figures 1 to 8. The instances of these phenomena given in these eight figures are illustrative of many thousands of observations for which the author has data on file.

In the last column of table 1 are numerous entries of increase of radio atmospherics at the same times as the other effects. These are all based on data published by R. Bureau, of France. They refer to an increase in atmospherics as recorded on frequencies between 27 and 40 kc/s, at observing points in France and Northern Africa.

The expression "Ter. mag. pulse", in the last column of table 1, means an abrupt change in one or more of the terrestrial magnetic elements, viz horizontal intensity, vertical intensity, and declination, usually in all three. Some typical examples are shown in figures 1 to 8. Most of the data on terrestrial magnetic effects were obtained from the magnetograms of the Cheltenham, Md., Observatory of the U. S. Coast and Geodetic Survey, supplemented in some cases by information from other magnetic observatories, particularly the Mt. Wilson, Calif., Observatory of the Carnegie Institution of Washington. A

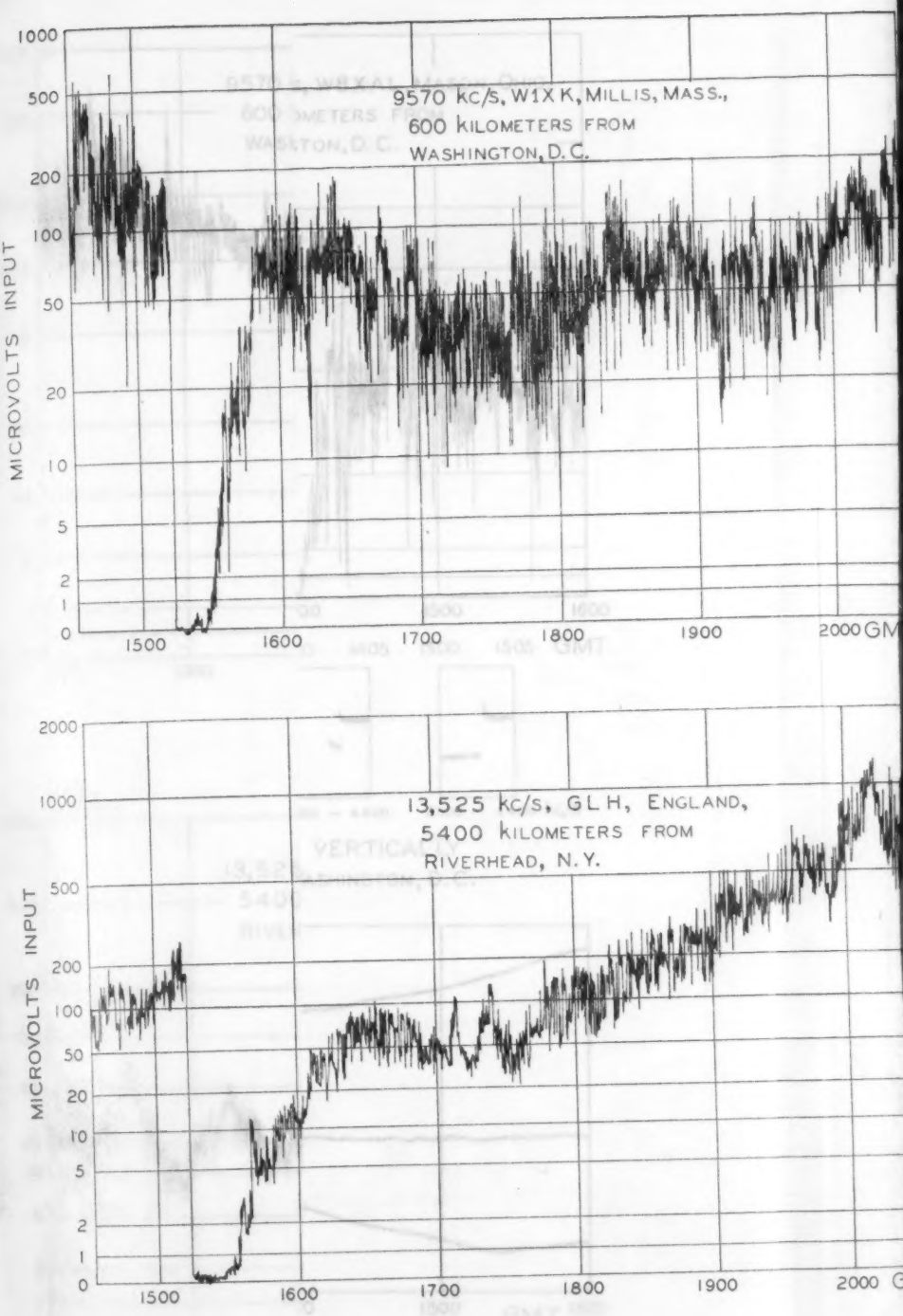

FIGURE 1.—*Sudden disturbance of the ionosphere on February 14,*

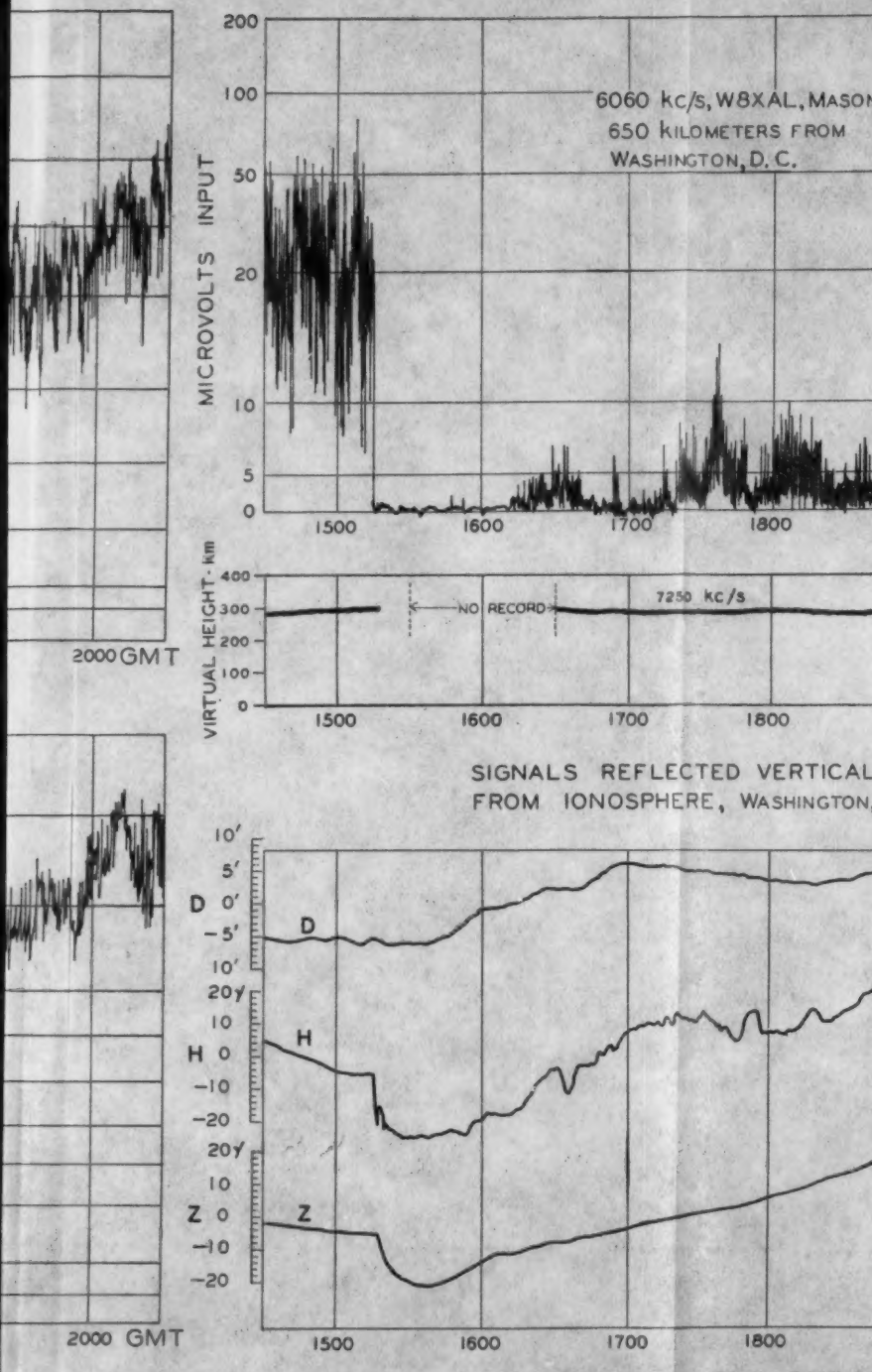

n February 14, 1936, as revealed by radio fadeout and terrestrial magnetic perturbation.

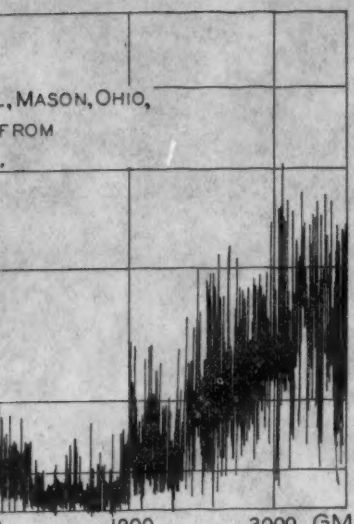

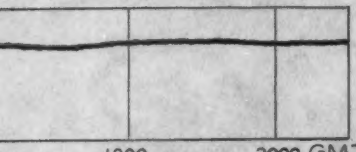

RTICALLY
HINGTON, D.C.

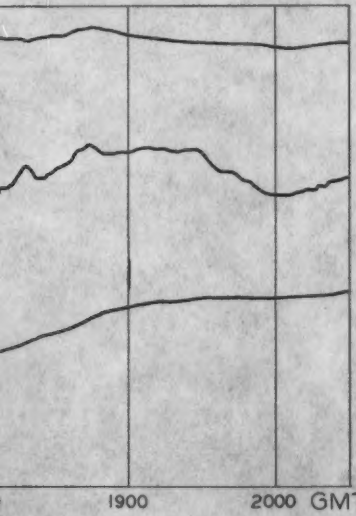

RECORD,

bation.

22—37 (Face p. 124) No. 1

UNIV. OF MICH.

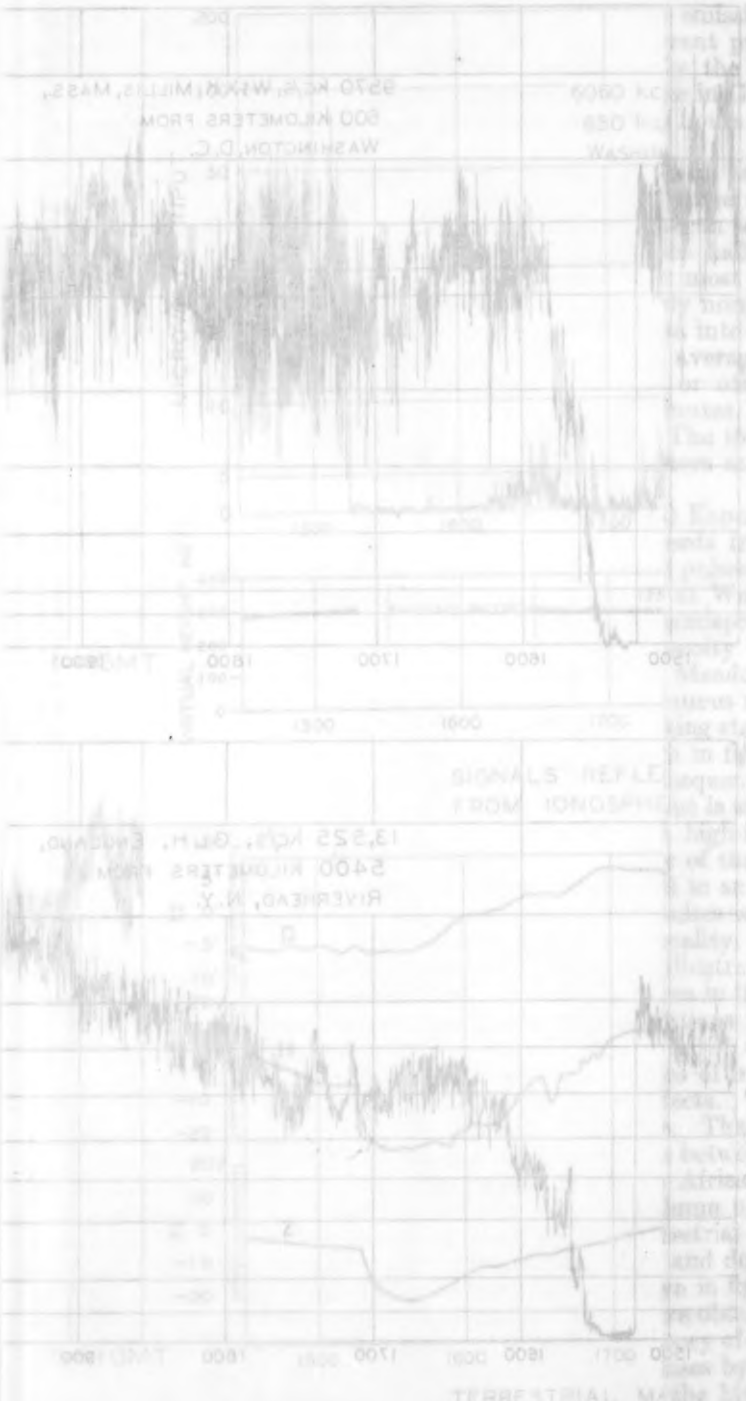
MICROVOLTS INPUT
MICROVOLTS INPUT

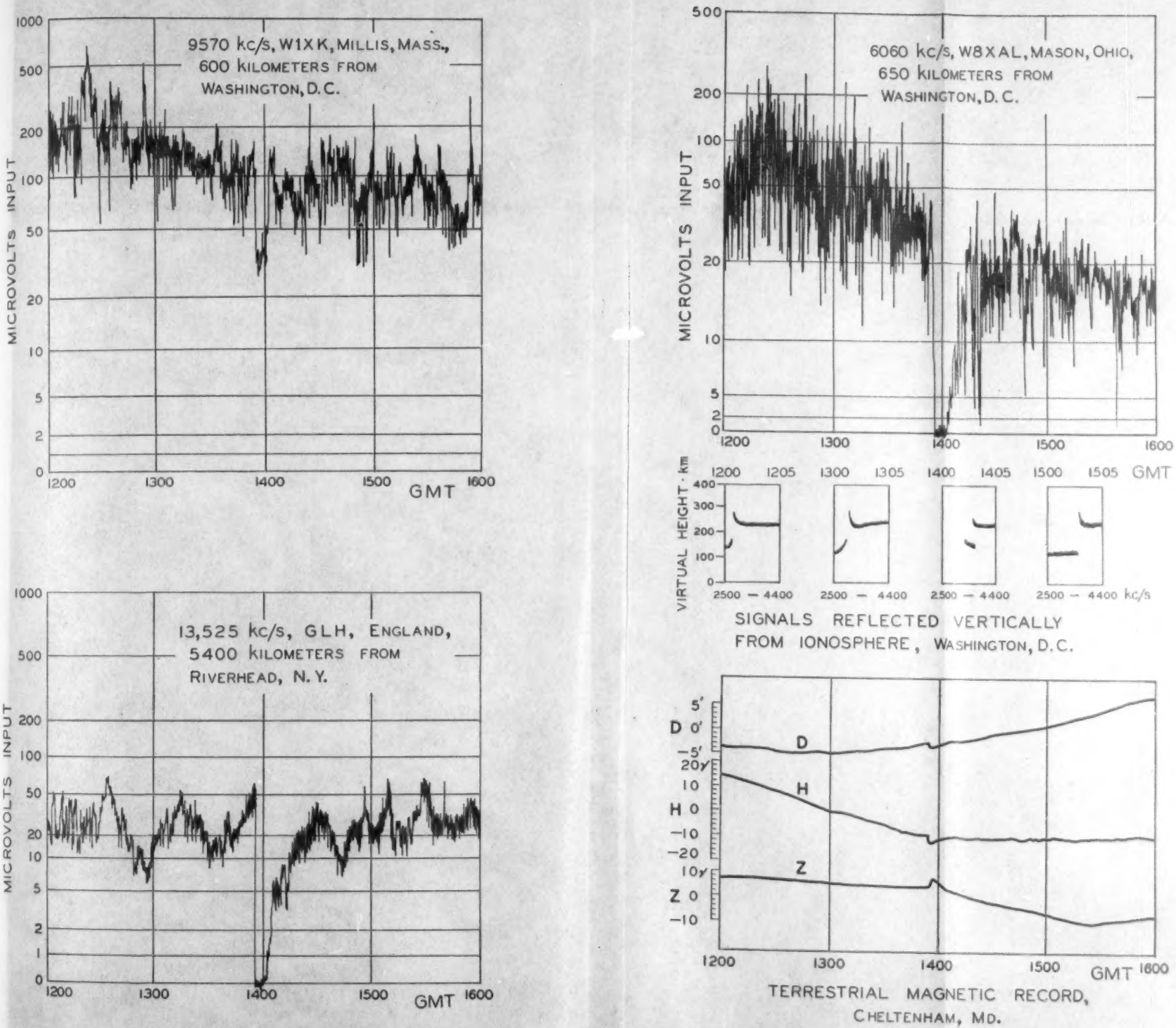

FIGURE 2.—*Sudden disturbance of the ionosphere on April 6, 1936, as revealed by radio fadeout and terrestrial magnetic perturbation.*

UNIV OF MICH

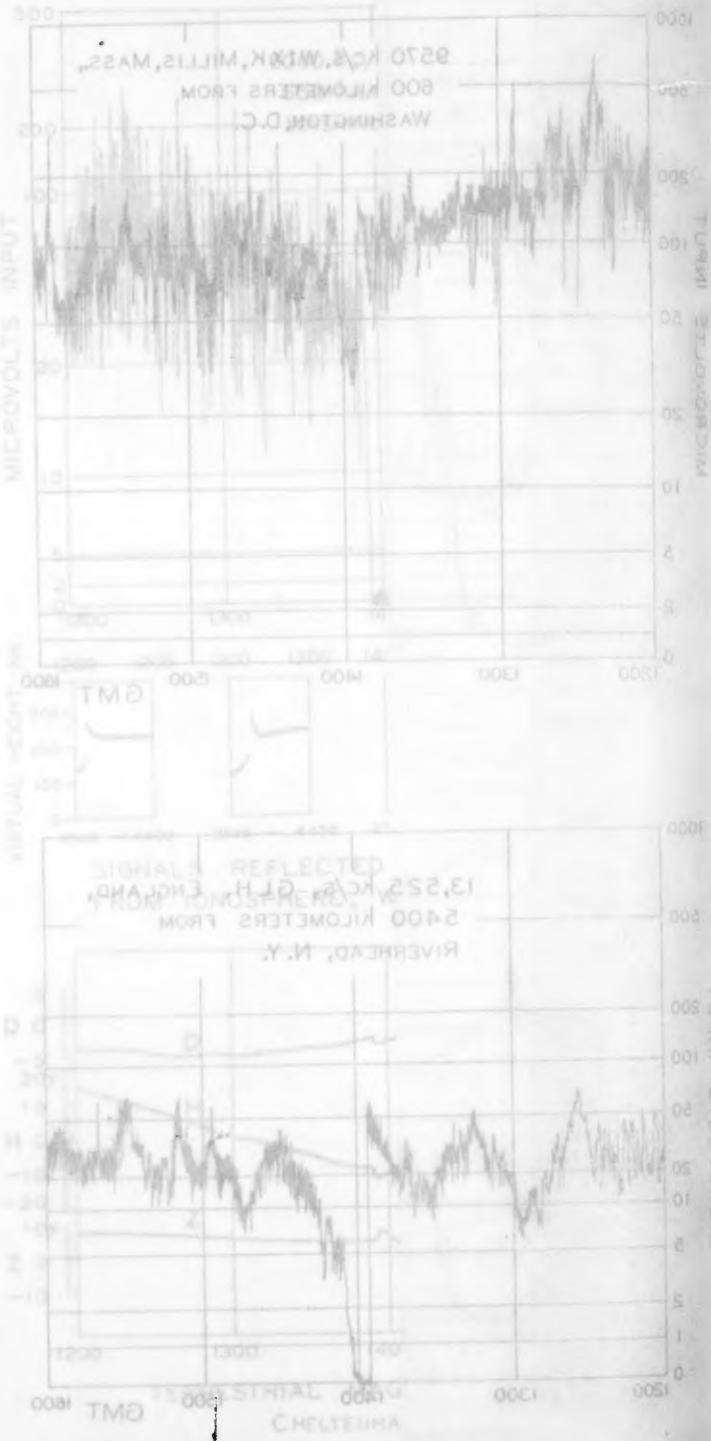
MICROVOLTS INPUT
MICROVOLTS INPUT
GMT
GMT
CHELTENHAM

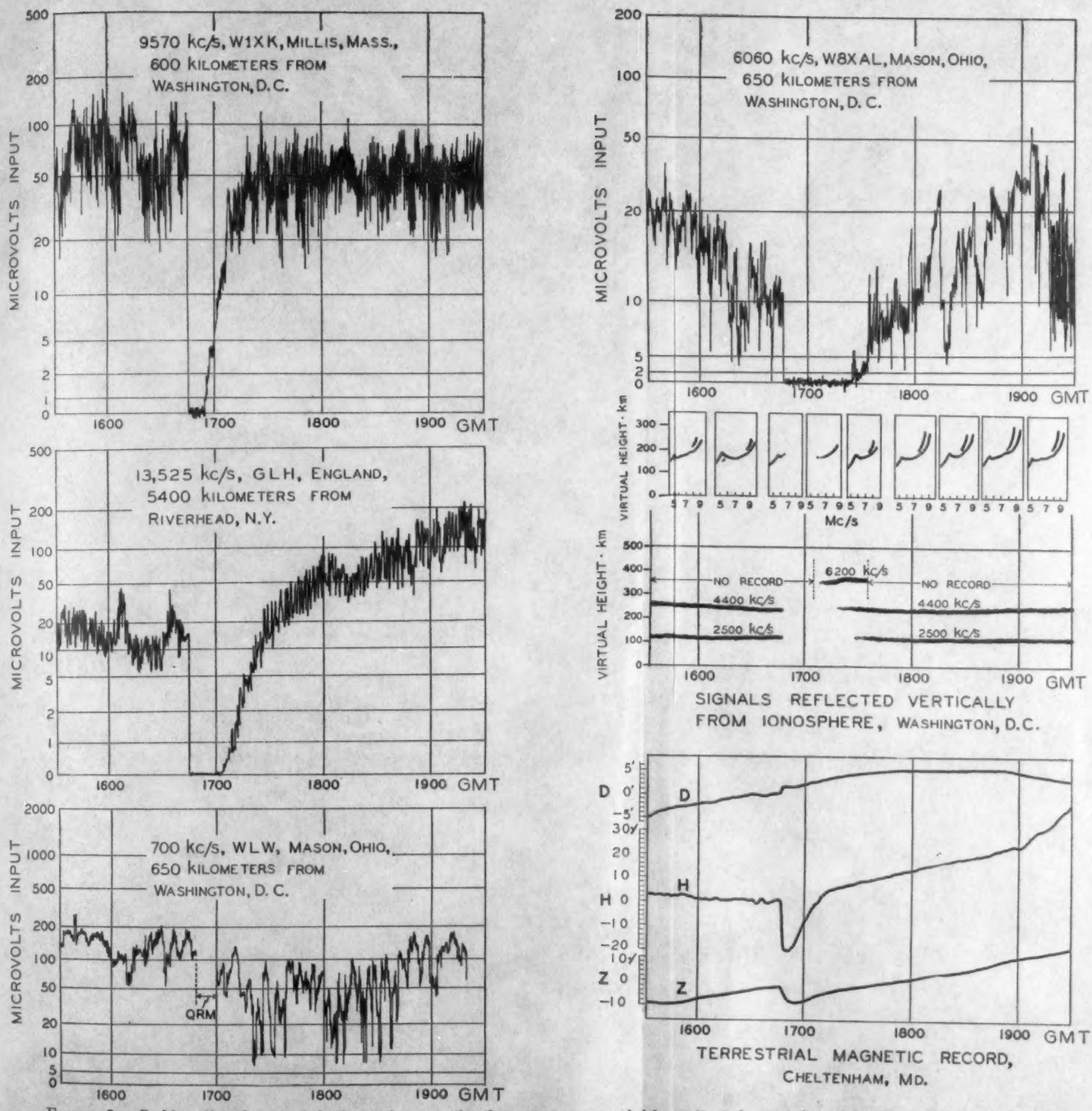

FIGURE 3.—*Sudden disturbance of the ionosphere on April 8, 1936, as revealed by radio fadeout and terrestrial magnetic perturbation.*

UNIV. OF MICH.

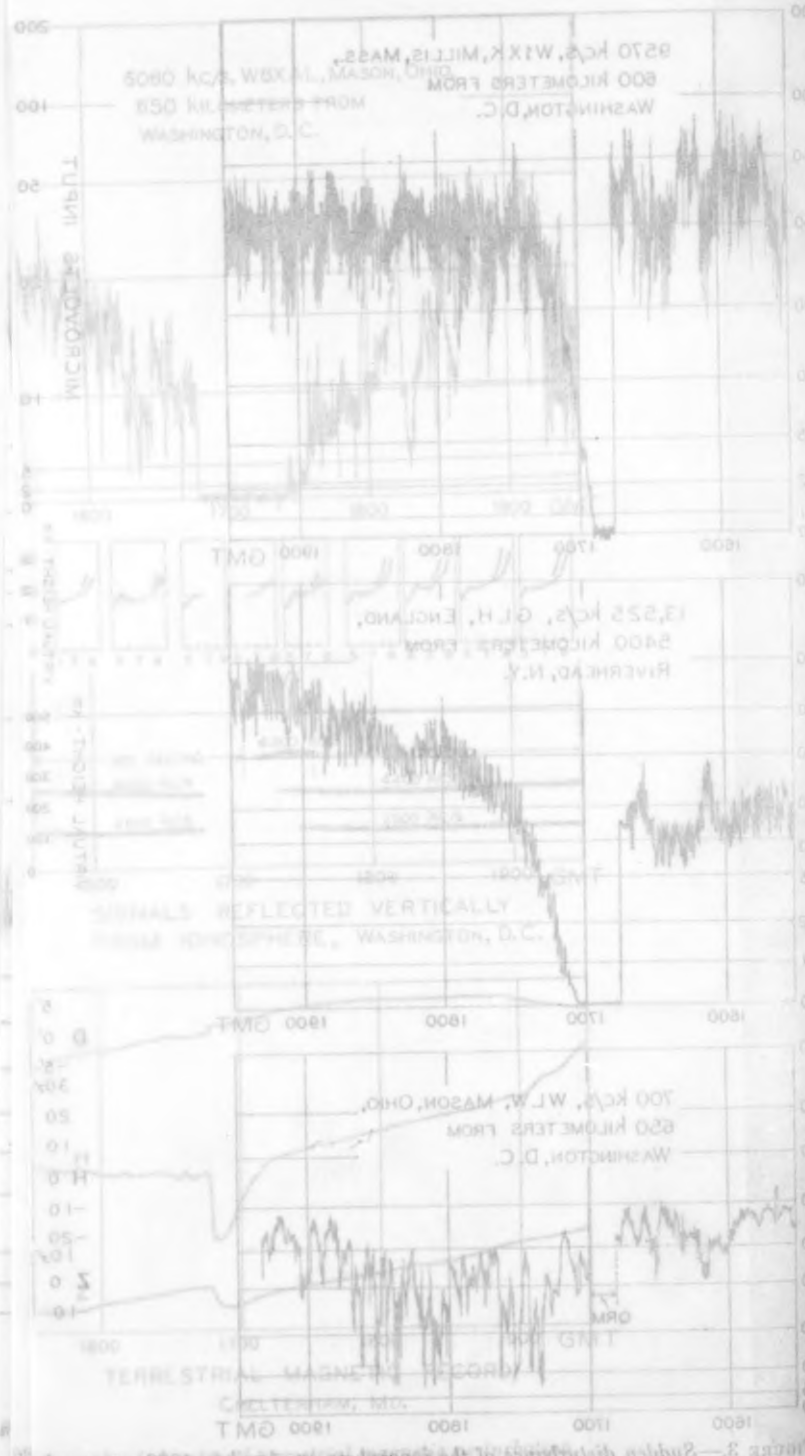
MICROVOLTS INPUT
1800 GMT
1700
1800

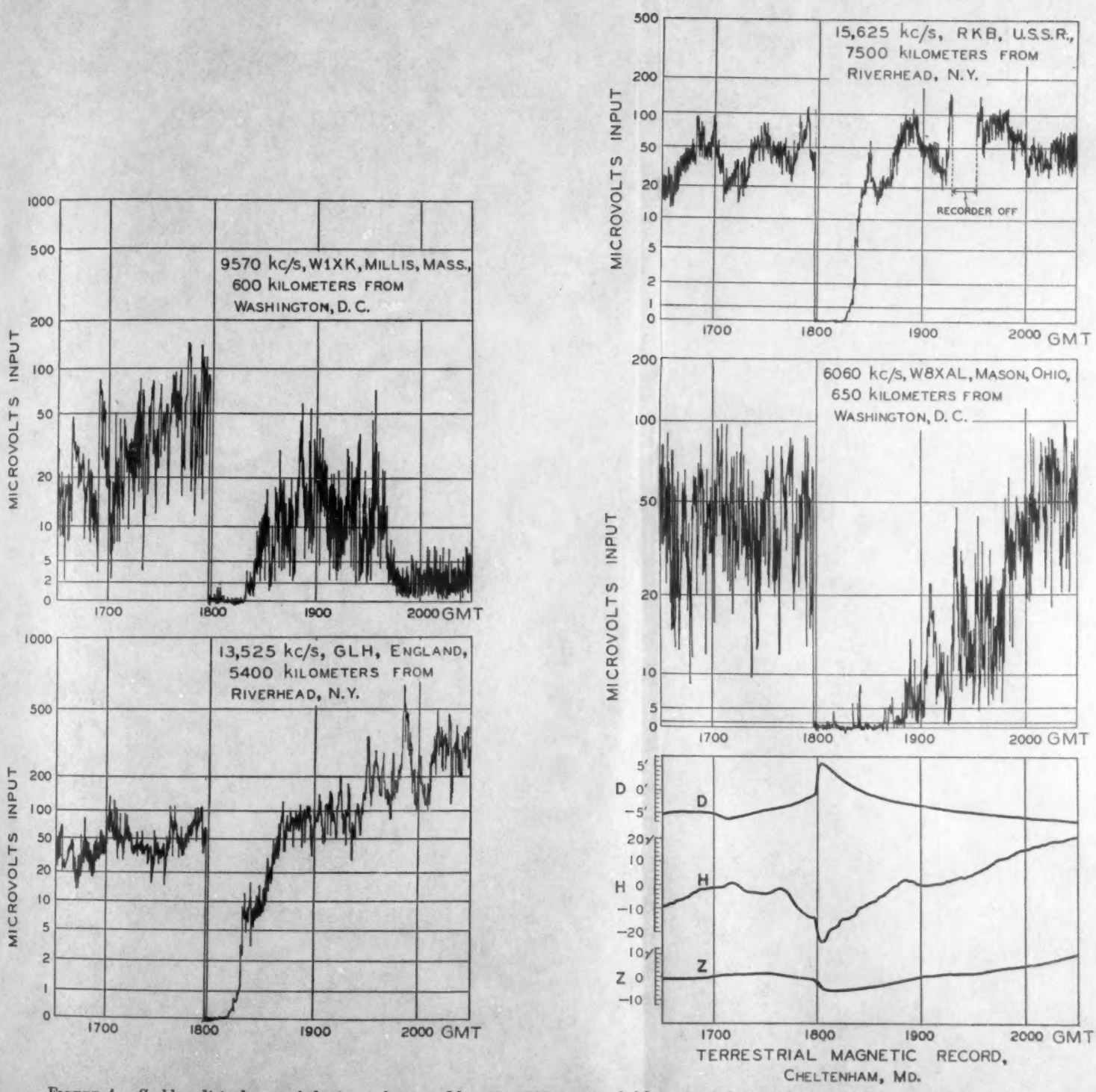

FIGURE 4.—*Sudden disturbance of the ionosphere on May 28, 1936, as revealed by radio fadeout and terrestrial magnetic perturbation.*

UNIV. OF MICH.

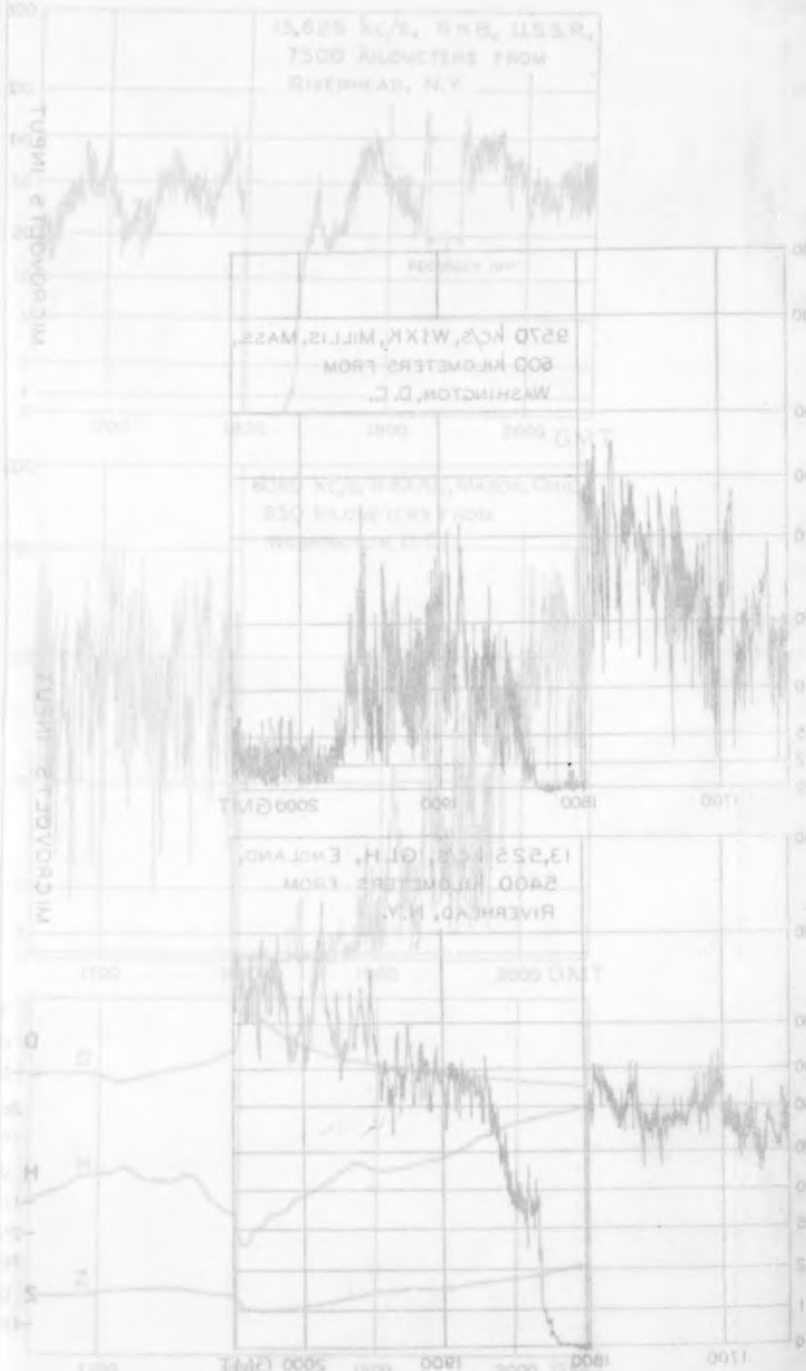

TERRESTRIAL MAGNETIC RECORD,
CHELTENHAM, MD.

FIGURE 4.—Sudden disturbance of the ionosphere on May 28, 1936, as recorded

TEM—37 (Over p. 126) No. 4

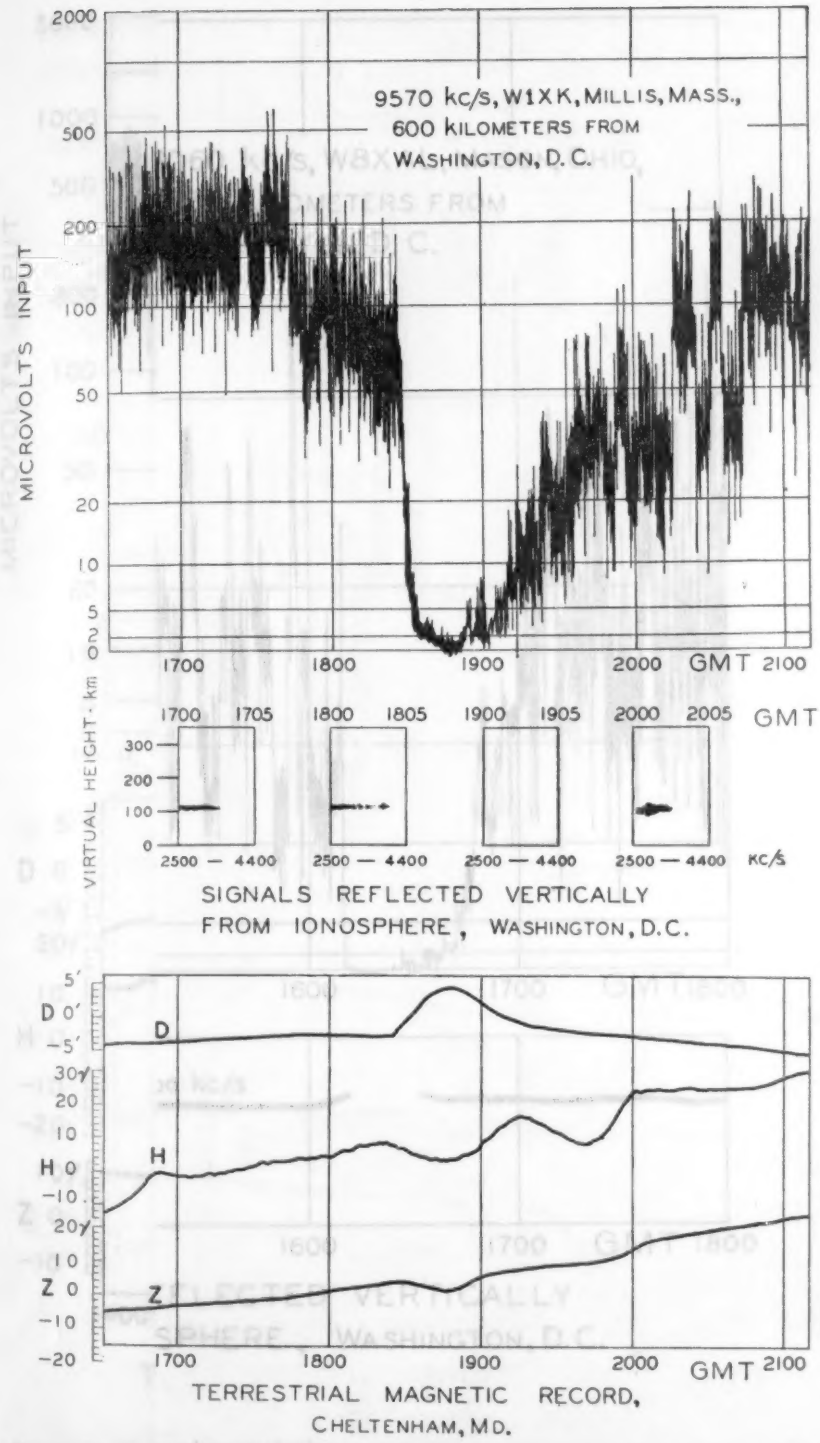

FIGURE 5.—*Sudden disturbance of the ionosphere on August 25, 1936, as revealed by radio fadeout and terrestrial magnetic perturbation.*

UNIV. OF MICH.

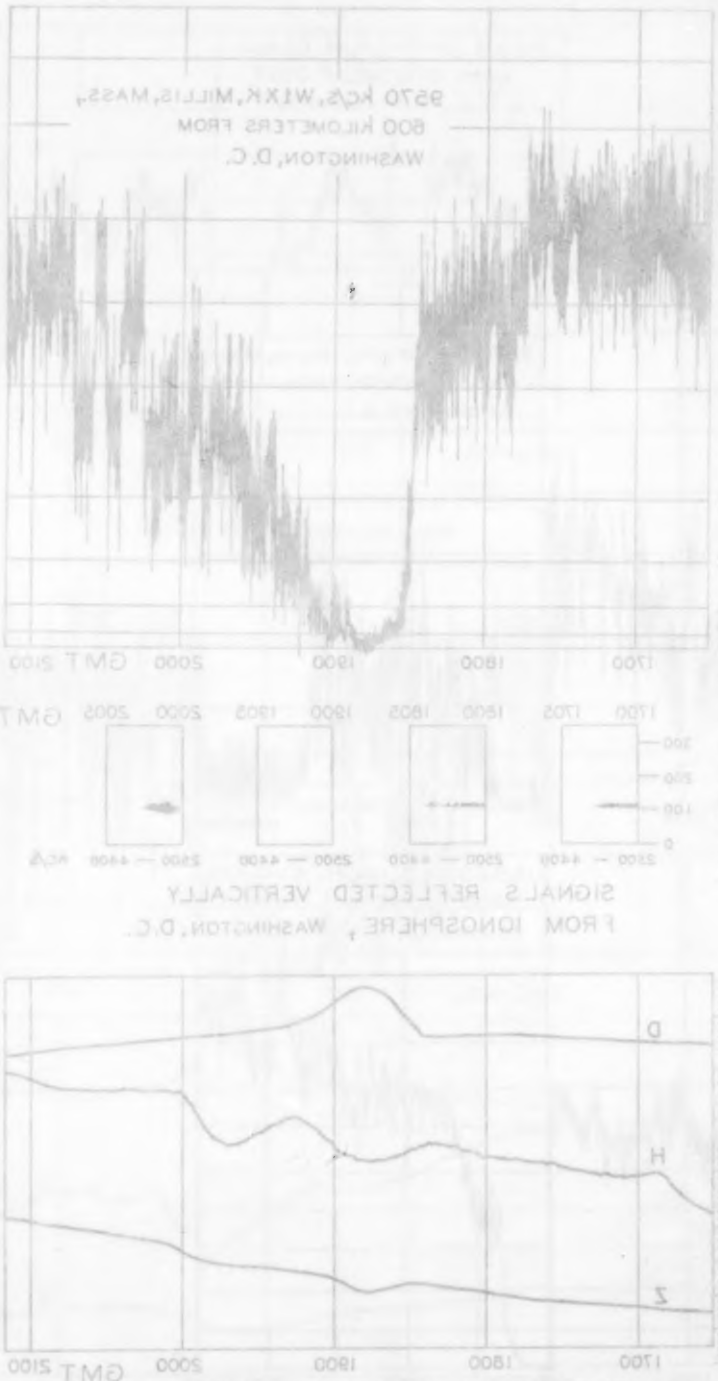

FIGURE 5.—Sudden disturbance of the ionosphere on August 25, 1939, as recorded by radio fadeout and terrestrial magnetic perturbation.

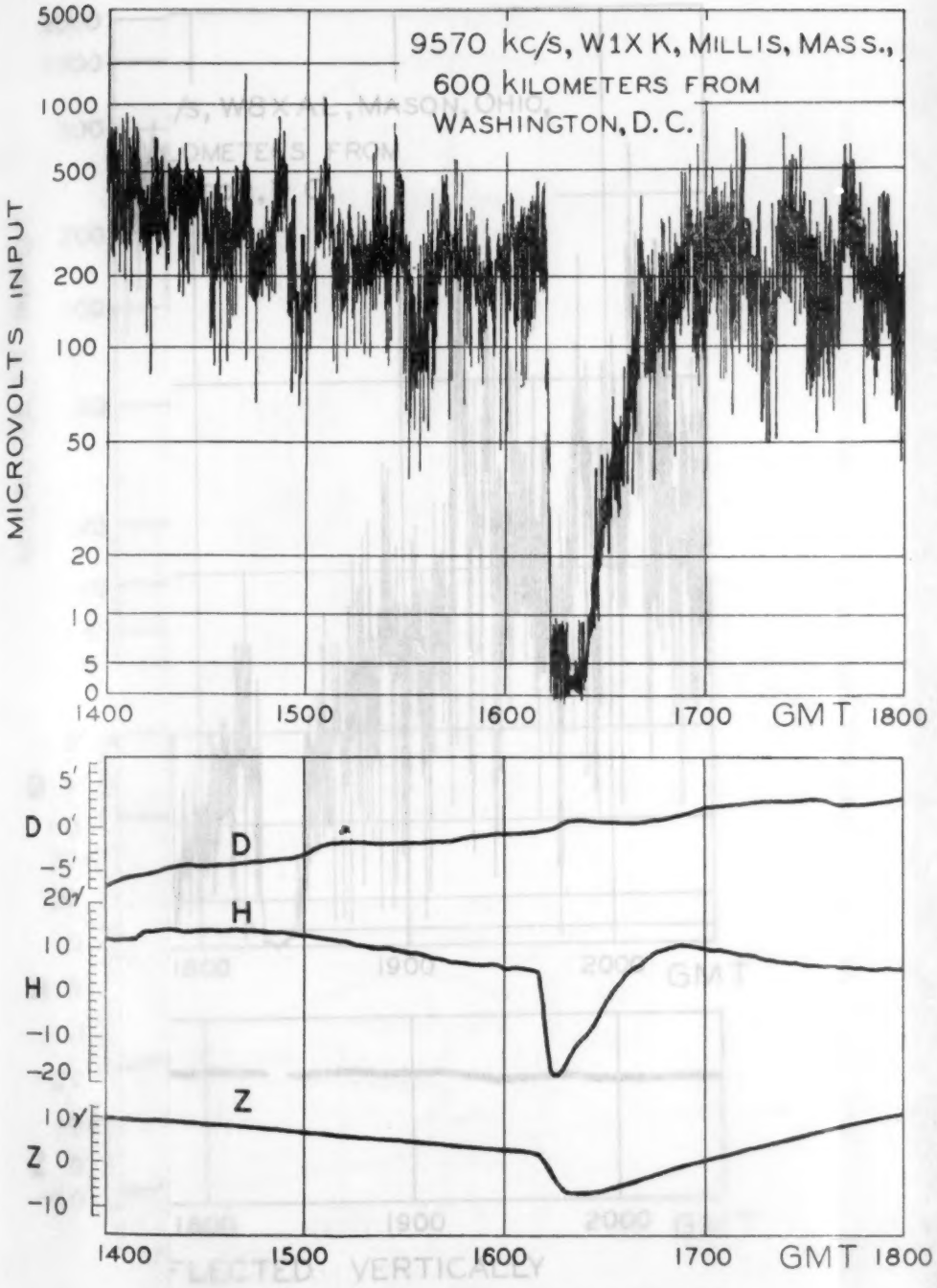

FIGURE 6.—*Sudden disturbance of the ionosphere on Novemb*

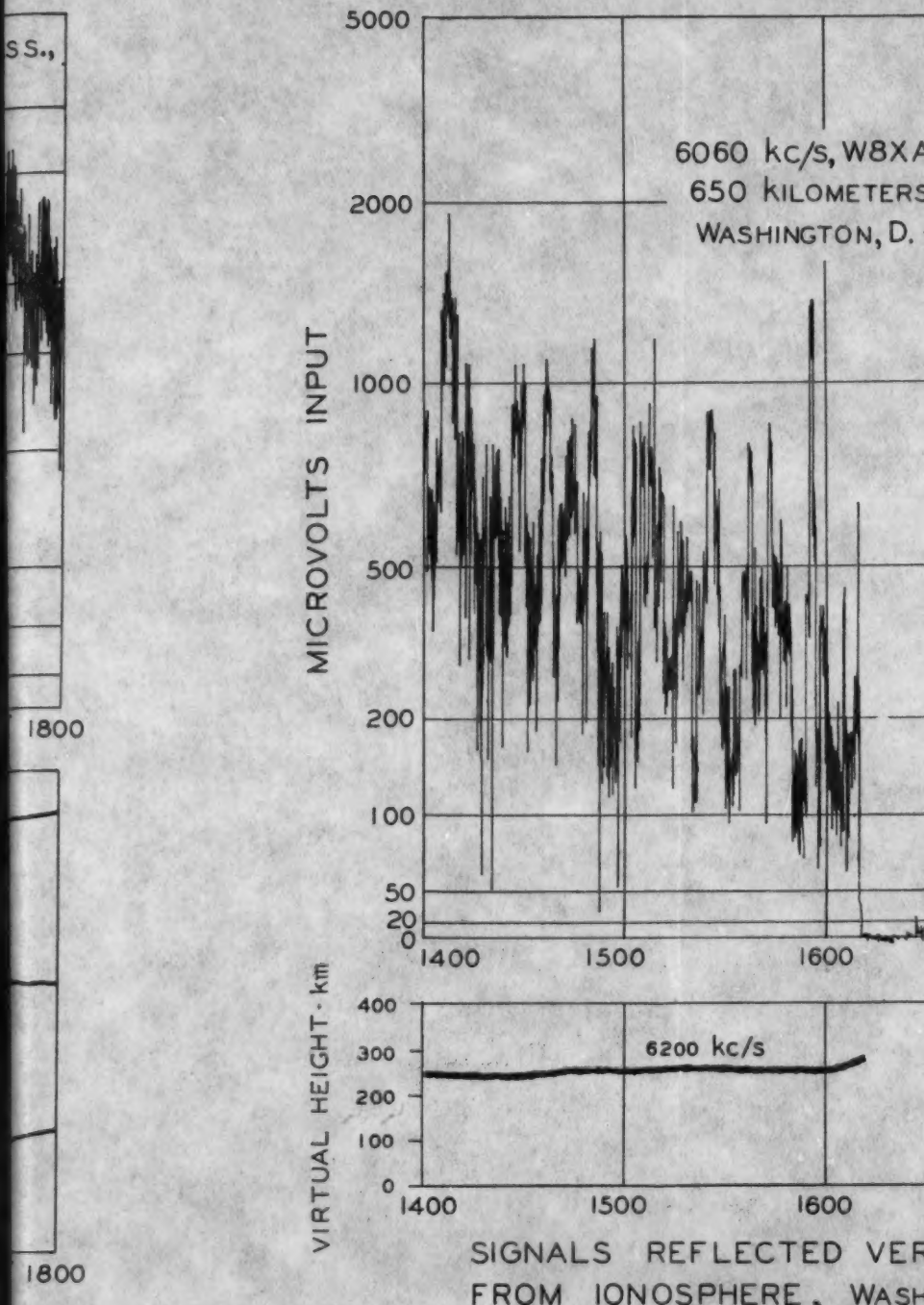

on November 6, 1936, as revealed by radio fadeout and terrestrial magnetic perturbation.

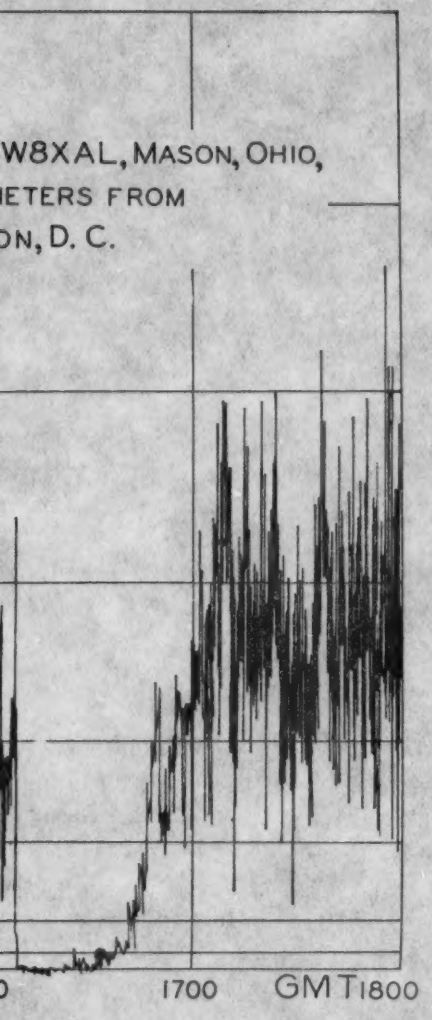

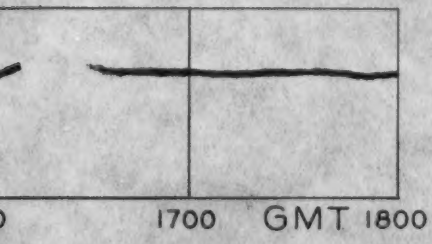

VERTICALLY
WASHINGTON, D.C.

722—37 (Face p. 124) No. 6

UNIV. OF MICH.

TERRESTRIAL MAGNETIC RECORD,
CHELTENHAM, MD.

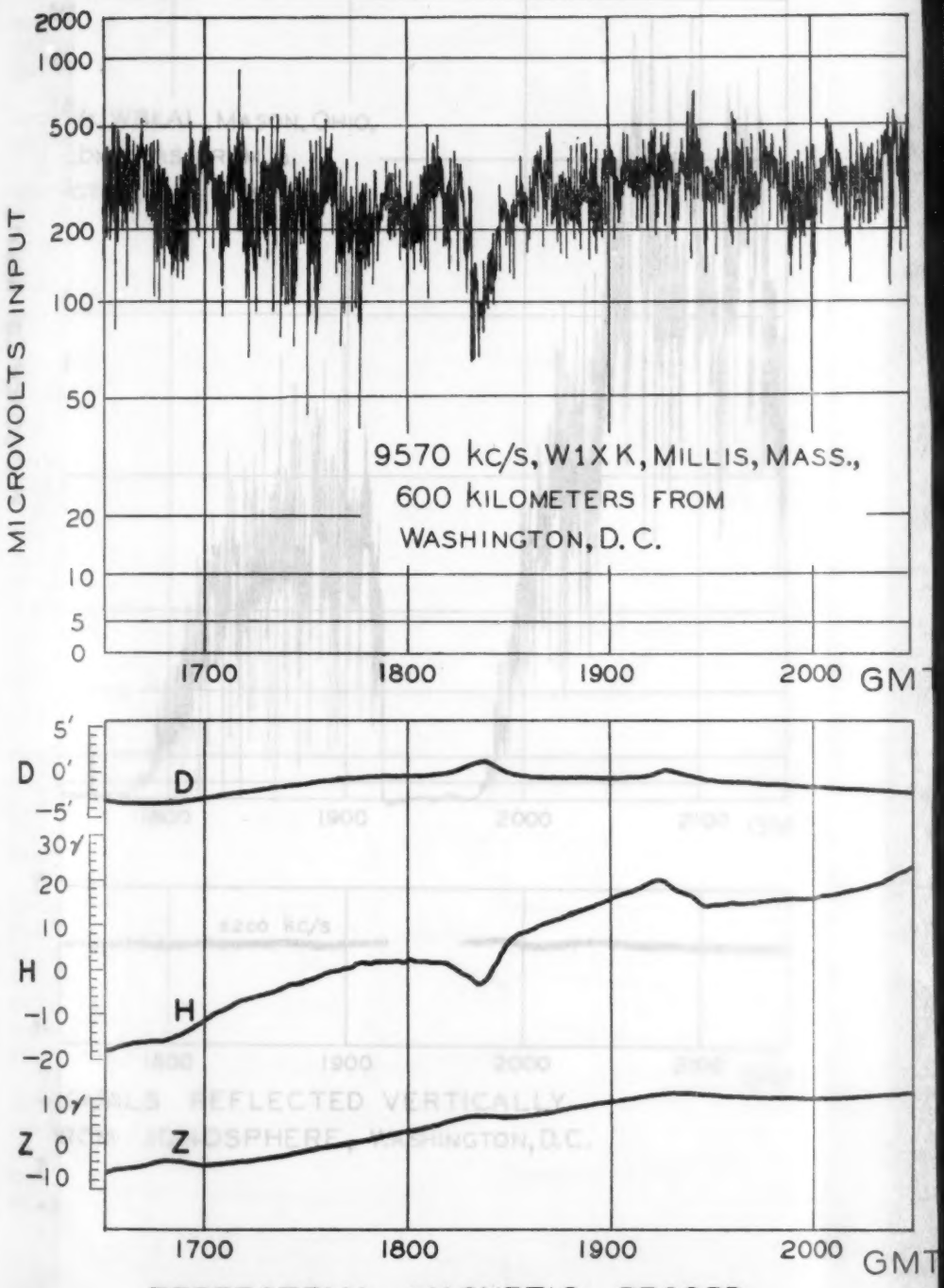

FIGURE 7.—*Sudden disturbance of the ionosphere on Novem*

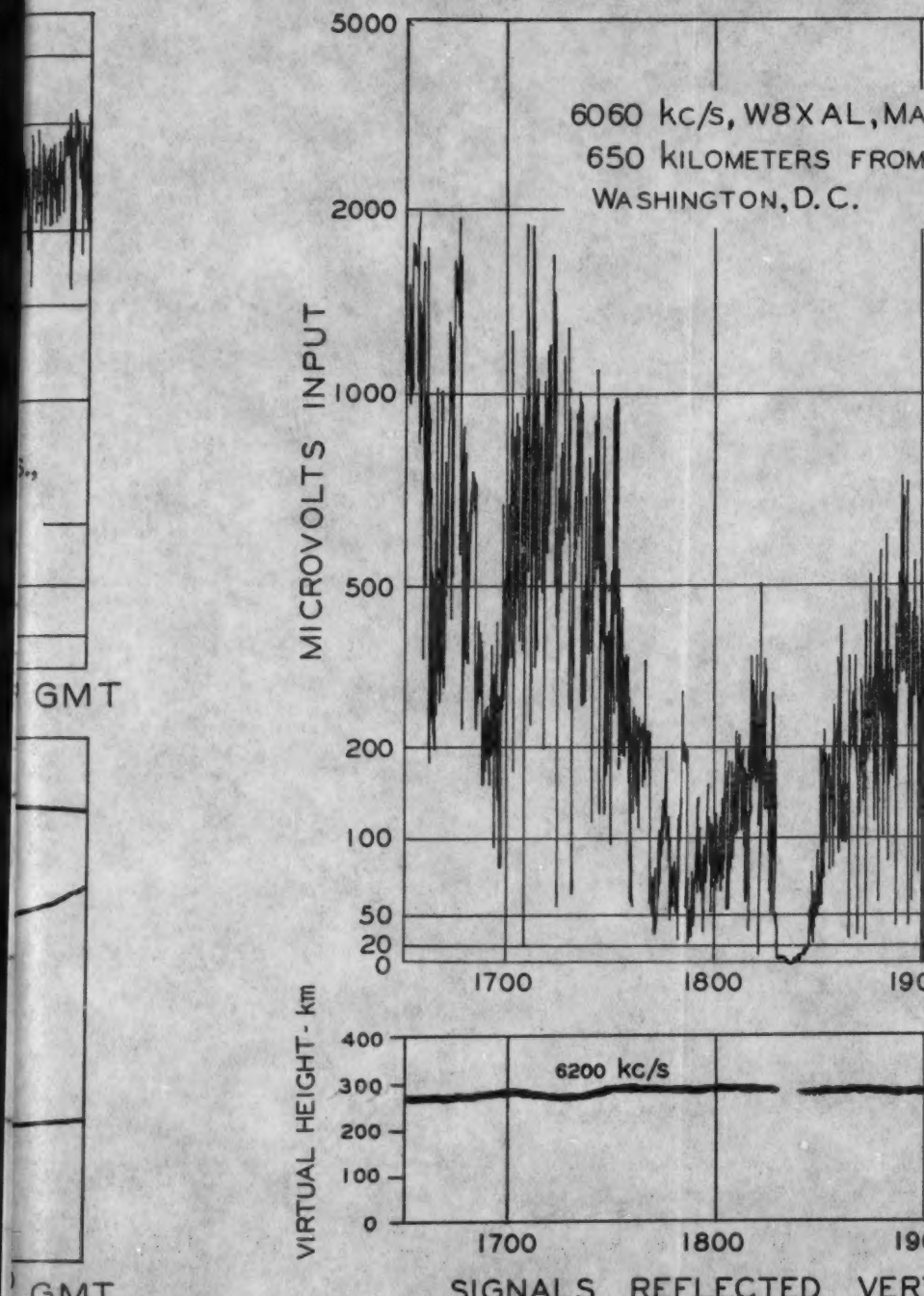

on November 8, 1936, as revealed by radio fadeout and terrestrial magnetic perturbation.

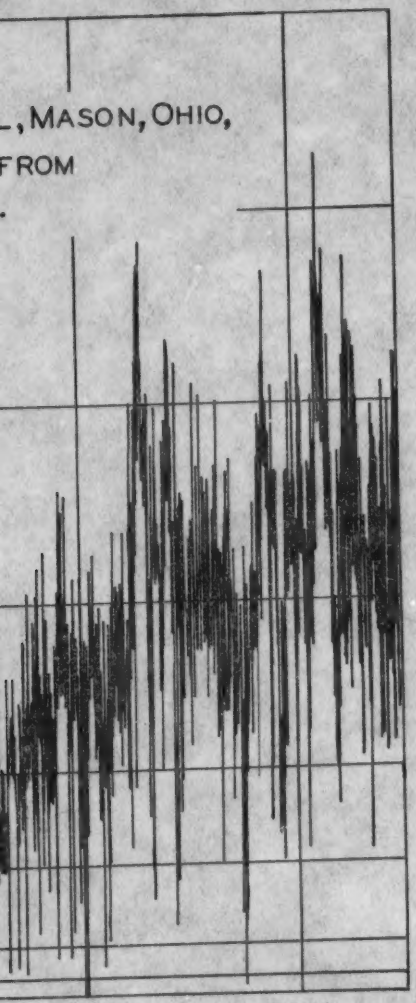

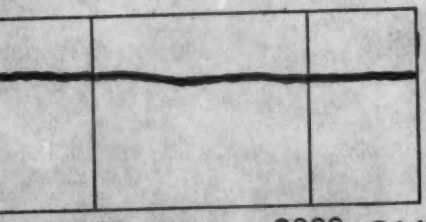

VERTICALLY

WASHINGTON, D.C.

n.

UNIV. OF MICH.

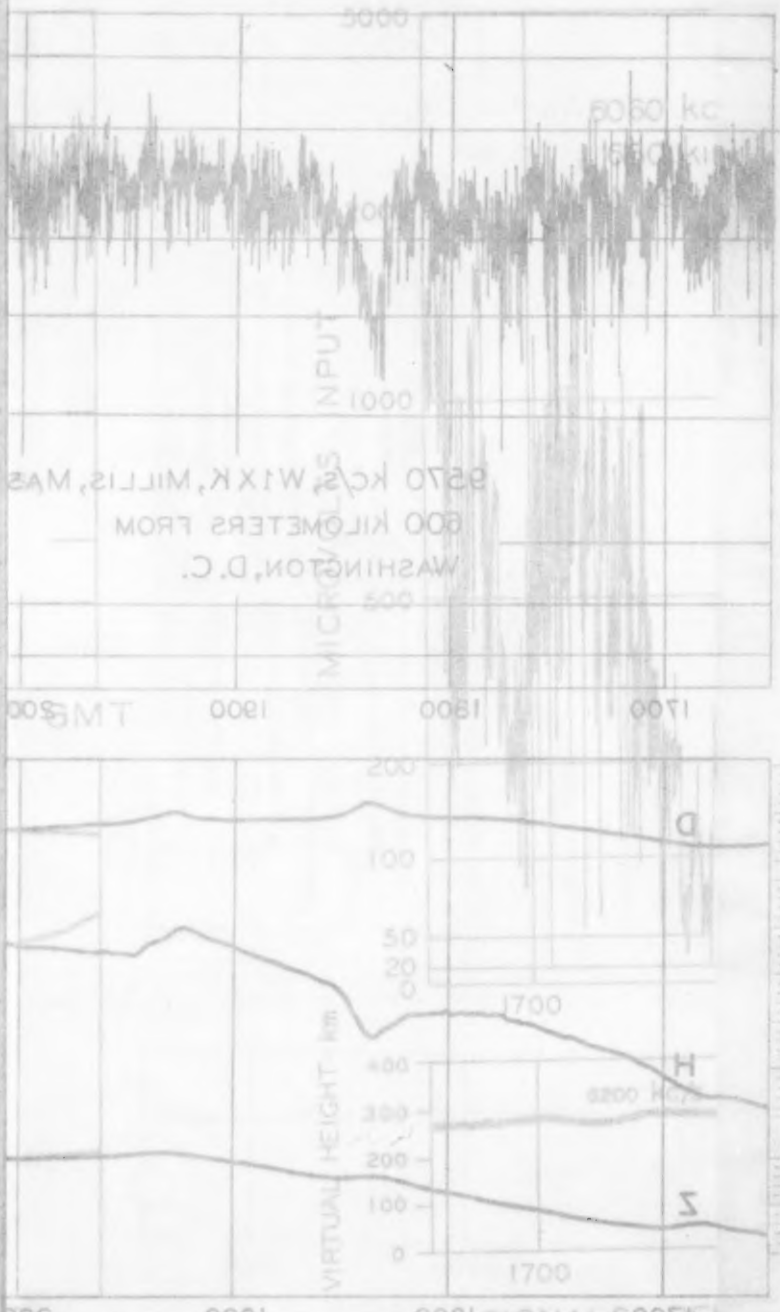

TERRESTRIAL MAGNETIC RECORD,
CHELTENHAM, MD.

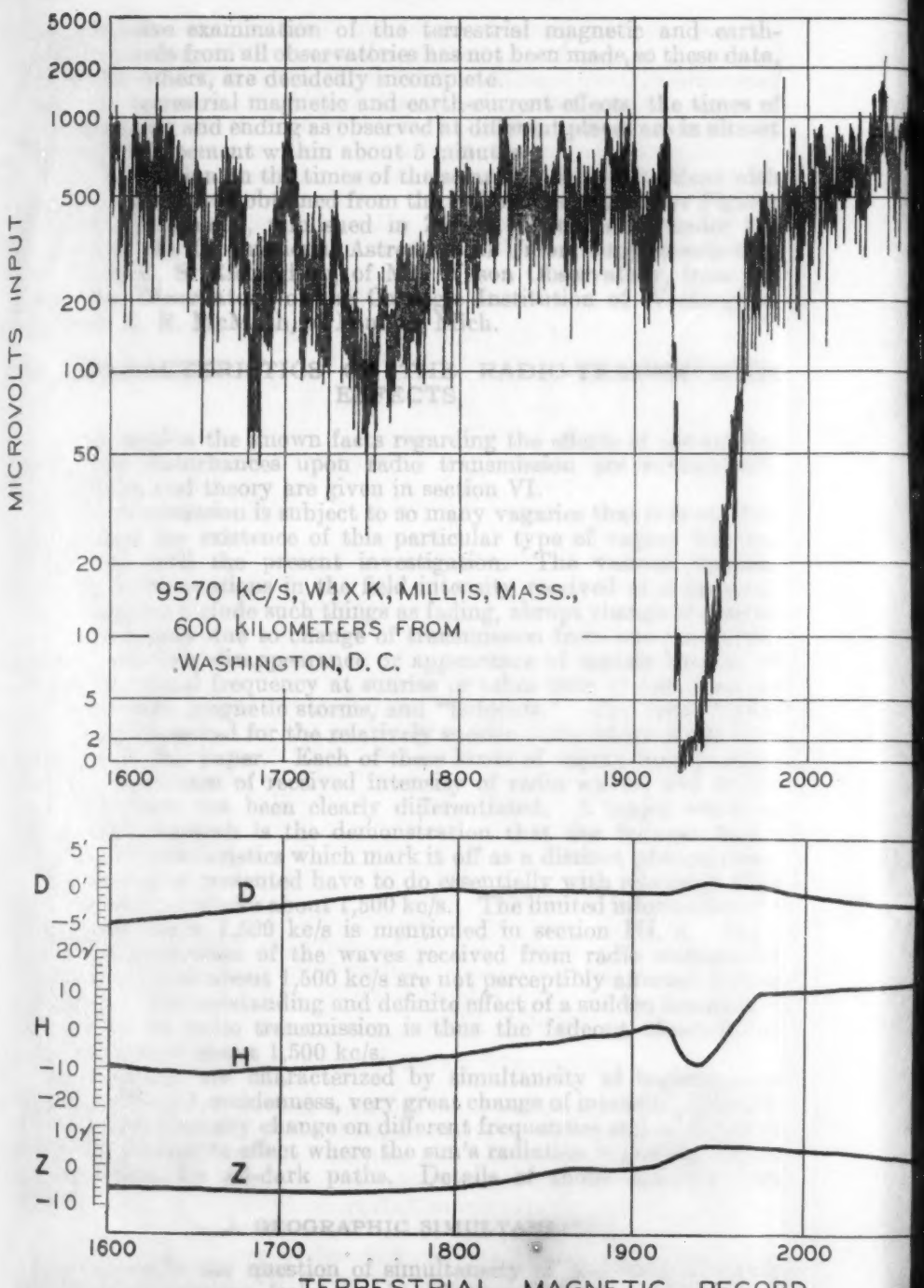

FIGURE 8.—*Sudden disturbance of the ionosphe*

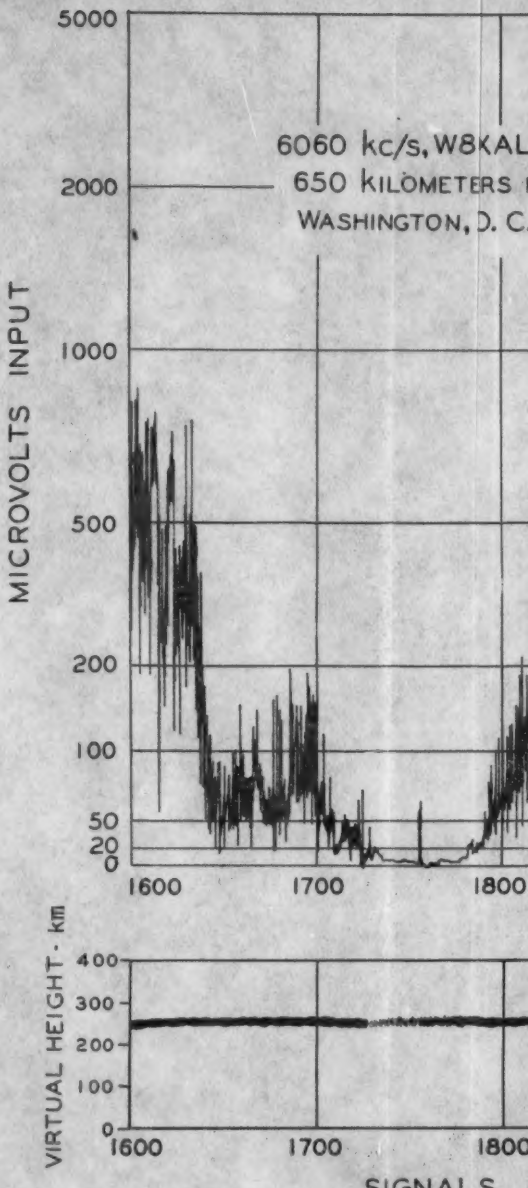

the ionosphere on November 24, 1936, as revealed by radio fadeout and terrestrial magnetic

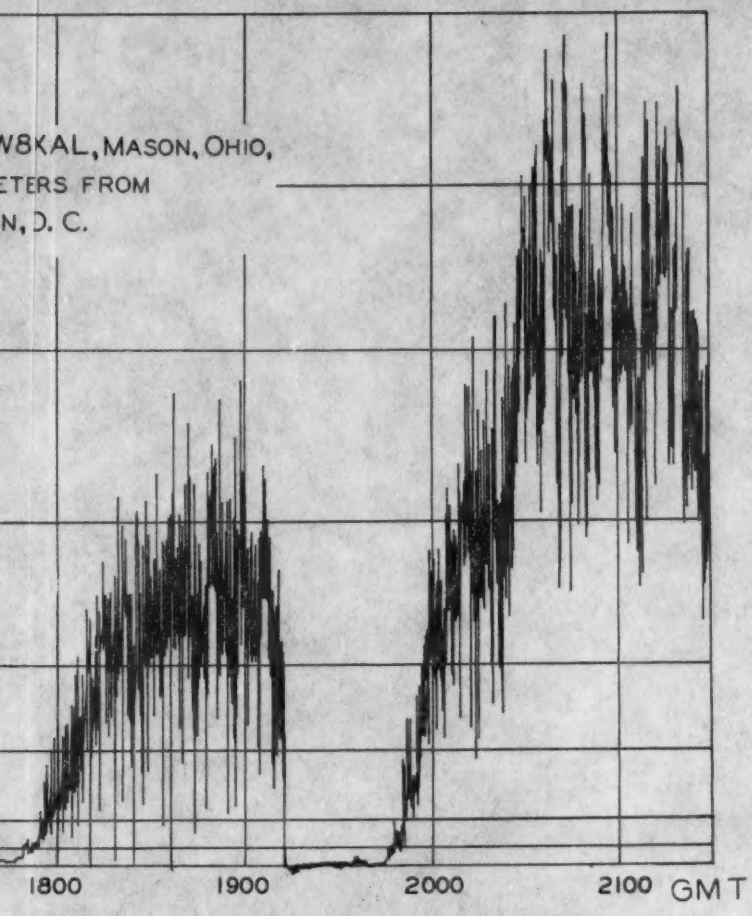

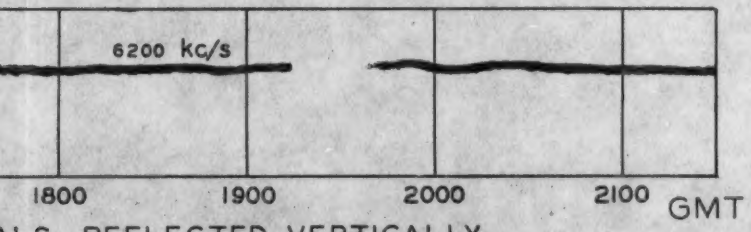

ALS REFLECTED VERTICALLY
I IONOSPHERE, WASHINGTON, D.C.

nagnetic perturbation.

UNIV. OF MICH.

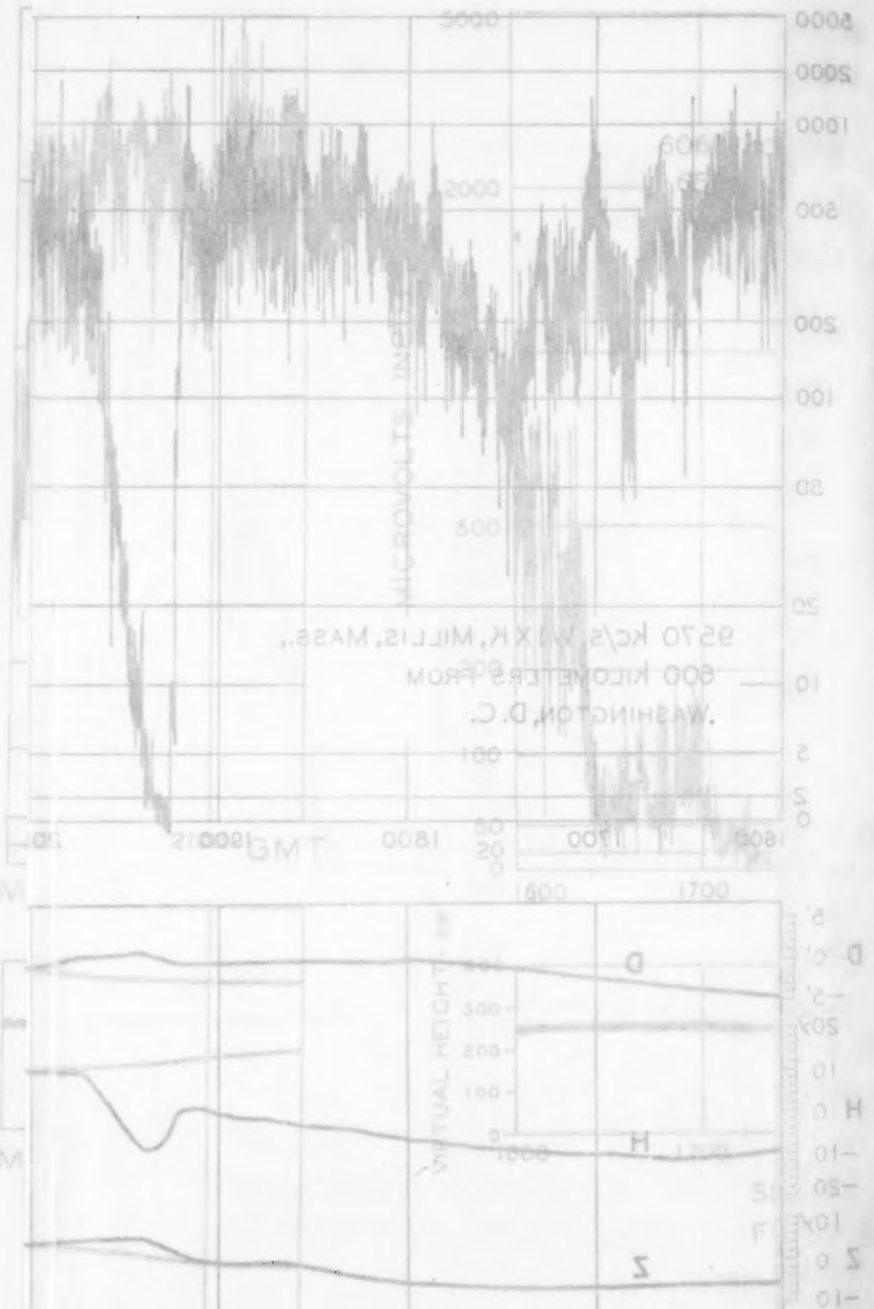

TERRESTRIAL MAGNETIC RECORD

CHELTENHAM, MD.

...as revealed by radio fadeout and...

comprehensive examination of the terrestrial magnetic and earth-current records from all observatories has not been made, so these data, like all the others, are decidedly incomplete.

For the terrestrial magnetic and earth-current effects, the times of both beginning and ending as observed at different places are in almost all cases in agreement within about 5 minutes.

The information on the times of the solar eruptions coincident with the other effects was obtained from the Bulletin for Character Figures of Solar Phenomena, published in Zurich, Switzerland, under the auspices of the International Astronomical Union, supplemented by data from R. S. Richardson, of Mt. Wilson Observatory, from the Huancayo Observatory of the Carnegie Institution of Washington, and from R. R. McMath, of Pontiac, Mich.

III. CHARACTERISTICS OF THE RADIO-TRANSMISSION EFFECTS

In this section the known facts regarding the effects of the sudden ionosphere disturbances upon radio transmission are summarized. Explanation and theory are given in section VI.

Radio transmission is subject to so many vagaries that it is not surprising that the existence of this particular type of vagary was not recognized until the present investigation. The various vagaries cause large fluctuations in the field intensity received at a distance. These vagaries include such things as fading, abrupt change of general level of intensity due to change of transmission from one ionosphere layer to another, disappearance or appearance of signals because of change of critical frequency at sunrise or other time of day, changes associated with magnetic storms, and "fadeouts." The term "fadeout" is here reserved for the relatively sudden radio effect of the type described in this paper. Each of these kinds of vagary may produce marked diminution of received intensity of radio waves, and in the past they have not been clearly differentiated. A major result of the present research is the demonstration that the fadeout has a number of characteristics which mark it off as a distinct phenomenon.

The data here presented have to do essentially with relatively high frequencies, i. e., above about 1,500 kc/s. The limited information for frequencies below 1,500 kc/s is mentioned in section III, 4. Ordinarily the intensities of the waves received from radio stations on frequencies below about 1,500 kc/s are not perceptibly affected during a fadeout. The outstanding and definite effect of a sudden ionosphere disturbance on radio transmission is thus the fadeout observed on frequencies over about 1,500 kc/s.

The fadeouts are characterized by simultaneity of beginning at all places affected, suddenness, very great change of intensity, differing duration and intensity change on different frequencies and at different distances, maximum effect where the sun's radiation is perpendicular, and no effect for all-dark paths. Details of these characteristics follow.

1. GEOGRAPHIC SIMULTANEITY

Leaving aside the question of simultaneity of the radio fadeouts with other phenomena (solar, etc.), a distinguishing characteristic of the radio fadeout is the simultaneity of its beginning at the various

places where it is observed. As shown in table 1, the beginning of a fadeout is in nearly all cases simultaneous within a few minutes. Variations of more than 10 minutes are reported in only 17 of the 118 cases, and these are probably attributable to incompleteness or inaccuracies of observation. It is likely that every fadeout began simultaneously within 3 minutes everywhere, and in many cases the simultaneity was doubtless well within 1 minute.

The time of ending of a fadeout, on the other hand, is very different at different radio frequencies, at different distances, and in different parts of the earth; this is discussed further in sections III, 4, and III, 5.

2. SUDDENNESS

The suddenness of the radio fadeouts has astonished many radio observers, operators, and amateurs. Radio signals being received at normal intensity suddenly begin to diminish and the intensity falls to zero, usually within a minute. The effect is on some occasions preceded by a short period of unusually violent fading, echoes, and noise (of a type different from atmospherics), but the effect usually comes without warning. There is sometimes also a period of violent fading, echoes, and noise (different from atmospherics) after as well as before a fadeout.

The suddenness of commencement of a fadeout is vividly illustrated by numerous reports in which the observer stated he thought that the power had gone off in the receiving station, or that a fuse had blown, or that the stations to which he was listening had stopped transmitting, or that his receiving apparatus had developed a sudden fault. Many an observer has dissected his receiving equipment on such occasions in the vain effort to determine why it suddenly went dead.

As may be seen from the examples in figures 1 to 8, the received radio-wave intensity drops from full value to zero, in most cases within a minute. In some of the more intense fadeouts, like that of February 14, 1936, shown in figure 1, the cutoff occurs within a few seconds. The duration of the effect is greater for the lower frequencies of the frequency range affected; this is discussed further in section III, 4. Sometimes the drop to zero is not quite so sudden for the higher frequencies as for the lower; this is illustrated in figure 6 (Nov. 6, 1936) and figure 8 (Nov. 24, 1936). In a few rare cases, such as the extra fadeout at 1715, November 24, 1936, shown in figure 8, the drop to zero was gradual, lasting 10 minutes or so; such a case was not one of the more intense fadeouts, and was not accompanied by a terrestrial magnetic effect.

3. DEGREE OF INTENSITY CHANGE

The sudden change of intensity in a fadeout is very great. In most fadeouts, there is a certain band of radio frequencies throughout which the intensity drops from normal value to zero. Sometimes the intensity does not drop all the way to zero for the higher frequencies; see for example figure 7 (Nov. 8, 1936). There is evidence that there is often a frequency limit above which radio transmission is merely weakened rather than reduced to zero, and sometimes a still higher limit above which radio-transmission intensity is not perceptibly reduced. Such is not always the case, however, for sometimes the sky wave intensity is reduced to zero throughout the entire high-frequency radio spectrum.

The sudden reduction of the intensity to zero when a fadeout occurs is an extraordinary experience. Not only does the radio station appear to stop transmitting, but in the more intense fadeouts even the background noise due to atmospherics "static" disappears. The impression of the observer is that reception goes dead. This enhances the effect of the suddenness of the fadeout and further impels the observer to look for trouble in his receiving equipment.

4. FREQUENCIES AFFECTED

The data on radio fadeouts indicate that they occur on all the high frequencies used for long-distance radio work, i. e., from about 1,500 to 30,000 kc/s. Reports are available on radio reception at lower frequencies during many of the fadeouts, and in nearly all cases they indicate that reception was not affected. Some automatic records made by the National Bureau of Standards indicated that the sky wave at broadcast frequencies was weakened during a fadeout. As the ground wave plays a large part in daytime transmission at broadcast and lower frequencies, and the ground wave is unaffected by ionosphere phenomena, fadeout effects would not be prominent and would tend to escape notice. In a very few cases there have been reports of a changed character of fading on broadcast or lower frequencies, or, very rarely, of an increase of intensity on the lower frequencies. Dr. R. Bureau, of France (see Reference, p. 141), has found that recorders of atmospherics on frequencies between 27 and 40 kc/s show an increase in numbers of atmospherics pulses recorded during many of the fadeouts; the times of such occurrences are given in table 1.

For the frequency range in which fadeout effects are conspicuous—i. e., from about 1,500 to 30,000 kc/s—the effects are greater on the lower frequencies. This is true in regard to the duration of the effects and the degree of intensity change. The variation of intensity change with frequency is described in section III, 3. The variation of the duration of a fadeout with frequency is illustrated in figures 1 to 8.

As shown in the figures, the beginning of a fadeout is simultaneous on all frequencies. This simultaneity is exact in most cases, and where not exact the times of beginning seldom differ more than 2 or 3 minutes and the effect occurs first on the lower frequencies. As also shown conspicuously in the figures, the duration or time of ending of a fadeout is very different on different frequencies. The time during which the received intensity is zero, and the time of recovery to normal intensity, are both greater the lower the frequency, other factors being the same. Interpretation of the variation of the effect with frequency in particular cases is complicated by the variation of the effect (discussed in next section below) with geographic location of the radio-transmission paths affected, and also by the variation with distance of transmission. Since, in long-distance transmission, the waves travel a much longer path through the lower ionosphere, the effects are greater for long distances than for short distances. Thus, a fadeout for a long-distance transmission path, on a given frequency, will have a greater reduction of intensity and a greater duration than for a short-distance transmission path. Expressed otherwise, the fadeout effects for a long-distance path correspond to those at a lower frequency for a short-distance path. Bearing this

in mind, the variation of fadeout effects with frequency is consistent in the figures and in all known fadeouts. H. A. G. Hess reported that during the intense fadeout of Nov. 6, 1936, which happened to occur during a time when long-distance transmission on 40,000 kc/s was possible, there was no diminution in transatlantic reception on about that frequency. This fadeout was not as intense as some others. As far as known, during the most intense fadeouts all high-frequency sky waves fail.

It is found, and it is consistent with the foregoing conclusion, that fadeouts which last longer are usually observed up to higher frequencies than those of shorter duration; where the duration is short, the higher frequencies are less affected. This is illustrated by a comparison of figure 1 and figure 7.

5. GEOGRAPHIC DISTRIBUTION

All of the fadeouts known to date, listed in table 1, have the characteristic discovered by the author in 1935 for the fadeouts then known, that they occur throughout the hemisphere illuminated by the sun and not in the dark hemisphere. More precisely stated, whenever a radio fadeout occurs some part of the radio-transmission path is in the daylight hemisphere. The continuous automatic recorders of the National Bureau of Standards, recording the field intensities of domestic stations and the normal-incidence ionosphere reflections, have detected no fadeouts between sunset and sunrise. Since many other observers throughout the world have been watching for the effects, the lack of any reports whatever of disturbances on all-dark paths may be taken as proof of their nonoccurrence. For many of the times when radio fadeouts were reported, there have also been specific reports from the dark hemisphere that radio transmission was unaffected. Sometimes a fadeout is reported as observed at a place where it is dark, but in every such case the fadeout occurs only on radio transmission paths which are partly in the hemisphere illuminated by the sun. Thus, fadeouts have in a few cases been observed at midnight in certain places, without violating this principle. Conspicuous examples are: Argentina, 0400 GMT April 2, 1936; California, 0728 GMT May 28, 1936; England, 0016 GMT July 31, 1936.

A study has been made to determine more specifically the variation of intensity of the effect with latitude, longitude, and direction. It is found that the effects are most pronounced in localities where the sun's radiation is perpendicular to the earth's surface. Thus they are most intense in the equatorial regions and diminish with increasing latitude. Similarly, they are most intense at longitudes where it is noon and diminish in both directions toward longitudes where it is night. These relations are true in respect to the suddenness of beginning of the radio fadeout, the time it lasts, the upper limit of frequency affected, and the degree of reduction of field intensity. A fadeout which, at the place where the sun's radiation is perpendicular, may be very intense and prolonged, may, for the same frequency, be a mere brief reduction of field intensity near the boundary of the illuminated hemisphere.

Variations with direction have not been completely analyzed, but they appear to be consistent with the foregoing relations. For example, at receiving points in the United States, reception from stations

in the southern hemisphere usually exhibits greater effects than reception from other directions (because of passing the equatorial regions). Similarly, a disturbance occurring in the morning usually exhibits greater effects in reception from the east than from the west, and vice versa for the afternoon (because of passing the region where it is noon).

Interpretation of particular cases is complicated by the variation of the effect with the radio frequency and distance.

IV. CHARACTERISTICS OF THE TERRESTRIAL MAGNETIC AND EARTH-CURRENT EFFECTS

In this section the known facts regarding the effects of the sudden ionosphere disturbances upon terrestrial magnetism and earth currents are summarized. The phenomena are explained in section VI.

In many respects the terrestrial magnetic and earth-current effects have the same characteristics as the radio transmission effects. These similar characteristics include geographic simultaneity, suddenness, limitation of occurrence to the illuminated hemisphere, and the same variation of intensity of effect with latitude and longitude. They are similar also in being only one among the many types of vagaries of terrestrial magnetism and earth currents, such as diurnal and seasonal variations, irregular fluctuations, and magnetic storms (i. e., times of violent magnetic fluctuation). Also, as in radio, the effects due to the sudden ionosphere disturbances have in the past not been recognized as something different from the other classes of vagaries; this study has shown that they have characteristics which mark them off as a distinct and separate type of magnetic perturbation.

1. LIMITATION TO ILLUMINATED HEMISPHERE

The data on terrestrial magnetism in table 1 are based principally on the magnetograms of the Cheltenham, Md., Observatory of the U. S. Coast and Geodetic Survey. These magnetograms were examined for the times of all the radio fadeouts. In a few cases data were available from the records of other observatories. In the more intense fadeouts, magnetic effects occurred simultaneously everywhere throughout the sun-illuminated hemisphere. In none of them did effects occur in the dark hemisphere.

The data on earth currents are highly fragmentary, as no systematic examination of earth-current records was made. The few entries of earth-current effects in table 1 are based on occasional reports to the author by various collaborators. The phenomena of earth currents and terrestrial magnetism are so closely interrelated that very probably earth-current effects occurred whenever there were perturbations of terrestrial magnetism.

2. SIMULTANEITY WITH RADIO FADEOUTS

Typical examples of the terrestrial magnetic effects are shown in figures 1 to 8, in which a few Cheltenham magnetograms are reproduced. The magnetic pulses, when they occur, are simultaneous with the radio effects, indicating that both are manifestations of an ionosphere change. As indicated in the table, the magnetic pulses occurred during many of the radio fadeouts but not all. The suddenness and the duration of the pulses may be judged from figures 1 to 8.

3. GEOGRAPHIC DISTRIBUTION

The geographic distribution of intensity of the terrestrial magnetic effects is, so far as the limited data indicate, the same as for the radio fadeouts. That is, they are most pronounced in the vicinity of that region of the earth's surface to which the sun's radiation is perpendicular, and diminish to zero near the boundary of the illuminated hemisphere. Thus the effects are greatest at low latitudes, and at longitudes where it is noon. They do not commonly occur in the night hemisphere.

4. COMPARISON WITH MAGNETIC STORMS

The geographic distribution of intensity of the effects is strikingly different from that of terrestrial magnetic and earth-current effects hitherto known. For example, a world-wide magnetic storm is characterized by a "sudden commencement", a pulse which is simultaneous over the whole earth. The magnetic storms and their sudden commencements thus differ markedly from the magnetic effects associated with sudden ionosphere disturbances in respect to distribution in longitude, since the latter occur only in the sun-illuminated hemisphere.

The two phenomena differ even more extraordinarily in respect to their distribution in latitude. Magnetic storms have minimum effects at the equator and maximum effects near the magnetic poles, just the opposite of the effects of sudden ionosphere disturbances. An interesting consequence of this is that the magnetic and earth-current pulses due to the sudden ionosphere disturbances are much more striking when observed in equatorial regions than in high latitudes. They may be of the same order of magnitude as the fluctuations caused by magnetic storms in equatorial regions, relatively small in middle latitudes, and negligible in high latitudes.

Besides these differences in the geographic distribution of the effects, magnetic storms and the sudden ionosphere disturbances differ in duration, the former lasting hours or days instead of the brief period of the latter.

A study has been made to determine whether there is any relation between times of occurrence of magnetic storms and the sudden ionosphere disturbances. None has been found, and the occurrence of each appears to be quite random with respect to the other. Sudden ionosphere disturbances usually occur during magnetically quiet times, but some occur during magnetic storms. In studying this subject, caution should be observed to consider the results observed at a number of different locations in order to be sure that an apparent effect of the sudden type really is one. Observations of the effect at a single location are often hard to distinguish from other types of vagaries.

One of the major results of this research is the discovery of a separate type of terrestrial magnetic disturbance, with remarkable characteristics which clearly differentiate it from magnetic storms or any previously known types of magnetic perturbations. This is analogous to the discovery of the fadeout as a distinct type of radio vagary.

V. SOLAR PHENOMENA ASSOCIATED WITH SUDDEN IONOSPHERE DISTURBANCES

In this section the known facts regarding solar phenomena having a bearing on the sudden ionosphere effects are summarized. Explanation and discussion follow in section VI.

1. EXACTNESS OF SIMULTANEITY

The times of the solar eruptions known to have occurred at the times of the sudden ionosphere disturbances are given in the last column of table 1. They were simultaneous in the sense that the reported time of the solar eruption overlapped the time of the sudden ionosphere disturbance.

The times stated for the solar eruptions are in most cases uncertain by many minutes. This is because of difficulties in their observation. They are sometimes seen with difficulty, and the observing astronomer can not be sure when a solar disturbance begins or ends. They are often obtained by photographs which may be taken at intervals of 15 minutes or more, so that the time of a phenomenon indicated by a difference between two successive photographs may be uncertain.

Because of the uncertainties of their observational material, different astronomers adopt different criteria. The conditions of seeing (presence of haze, etc.) are also different at different observatories at any one time. It results that different solar observers differ considerably in the times they report for the beginning and end of solar eruptions. For example, the solar eruption of August 5 listed in the table was reported by Mount Wilson Observatory as ending at 1613 and by Zurich Observatory as ending at 1648. As another example, the eruption listed for August 28 was reported by Zurich Observatory as ending at 1030, and was reported by Greenwich Observatory as still in progress at 1130. Likewise, an eruption was reported by Zurich Observatory as having begun on July 4, 1936, at 1655, and the same eruption was reported by Mount Wilson Observatory as having begun at 1707. These cases were all major eruptions, more easily visible than most solar eruptions. It is evidently impossible to determine the times of solar changes within a small number of minutes.

The lack of precision of the solar data thus makes it impossible to say how close is the correspondence of times of the solar eruptions and the terrestrial effects. All of the cases listed in table 1 may reasonably be described as simultaneous occurrences within the limits of our knowledge.

2. PROPORTIONATE NUMBER OF SIMULTANEOUS OCCURRENCES

Of the 118 ionosphere disturbances listed in the table, 59 (exactly half) are shown to have been coincident in time with solar eruptions. There may have been a much larger proportion than shown. The sun is not under continuous observation and hence it is not known whether a visible solar eruption occurred or not at the time of any ionosphere disturbance for which no solar eruption is reported. Most solar observatories have in the past carried on observations for not more than an hour each day. An arrangement is in effect by which observatories in different parts of the world stagger their times of observation with a view to a continuous watch on the sun. Cloudy weather and other conditions, however, prevent the full attainment of this program.

On the other hand, however, when we examine the solar records in the Bulletin for Character Figures of Solar Phenomena, we find that many solar eruptions occur when no ionosphere disturbances are known to have occurred. For example, from January to June 1936, the above mentioned bulletin lists 302 solar eruptions, and only 29 of these were simultaneous with known disturbances of the ionosphere. A larger proportion of coincidences is found if we consider only the more intense solar eruptions (those of arbitrary intensities 2 or 3); there were in the same period 69 of these listed, of which 17 were simultaneous with known disturbances of the ionosphere. It is probable that many of the visible solar eruptions were not accompanied by detectable ionosphere disturbances, although the converse may not be true. Many of these eruptions may rise high enough in the solar atmosphere to permit the escape of visible light but not high enough to permit the escape of the ultraviolet radiation responsible for the sudden bursts of ionization in the earth's atmosphere. The use of automatic radio and magnetic recorders continuously has assured knowledge of the occurrence of practically all ionosphere disturbances in the western hemisphere.

3. CHARACTER OF ERUPTIONS

The eruptions here discussed are bright chromosphere eruptions. They are visible as sudden increases of brightness of large bright patches on the sun's surface, and when occurring at the limb of the sun are seen as eruptive prominences. An eruption usually, but not always, takes place near an active sunspot group. Most of the eruptions simultaneous with sudden disturbances of the ionosphere are much brighter than the average.

4. LOCATION OF ERUPTIONS ON SUN

It is of interest to know whether the eruptions causing sudden ionosphere disturbances occur wholly or predominantly at any particular location on the sun's surface. It might be thought, for instance, that the radiation would be effective only when projected radially from the sun to the earth, i. e., when the eruptive area is in the center of the sun's disk. The solar locality of all the visually observed eruptions simultaneous with sudden ionosphere disturbances is known, and has been examined in this connection. It is found to be random, which means that the eruptions send out their radiations in all directions from the sun's surface; the terrestrial effects occur regardless of where the eruption takes place, near the sun's limb, at or near the center of the disk, or anywhere between.

The locations of the eruptive areas on the sun have also been examined to find out whether particular areas give rise to repeated effects, and especially whether such effects are repeated after one or more rotations of the sun. On a number of occasions, successive eruptions from a given solar area, accompanying sudden ionosphere disturbances, have occurred in the course of a day or two. Little evidence, however, has been found of any repetition of eruptions from a particular area after one or more rotations of the sun.

5. RECURRENCE TENDENCY

A possible periodic tendency in the times of occurrence of the sudden ionosphere disturbance was suggested by the occurrence of the ones first known to the author, and listed first in table 1, at intervals of approximately 55 days. This is shown graphically in figure 9, in which all the occurrences are plotted. The intensity of each occurrence was weighted on an arbitrary basis, having regard to the duration and magnitude of the effect, the number of places from which reported, etc. The intensities thus weighted by two persons independently agreed very well and were plotted as ordinates on an arbitrary scale in figure 9. The abscissas are time, each

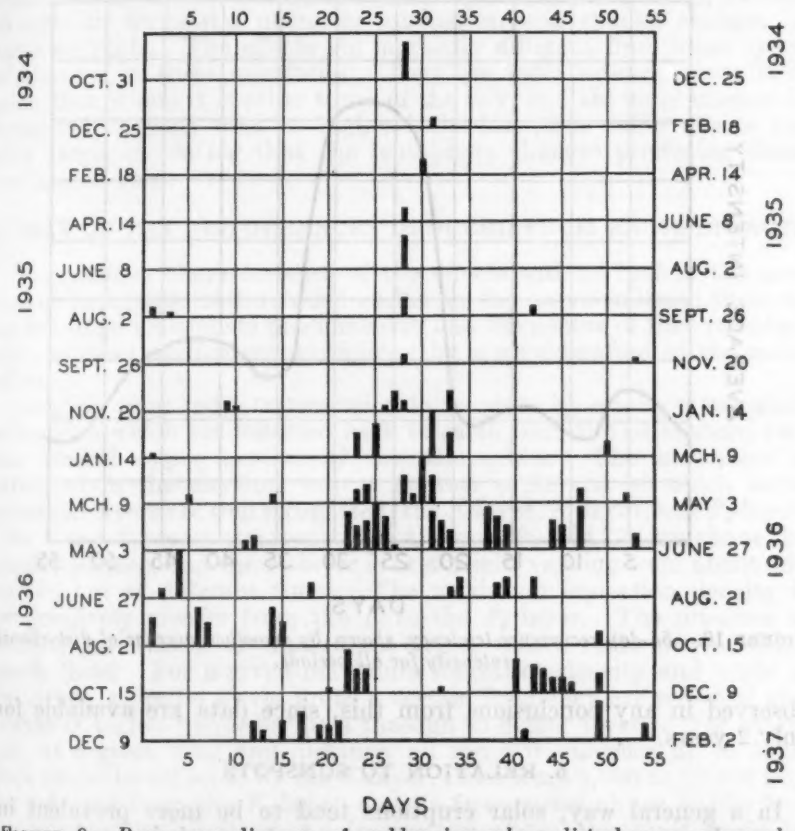

FIGURE 9.—*Recurrence diagram of sudden ionosphere disturbances, arranged in 55-day periods; intensity of disturbance is approximately indicated by ordinate.*

horizontal line being an interval of 55 days. In figure 10 is plotted an average curve for all the 55-day periods. The existence of a 55-day recurrence tendency is indicated. This should not be taken as proved, as 2 years is not considered to be a sufficient time to establish such a tendency with certainty. It may be mentioned that the 55-day recurrence tendency remains very marked even if the first seven cycles, in which it is so pronounced, be disregarded. Further analysis has indicated that the recurrence tendency averages slightly less than 55 days, but it is closer to 55 than 54.

It is of interest that there is no indication of a recurrence tendency of the order of 27 days. The sun rotates on its axis in a remarkable way, rotating faster at the equator than elsewhere. The rotation period is about 24 days at the sun's equator and about 36 days near its poles. The average rotation period of the portion of the sun in which the eruptions take place, and also incidentally the period for which terrestrial magnetic disturbances show a recurrence tendency (presumably dependent upon some unidentified type of solar eruptions), is between 27 and 28 days. Thus the tendency to a recurrence period of 55 days, of the ionosphere disturbances, is twice the well-known solar period of approximately 27 days. Again, caution should be

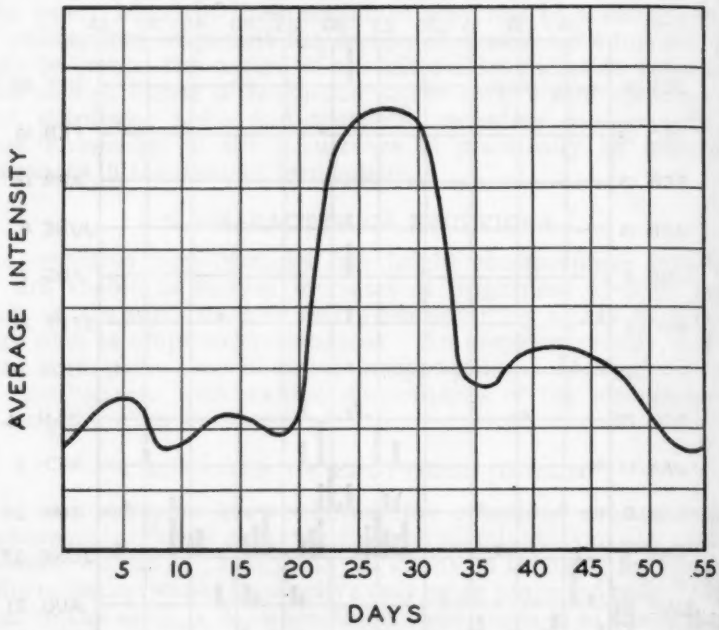

FIGURE 10.—*55-day recurrence tendency, shown by smoothed average of disturbance intensity for all periods.*

observed in any conclusions from this, since data are available for only 2 years.

6. RELATION TO SUNSPOTS

In a general way, solar eruptions tend to be more prevalent in years when sunspots are more numerous, and thus their number may be expected to wax and wane in an 11-year cycle with the sunspots. There is no evidence, however, of any short-time correlation with sunspot numbers of the sudden ionosphere disturbances or the particular solar eruptions accompanying them. The number of sudden ionosphere disturbances certainly does not vary from day to day, or from month to month, in accordance with the sunspot numbers. Data are not available over a long enough time to permit a conclusion as to whether there is any correlation of yearly averages.

VI. DISCUSSION AND EXPLANATION

The foregoing facts clearly outline a phenomenon which is some type of sudden change somewhere in the ionosphere. Whenever the phenomenon occurs, it is most intense in that region of the earth where the sun's radiation is perpendicular and diminishes to zero at the outer edge of the illuminated hemisphere. Its onset usually occurs within a minute, and is simultaneous throughout the hemisphere affected. Its various effects begin simultaneously, and last from about 10 minutes to several hours, the occurrences of greater intensity in general producing effects of longer duration. The effects include the sudden blotting out of high-frequency radio sky-wave transmission, sudden changes in low-frequency atmospherics, sudden changes in terrestrial magnetic intensities, and sudden changes in earth currents. The effects are markedly different from other types of changes in these quantities. They are more intense where it is noon than where it is other times of the day, and are more intense in equatorial regions than in higher latitudes. The radio effects are very large, indicating that the ionosphere changes producing them are intense ones.

1. SEAT OF THE DISTURBANCES DEDUCED FROM RADIO EFFECTS

The various characteristics of the effects summarized in the preceding paragraph and detailed earlier in the paper indicate them to be due to an ionosphere phenomenon; and the nature of that phenomenon is more particularly elucidated by a consideration of the radio effects.

Long-distance radio transmission takes place by means of so-called sky-waves which are reflected back to earth from the ionosphere, i.e., the ionized upper portion of the atmosphere. The ionization is stratified in the daytime into a number of layers, of which three principal layers are well recognized; the E-layer, F_1-layer, and F_2-layer. The E and F_1 layers are, respectively, about 120 and 220 km above the earth's surface, and the F_2-layer is at a height varying from about 250 to 400 km at different times. The maximum ionization density is progressively greater from the E to the F_2 layer. The presence of ionized particles of air makes the layers reflect radio waves which reach them. For a given maximum ionization density and angle of incidence, all radio waves up to a certain frequency are reflected and waves of higher frequency pass through to higher layers. For example, at a given time and distance, all radio frequencies up to 9,000 kc/s might be reflected by the E-layer, those from 9,000 to 30,000 kc/s be reflected from the F_2-layer, and no frequencies above 30,000 kc/s be reflected at all (i. e., no frequencies above this limit could be received over the distance considered).

An increase in the maximum ionization density of a layer raises the upper limit of frequency of radio waves which it can reflect. During a number of the sudden ionosphere disturbances measurements or recordings were in progress to determine this upper limit of frequency for the several layers, E, F_1, and F_2. In no case was an appreciable change observed during or just after the disturbance. (It is possible to speak of radio observations being in progress during a fadeout because there were usually some frequencies, distances, or locations for which radio transmission continued, while for others the radio

transmission was annihilated—see section III). It may be concluded that the sudden ionosphere disturbances change the maximum ionization density of the E, F_1, or F_2 layers either not at all or very slightly.

On the other hand, ionosphere studies have amply proved that an increase in the ionization density of a region *through* which radio waves pass on the way to being reflected by a higher layer causes an increase in absorption of the radio waves' energy and results in a diminution of the received wave intensity. This is exactly what happens, and, indeed, to a striking degree, during one of the sudden disturbances.

It may therefore be concluded that these sudden disturbances involve a sudden great increase of ionization in some region through which radio waves pass on the way to being reflected by a higher region. Since the fade-out occurs in radio waves reflected by the E as well as the higher layers, the absorbing medium must be below the E-layer.

The seat of the sudden large increase of ionization is thus below the E-layer, i. e., lower than 120 km above the earth's surface. The E-layer is thus not the lowest part of the ionosphere. This is in harmony with some other facts which have been discovered recently. It is now known that waves of broadcast and lower frequencies are propagated in the daytime at certain seasons by reflection from a layer lower than the E-layer. This was discovered[5] by observation of the changes in the characteristics of received waves near sunset and sunrise, showing a change from E-layer at night to a lower layer in the daytime and back to the E-layer at night.

This low layer may perhaps be called the D-layer. Not enough is yet known about it to be sure that this designation is appropriate. There may be several layers acting, whose combined effect we observe, or one or another of them may predominate at different times. Or the effective layer may more or less merge into the E-layer. With our present limited knowledge it is perhaps as well to think tentatively of a single low layer or region in which low-frequency transmission takes place, and in which the sudden ionosphere disturbances occur.

For low frequencies (below about 1,500 kc/s), a sudden ionosphere disturbance does not produce as complete a fadeout as at higher frequencies, because radio waves tend to be reflected by, instead of passing through, the layer in which the sudden increase of ionization occurs. Indeed, the sudden increase of ionization may even tend to increase rather than decrease the very low-frequency radio-wave intensity; this is in harmony with the results of R. Bureau on low-frequency atmospherics (30 to 40 kc/s).

For frequencies above about 1,500 kc/s, the ionization of the low layer is ordinarily not great enough to reflect the waves. They pass through and are reflected from the E or higher layers where the ionization density is greater. When the sudden increase of ionization in the low layer occurs, however, the ionization suddenly becomes great enough to produce large absorption of the radio-wave energy and a fadeout occurs. There is less interchange of energy between the ions and the radio waves, the higher the frequency, and therefore for very high frequencies the fadeout effects are less pronounced; this in accordance with experience, as described in section III and illustrated in

[5] Smith and Kirby, Critical frequencies of low ionosphere layers, Phy. Rev. **51**, 890 (May 15, 1937).

figures 1 to 8. It is also clear from this conception why the effects on a given frequency for normal-incidence transmission are the same as the effects on a much higher frequency for grazing-incidence transmission: the waves at grazing incidence travel a much longer path through the abnormally ionized layer and thus experience an added amount of energy interchange with the ions, thus compensating for their higher frequency.

The source of the sudden ionization changes must be outside the earth, and therefore has to come through the E, F_1, and F_2 layers. It must have a character, therefore, distinctly different from the source of ionization of those layers. It produces its effect at a level where the air density is great enough to insure numerous collisions of moving ions and hence rapid absorption of the radio-wave energy. The radiation producing this effect is therefore of a type which can penetrate the better known higher layers and produce ionization where the mean free path is shorter than at the higher levels. The effect must be produced by a very sudden burst of very penetrating radiation, which reaches and ionizes a level of the atmosphere where the air density is great enough to insure rapid recombination of the ions as well as rapid absorption of the energy of radio waves reaching such region. This explains the great reduction of the radio-wave intensity and the short duration of the effect, as well as the suddenness of the drop of radio intensity.

The recombination proceeds so fast that the ionization and the ionizing energy are probably very nearly in equilibrium at all times. As the ionizing radiation from the sun dies out, in accordance with the disappearance of the solar eruption, the intense ionization in the lower ionosphere wanes, and the highest radio frequencies affected are soon freed of its effects. As the ionization diminishes, lower and lower frequencies recover from the effects. The duration of a fadeout at a given frequency is probably dependent not only on the intensity of the burst of ionizing energy but also on the duration of the solar eruption.

2. MAGNETIC EFFECTS

The occurrence of the sudden ionization being thus inferred and explained from the radio effects, it is clear why simultaneous changes are sometimes observed in terrestrial magnetism and earth currents. Both of the latter phenomena are due in part to the motion or drift of ions in the earth's atmosphere, constituting in the aggregate vast currents whose associated magnetic field constitutes a portion of the earth's magnetism and whose fluctuations account for the variations in terrestrial magnetism and earth currents. When a sudden ionosphere disturbance of the type here considered takes place, the sudden increase in ionization permits a simultaneous sudden change in net current flowing and thus perturbations in terrestrial magnetism and earth currents. It is to be noted that such perturbations do not depend entirely on the amount of the ionization, as do the radio effects, but involve also drift or motion of the ions. The radio effects are therefore not always accompanied by magnetic and earth-current perturbations. Whether the latter become observable or not depends on the complicated circumstances of the earth's magnetism at various places and times. When observed, they share the characteristics of the radio effects and the acting cause in the ionosphere, i. e., simul-

taneity throughout the portion of the earth affected, absence in the dark hemisphere, suddenness, and maximum intensity where the sun's radiation is perpendicular.

As previously stated, this type of perturbation of terrestrial magnetism and earth currents is strikingly different from the perturbations associated with "magnetic storms." Radio effects have shown that during magnetic storms the ionization density of the highest layer of the ionosphere (F_2 layer) is reduced and the ionization is diffused rather than sharply stratified. These effects thus prove that at least part of the phenomena of magnetic storms have their seat in the F_2 layer.[6 7 8]

It has here been shown, on the other hand, that the sudden ionosphere disturbances have their seat below the E-layer, and the phenomena causing the terrestrial magnetic and earth-current perturbations associated therewith must therefore also have their seat below the E layer.

Thus the two kinds of magnetic phenomena arise in entirely different portions of the ionosphere, in entirely different ways, and are probably due to ionizing agents of different characteristics. We thus have a new tool for analysis of the characteristics of terrestrial magnetism and for determination of their causes. There has hitherto been little known as to the locations of the vast ionosphere current systems which cause the fluctuations of terrestrial magnetism. The new possibility of localizing the levels in which different types of perturbations originate will aid in deciding between rival theories of terrestrial magnetism and should do much to bring to light the hitherto unknown mechanisms of terrestrial magnetic variations.

3. SOLAR SOURCE

The sun is in an extremely turbulent state, and on it occur frequent eruptions from which are emitted radiations having a great range of wave lengths. There is no reason to doubt that some of the radiations from some of these eruptions are the sudden bursts which cause the sudden disturbances of the ionosphere of this planet. This is strongly indicated by the numerous observations of such eruptions and ionosphere disturbances coinciding in time.

The lack of occurrence of an ionosphere disturbance during every visible solar eruption does not at all vitiate the idea of a causal relation, because many different kinds of radiation are emitted in solar eruptions and visible radiation is not the kind which affects the ionosphere. The existence of visible solar effects during the solar cataclysms which cause the ionosphere disturbances is fortuitous. The simultaneous occurrence of an ionosphere disturbance and the flare of light which makes the solar eruption visible indicates that the radiation causing the ionosphere disturbance travels to earth with the velocity of light. As shown above, the radiation which causes the sudden large increase of ionization of a low region of the ionosphere is of a very penetrating type; it is therefore electromagnetic radiation of frequency far above visible light.

[6] S. S. Kirby, T. R. Gilliland, E. B. Judson, and N. Smith. *The ionosphere, sunspots, and magnetic storms.* Phys. Rev. **48,** 849 (1935).
[7] S. S. Kirby, T. R. Gilliland, N. Smith, and S. E. Reymer. *The ionosphere, solar eclipse, and magnetic storms.* Phys. Rev. **50,** 258 (1936).
[8] S. S. Kirby, N. Smith, T. R. Gilliland, and S. E. Reymer. *The ionosphere and magnetic storms.* Phys. Rev. **51,** 992 (1937).

This doubtless gives the explanation why not all visible solar eruptions cause ionosphere disturbances. Evidently some eruptions emit the particular type of radiation which penetrates to the region below the E layer and ionizes it, and some do not.

The ionosphere disturbances and their associated effects are the only known means of detecting the causative solar radiation, because this radiation can not penetrate the relatively dense lower atmosphere and reach the earth's surface and thus can not be directly detected by any instrumental means. We have thus come into possession of a means of studying a new class of invisible solar radiation, not hitherto accessible to detection or measurement.

The results of this research prove conclusively that ultraviolet radiation from the sun can cause terrestrial magnetic fluctuations. Dr. E. O. Hulbert has advocated similar ideas in numerous papers during the past 10 years.

Ionosphere phenomena should be of very great value in increasing our knowledge of the sun. The ionization phenomena of the F_2 layer are decidedly different from those of the E layer, and there may thus be differences in the causative radiations for the two layers. Certain effects in the F_2 layer, associated with magnetic storms, may be caused by a different type of radiation. As we have seen, the radiation causing the sudden ionosphere disturbances is of still different character. All of these classes of radiation can be studied only by their ionosphere effects, as they do not penetrate down to the earth's surface. Ionosphere phenomena, as detected by radio, terrestrial magnetic, and earth-current effects, thus become the unique means by which we can study various classes of radiation from the sun.

The physical nature of the sun is extremely interesting and presents many mysteries. One of the chief mysteries is the eruptions. Little is known about the precise relation of the eruptions to sunspots or about the cause of either. The sun is a rotating sphere of very hot gas, and a sunspot is a vortex resulting from a great cataclysmic change in a portion of the sun. A sunspot lasts from a few days to a few months. The sudden eruptions, usually lasting only a few minutes, commonly occur during the early stages of a neighboring sunspot group; they may be connected with the process which gives birth to sunspots. This process is thought by astronomers to be the sudden formation of vast quantities of helium from hydrogen by the combination of four hydrogen atoms to form one of helium, with great energy liberation. Determination of the wave lengths of the radiation accompanying sudden pulses which occur during this process should aid in further identifying its nature and the obscure cause within the sun. Such determination is among the possibilities of future study of the sudden ionosphere disturbances. The duration of some of the phenomena during eruptions may also be learned through this study.

Another aspect of the sudden ionosphere disturbances, which is worthy of study in connection with solar phenomena, is the time grouping of the disturbances. As shown in figure 9, the major disturbances showed a very marked 55-day recurrence tendency from November 1934 to May 1936, then in May and June 1936, there was an extraordinary outburst of them, after which there were relatively few of them for several months.

A study of the solar circumstances of the eruptions accompanying such disturbances, and the possible future determination of the wave

lengths of the solar radiation associated with them, may eventually elucidate the nature of the eruptive processes within the sun and the causes of sunspots.

The work here reported has been in large measure a world-wide cooperative study. Many individuals and organizations have sent me reports of their observations of various aspects of the sudden disturbances of the ionosphere as they occurred.

The most consistent source of data has been the continuous records of field intensity of high-frequency stations, and the records of ionosphere phenomena, made by my colleagues in the National Bureau of Standards, S. S. Kirby, N. Smith, T. R. Gilliland, and S. E. Reymer.

Dr. R. Jouaust, of the Laboratoire Central de Radioélectricité, France, and the author have regularly interchanged data during this study. Dr. Jouaust has compiled and distributed comprehensive bulletins of data on the radio fadeouts, principally as observed in Europe. These were forwarded from the French National Committee to the other National Committees of the International Scientific Radio Union, and this service is being continued.

The Carnegie Institution of Washington has collaborated in the supplying of solar and terrestrial magnetic data. In particular, Dr. R. S. Richardson, of the Mount Wilson Observatory, California, has cooperated with the author through the supplying of information monthly on solar eruptions.

The Coast and Geodetic Survey has assisted by supplying copies of its daily magnetograms made at its terrestrial magnetic observatory at Cheltenham, Md.

Regular reports on radio fadeouts as observed during the handling of radio-communication traffic have been furnished by:

H. H. Beverage, chief research engineer, RCA Communications Inc.
H. Pratt, chief engineer, Mackay Radio and Telegraph Co.
L. Espenschied, Bell Telephone Laboratories.
N. Koomans, chief, Staatsberdreijf der P. T. T., Holland.
T. Nakagami, chief engineer, Kokusai-Denwa Kaisha Ltd., Japan.

Reports have been furnished on particular radio fadeouts and related phenomena by many others, including:

Chief Signal Officer, War Department, U. S. A.
Naval Communication Service, U. S. A.
Aeronautical Radio Inc., U. S. A.
British Broadcasting Corporation, England.
W. Calloway, Office of Posts and Telegraphs, Kuala Lumpur, Malaya.
J. H. McMullin, Commissioner of Police, British Columbia, Canada.
C. P. Edwards, Department of Transport, Ottawa, Canada.

Reports on numerous radio fadeouts have been supplied by many radio amateurs, forwarded through the American Radio Relay League. Of these, the reports of F. D. Jenkins, of Atlanta, Ga., have been particularly helpful.

VII. BIBLIOGRAPHY

J. H. Dellinger. *A new cosmic phenomenon.* Science **82**,, 351 (Oct. 11, 1935).

J. H. Dellinger. *A new radio-transmission phenomenon.* Phys. Rev. **48**, 705 (Oct. 15, 1935).

J. H. Dellinger. *Confirmation of cosmic phenomenon.* Science **82**, 548 (Dec. 6, 1935).

J. H. Dellinger. *New radio-transmission phenomenon.* QST **19,** p. 21 of Dec. 1935.
J. H. Dellinger. *A new solar radio disturbance.* Electronics **9,** 25 (Jan. 1936).
R. S. Richardson. *The hydrogen outburst on the sun and radio fading.* Science **83,** 6 supp. (Jan. 10, 1936).
J. H. Dellinger. *New cosmic phenomenon.* QST **20,** p. 8 of Jan. 1936.
R. S. Richardson. *Sunspot activity and radio-transmission fadeouts.* Trans. Amer. Geophys. Union, part I, 172 (1936).
J. H. Dellinger. *High-frequency radio fadeouts continue.* QST **20,** p. 37 of June 1936.
R. S. Richardson. *The bright hydrogen eruption and radio fadeout of April 8, 1936.* Ter. Mag. & Atmos. Elec. **41,** 197 (June 1936).
O. W. Torreson, W. E. Scott, H. E. Stanton. *A conspicuous solar eruption on April 8, 1936, and simultaneous disturbances on magnetic, ionospheric, and earth-current records at Huancayo magnetic observatory.* Ter. Mag. & Atmos. Elec. **41,** 199 (June 1936).
G. Leithäuser. *On abnormal upper-atmospheric ionization on Feb. 14, 1936.* Funktech. Monatsheft **2,** 241 (July 1936).
D. Arakawa. *Abnormal attenuation in short radio-wave propagation.* Report of Radio Research in Japan **6,** 31 (1936).
K. Ohno, M. Nakagami, and K. Miya. *On the fall of short-wave intensity of short duration.* (In Japanese.) J. Inst. Elec. Engrs. (Japan) p. 938 (August 1936).
A. M. Braaten. *Fadeout observations at Riverhead, N. Y.* T. & R. Bul. (London) **12,** 111 (Sept. 1936).
M. Waldmeier. *The great solar eruption of Aug. 28, 1936.* Naturwiss. **24,** 638 (Oct. 2, 1936).
R. S. Richardson. *The bright eruption and radio fadeout of August 25, 1936.* Pub. Astron. Soc. Pacific **48,** 278 (Oct. 1936).
The ionosphere; the Dellinger wipe-out. T. & R. Bul. (London) **12,** 214 (Nov. 1936).
R. Bureau and J. Maire. *Ionospheric anomalies of sudden onset.* Compt. rend. **203,** 1257 (Dec. 7, 1936).
H. W. Newton. *Radio fadings and bright solar eruptions.* Nature **138,** 1017 (Dec. 12, 1936).
J. H. Dellinger. *Direct effects of particular solar eruptions on terrestrial phenomena.* Phys. Rev. **50,** 1189 (Dec. 15, 1936).
R. Jouaust, R. Bureau, and L. Eble. *The probable causes of sudden fadeouts of short radio waves and their relation to magnetic phenomena.* Compt. rend. **203,** 1534 (Dec. 28, 1936).
J. A. Fleming. *Notes on radio fadeout of August 25, 1936.* Ter. Mag. & Atmos. Elec. **41,** 404 (Dec. 1936).
O. W. Torreson, W. E. Scott, F. T. Davies, and H. E. Stanton. *A solar eruption on November 6, 1936, and disturbances in earth's magnetism, earth-currents, and the ionospheric regions.* Ter. Mag. & Atmos. Elec. **41,** 409 (Dec. 1936).
D. Arakawa. *Abnormal attenuation in short radio-wave propagation (Second Report).* Report of Radio Research in Japan **6,** 169 (1936).
Solar eruptions and radio fadeouts. Nature **139,** 61 (Jan. 9, 1937).
R. Bureau. *Abnormalities of the ionosphere and bright solar eruptions.* Nature **139,** 110 (Jan. 16, 1937).
J. H. Dellinger. *Radio fadeouts through 1936.* QST **21,** p. 35 of Feb. 1937.
A. G. McNish. *Magnetic effects associated with bright solar eruptions and radio fadeouts.* Nature **139,** 244 (Feb. 6, 1937).
J. H. Dellinger. *Sudden ionospheric disturbances.* Ter. Mag. & Atmos. Elec. **42,** 49 (March 1937).
F. T. Davies, O. W. Torreson, W. E. Scott, and H. E. Stanton. *A solar eruption of November 27, 1936, and simultaneous disturbances in earth's magnetism, earth-currents, and the ionospheric regions.* Ter. Mag. & Atmos. Elec. **42,** 93 (March 1937).
H. A. G. Hess. *Observations on the Dellinger-effect on November 6, 1936.* Funktech. Monatsheft **3,** 74 (March 1937).

WASHINGTON, May 26, 1937.

U. S. DEPARTMENT OF COMMERCE NATIONAL BUREAU OF STANDARDS

RESEARCH PAPER RP1017

Part of Journal of Research of the National Bureau of Standards, Volume 19, August 1937

INFRARED ABSORPTION OF NINETEEN HYDROCARBONS, INCLUDING TEN OF HIGH MOLECULAR WEIGHT [1]

By Frank W. Rose, Jr. [2]

ABSTRACT

The absorption spectra of 9 hydrocarbons of low molecular weight (C_8 to C_{10}) and of 10 hydrocarbons of high molecular weight (C_{24} to C_{32}) have been recorded in the near infrared from 5400 to 8900 cm^{-1} (1.82 to 1.12 μ) with a recording infrared-glass spectrograph. Molal absorptive indices have been calculated and plotted against wave numbers. Qualitative correlations of the differences in the various spectral characteristics of certain structural types have been noted and some limitations on such interpretations indicated.

It appears that these data can now be correlated quantitatively with respect to structural units of hydrocarbon molecules. The results of such a study on the infrared absorption spectra of 54 hydrocarbons follow in a subsequent report.

CONTENTS

	Page
I. Introduction	143
II. Experimental procedure	144
III. Source and nature of the hydrocarbons	144
IV. Results	146
1. Hydrocarbons of low molecular weight	147
(a) Absorption from 7900 to 8900 cm^{-1}	147
(b) Absorption from 6400 to 7400 cm^{-1}	148
(c) Absorption from 5400 to 6400 cm^{-1}	149
2. Hydrocarbons of high molecular weight	150
(a) Absorption from 7900 to 8900 cm^{-1}	150
(b) Absorption from 6400 to 7400 cm^{-1}	153
(c) Absorption from 5400 to 6400 cm^{-1}	155
V. Discussion of results	156
VI. References	161

I. INTRODUCTION

The association of the infrared absorption spectra of hydrocarbons with their structural types was substantiated in a previous report on 35 hydrocarbons of low molecular weight [1].[3] The development of the theory may be found in the literature there cited.

In order to make the results, in conjunction with certain other properties, of greater value in the problem of identifying the hydrocarbon constituents of petroleum, data on more compounds of different types, and especially those of higher molecular weight, were needed. The present report gives new experimental data for 19 hydrocarbons, 9 of low and 10 of high molecular weight, together with additional correlations of their spectra with respect to structural groups.

[1] Financial assistance has been received from the research fund of the American Petroleum Institute. This work is part of Project 6, The Separation, Identification, and Determination of the Constituents of Petroleum.

[2] Research Associate at the National Bureau of Standards, representing the American Petroleum Institute.

[3] Figures in brackets here and throughout the text refer to the references at the end of the paper.

U. S. Department of Commerce National Bureau of Standards

RESEARCH PAPER RP1017

Part of Journal of Research of the National Bureau of Standards, Volume 19, August 1937

INFRARED ABSORPTION OF NINETEEN HYDROCARBONS, INCLUDING TEN OF HIGH MOLECULAR WEIGHT [1]

By Frank W. Rose, Jr. [2]

ABSTRACT

The absorption spectra of 9 hydrocarbons of low molecular weight (C_8 to C_{10}) and of 10 hydrocarbons of high molecular weight (C_{24} to C_{32}) have been recorded in the near infrared from 5400 to 8900 cm^{-1} (1.82 to 1.12 μ) with a recording infrared-glass spectrograph. Molal absorptive indices have been calculated and plotted against wave numbers. Qualitative correlations of the differences in the various spectral characteristics of certain structural types have been noted and some limitations on such interpretations indicated.

It appears that these data can now be correlated quantitatively with respect to structural units of hydrocarbon molecules. The results of such a study on the infrared absorption spectra of 54 hydrocarbons follow in a subsequent report.

CONTENTS

	Page
I. Introduction	143
II. Experimental procedure	144
III. Source and nature of the hydrocarbons	144
IV. Results	146
1. Hydrocarbons of low molecular weight	147
(a) Absorption from 7900 to 8900 cm^{-1}	147
(b) Absorption from 6400 to 7400 cm^{-1}	148
(c) Absorption from 5400 to 6400 cm^{-1}	149
2. Hydrocarbons of high molecular weight	150
(a) Absorption from 7900 to 8900 cm^{-1}	150
(b) Absorption from 6400 to 7400 cm^{-1}	153
(c) Absorption from 5400 to 6400 cm^{-1}	155
V. Discussion of results	156
VI. References	161

I. INTRODUCTION

The association of the infrared absorption spectra of hydrocarbons with their structural types was substantiated in a previous report on 35 hydrocarbons of low molecular weight [1].[3] The development of the theory may be found in the literature there cited.

In order to make the results, in conjunction with certain other properties, of greater value in the problem of identifying the hydrocarbon constituents of petroleum, data on more compounds of different types, and especially those of higher molecular weight, were needed. The present report gives new experimental data for 19 hydrocarbons, 9 of low and 10 of high molecular weight, together with additional correlations of their spectra with respect to structural groups.

[1] Financial assistance has been received from the research fund of the American Petroleum Institute. This work is part of Project 6, The Separation, Identification, and Determination of the Constituents of Petroleum.

[2] Research Associate at the National Bureau of Standards, representing the American Petroleum Institute.

[3] Figures in brackets here and throughout the text refer to the references at the end of the paper.

II. EXPERIMENTAL PROCEDURE

The spectrograph employed in the present, as well as the previous [1] investigation, was described in its mechanical details by Brackett and Liddel [2]. The intensity of transmitted radiation is measured by a thermocouple and automatically recorded on a photographic plate as deflections of a sensitive galvanometer. The manipulation of the apparatus and the experimental technique involved have been adequately explained in earlier papers by Wulf and Liddel [1, 3, 4].

After applying the appropriate corrections as noted by these authors there is obtained the fraction of the incident light transmitted, I/I_0, through the solution at the various wave lengths. From these data, the molal absorptive index may be calculated,

$$K=\frac{-\log_{10}I/I_0}{cd},$$

where I is the intensity of the transmitted light, I_0 the incident light, c the concentration in moles per liter, and d the cell depth in centimeters. The molal absorptive index, K, is then plotted against wave number (the wave number is $1/\lambda$, where λ is the wave length in centimeters).

Solutions of the hydrocarbons in purified carbon tetrachloride were utilized in all cases (since this solvent has no significant absorption in this region). The solutions, studied in a 10-cm absorption cell, had the following approximate concentrations: for the hydrocarbons of low molecular weight, 0.5 molal for the region 6400 to 8900 cm^{-1} and 0.1 molal for the region 5400 to 6400 cm^{-1}; for the hydrocarbons of high molecular weight the concentrations for these regions were 0.1 and 0.02 molal, respectively.

III. SOURCE AND NATURE OF THE HYDROCARBONS

The nine hydrocarbons of low molecular weight included in this report are:

2-Methylnonane.	*n*-Propylbenzene.
3-Methylnonane.	Isopropylbenzene.
4-Methylnonane.	3, 5, 5-Trimethylheptane.
5-Methylnonane.	3, 4, 5, 5-Tetramethylhexane.
	Ethylcyclohexane.

The samples of 2-methylnonane, 3-methylnonane, 4-methylnonane, and 5-methylnonane were obtained from Dr. G. Calingaert of the Ethyl Gasoline Corporation, who has already described their synthesis and properties [5]. The samples of 3, 5, 5-trimethylheptane and 3, 4, 5, 5-tetramethylhexane were obtained from Prof. N. L. Drake of Maryland University, and their synthesis and properties will be described in a forthcoming publication [6]. The sample of isopropylbenzene was prepared by careful fractionation, at 215 mm Hg pressure, in a distilling column packed with 240 cm of locket-chain from crude synthetic stock obtained from Prof. W. B. Holton of American University [7]. The sample of *n*-propylbenzene was purified by distillation (in the same manner as the isopropylbenzene) from crude synthetic stock obtained from Prof. E. E. Reid of the Johns Hopkins University [8]. The sample of ethylcyclohexane was syn-

thesized by Rose and White, who described its properties [9]. The properties of the isopropyl- and *n*-propylbenzene will be described in forthcoming publications [17]. Figures are not given for the purities of the samples used, although, with the exception of 3, 5, 5-trimethylheptane and 3, 4, 5, 5-tetramethylhexane, the purity of all the samples was considered more than adequate for this work (95%). Furthermore the impurities are probably similar hydrocarbons whose effect is relatively small. These samples may, of course, be identified by their physical properties found in the references cited. Each of the exceptions noted may contain substantial amounts of the other.

REFERENCE NUMBER	NAME	STRUCTUAL FORMULA
1	1-Phenyl-n-octadecane	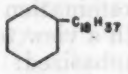
11	1-Cyclohexyl-n-octadecane	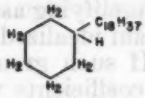
12	5-Cyclohexyl-n-docosane	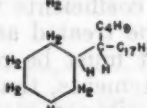
31	1-(7-Tetrahydronaphthyl)-n-octadecane	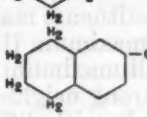
33	5-(7-Tetrahydronaphthyl)-n-docosane	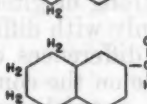
34	5-(7-Tetrahydronaphthyl)-n-docosene-5	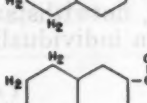
39	5-(2-Decahydronaphthyl)-n-docosane	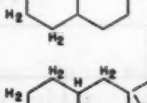
40	1-(p-Diphenyl)-n-octadecane	
41	5-(p-Diphenyl)-n-docosene-5	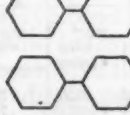

FIGURE 1.—*Structural formulas of high molecular weight hydrocarbons.*

The reference numbers in this figure are the same as those used in Mikeska's paper [10].

The hydrocarbons of high molecular weight whose names and formulas are given in figure 1 were kindly lent for this and other work by Dr. L. A. Mikeska of the Standard Oil Development Co., who synthesized these compounds and determined a number of their properties [10]. Mikeska reported that "No attempt has been made to establish the relative position of the substituents in the benzene derivatives nor

the exact location of the side chain or chains in the naphthalene derivatives." It is likely that, because of the similarity in the method of synthesis, the position is identical for all derivatives of the same aromatic nucleus. Furthermore, such a distinction lies somewhat beyond the scope of the present investigation.

The *n*-nonacosane ($C_{29}H_{60}$) was a sample of high purity, prepared by Dr. K. S. Markley, Bureau of Plant Industry, U. S. Department of Agriculture, from the cuticle of Rome Beauty apples. The physical constants of this compound have been described [11], [12]. A determination of the carbon-hydrogen ratio in this laboratory gave further proof of its purity [13].

IV. RESULTS

In the examination of the curves of absorption coefficients in the infrared with a view to their use in identification, the following points must be emphasized:

1. The simplifying assumption is often made that the molecule consists of certain idealized types of linkages (such as primary or methyl, $-CH_3$).[4] If such groups have, for a definite wave number, fixed absorption coefficients which are additive, the molecular absorption curve can be treated as the composite of these generalized linkages. However, it must be remembered, as a qualification upon all such general statements, that changes in intramolecular action caused by various substituents may modify both the position and amount of the absorption maximum [14].

2. A small maximum may be apparently displaced by the presence of a very strong neighboring maximum, and in some cases it may be discerned only with difficulty.

3. Small differences can not be emphasized until more intensive work is done on the compounds in question.

However, notwithstanding these limitations, the hydrocarbons do show certain individualities, and these form the basis of the present discussion.

TABLE 1.—*Position of maxima*

Region	Type of absorbing group [a]				
	$-\overset{H}{\underset{H}{C}}-H$	$\overset{H}{\underset{H}{\diagdown C \diagup}}$	$-C-H$	$>CH$ Aromatic	Naphthene
cm^{-1}	cm^{-1}	cm^{-1}	cm^{-1}	cm^{-1}	
7900 to 8900	8400 [b] (8680)	[c] 8250	8150	8700 to 8800 [c] 8750	Complex.
6400 to 7400	7350 [b] (6975)	[d] 7075 7175	6950	Weak multiple structure	
5400 to 6400	5860 5900	5670 5790		[f] About 5900	Similar to *n*-aliphatics.

[a] See footnote 4, p. 146.
[b] Weak.
[c] Median of absorption shifts to lower frequencies with increasing length of chain.
[d] Affected by substitution.
[e] Constant in position and magnitude for monosubstituted derivatives. With polysubstitution varies ±100 cm^{-1}.
[f] Three peaks appear near this point. Substitution radically changes the relative intensities.

[4] Hereafter an incomplete valence bond indicates the attachment to the remainder of the molecule through another C atom.

In table 1 are given the generalizations of the previous work [1], together with two additions from the present investigation. The wave numbers given for any absorption peak may vary over a range of ± 50 wave numbers, depending on the nature of the remainder of the molecule. This table is given merely as an aid in interpreting the diagrams, and the values given should not be construed as exact numerical data.

1. HYDROCARBONS OF LOW MOLECULAR WEIGHT

(a) ABSORPTION FROM 7900 TO 8900 cm^{-1}

The *n*-propyl- and isopropylbenzenes (fig. 2) reveal maxima in the absorption curves in accord with those of simpler compounds. Briefly the peaks and associated groups are: 8750 cm^{-1}, aromatic; 8400 cm^{-1}, primary aliphatic ($-CH_3$); 8250 cm^{-1}, secondary aliphatic ($>CH_2$); and 8150 cm^{-1}, tertiary aliphatic linkages ($\geqslant CH$). In contrast with the variations shown by polysubstituted phenyl derivatives, the mono-

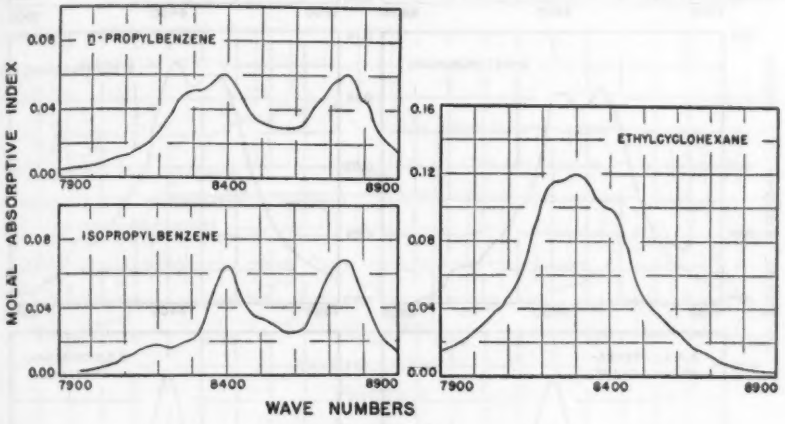

FIGURE 2.

substituted derivatives have maxima at 8750 cm^{-1} fairly constant both as to magnitude and position of the peak. The absorption due to the aliphatic portions of the molecules is consistent with the conclusions previously drawn [1].

The curves of ethylcyclohexane (fig. 2) are quite similar to those previously recorded for cyclohexane and methylcyclohexane [1].

The curves of the methylnonanes (fig. 3) show little variation in form but do not have the same values for the absorptive index at their maxima. These maxima show no significant displacement in frequency with change in the position of the methyl group. In the 4-methylnonane, the absorption due to the methyl groups (at 8400 cm^{-1} and 8650 cm^{-1}) seems to be more intense than in the other isomers. The absorption characteristic of a single tertiary group ($\geqslant CH$) in such a large molecule is apparently not detectable, since there is no indication of a peak at 8150 cm^{-1}. It is interesting to note that the methylnonanes (three primary ($-CH_3$) and six secondary groups ($>CH_2$), ratio 1:2) show the same relation between the maxima at 8400 and 8250 cm^{-1} as does *n*-hexane [1], (two primary ($-CH_3$) and four secondary groups ($>CH_2$), ratio 1:2).

The compounds 3,4,5,5-tetramethylhexane and 3,5,5-trimethylheptane (fig. 3) are highly methylated, having six and five primary ($-CH_3$) groups, respectively. Both show the expected characteristic peak at 8400 cm^{-1}, the latter having somewhat greater secondary ($>CH_2$) absorption at 8250 cm^{-1}. Neither shows obvious absorption characteristics of tertiary ($\geqslant CH$) groups.

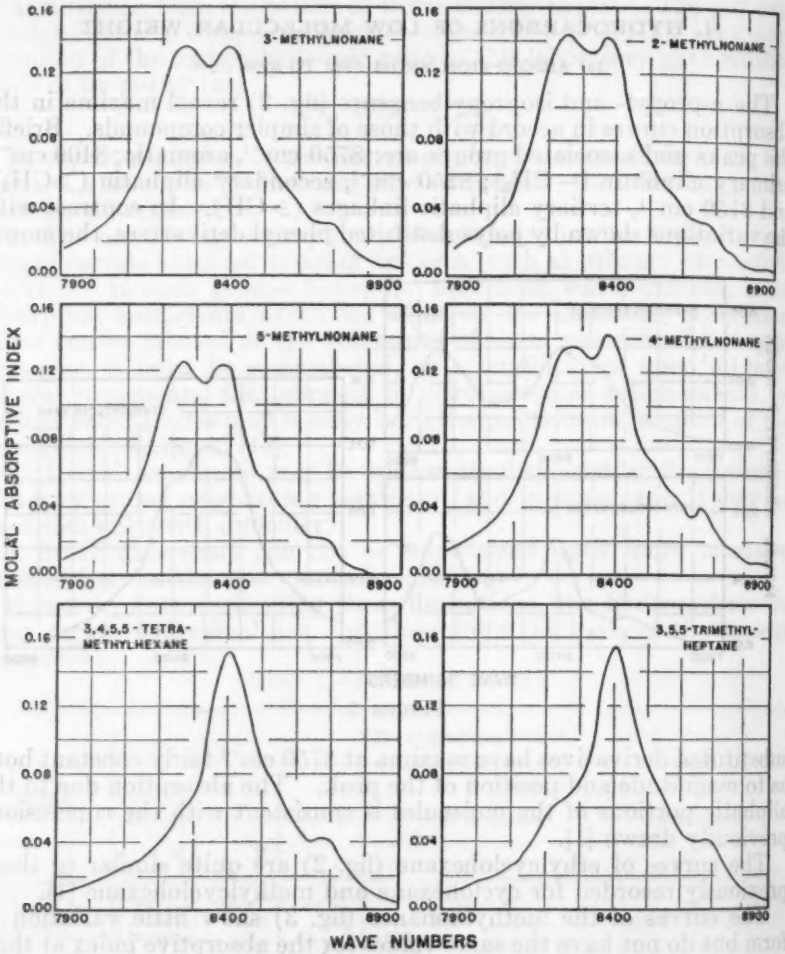

FIGURE 3.

(b) ABSORPTION FROM 6400 TO 7400 cm^{-1}

In this region, *n*-propylbenzene and isopropylbenzene (fig. 4) show the weak multiple absorption typical of aromatic derivatives.

The ethylcyclohexane curve (fig. 4) is quite similar to those of methylcyclohexane and cyclohexane, and is similar to those of the *n*-aliphatics but less intense.

The absorption curves of the methylnonanes (fig. 5) are indistinguishable from each other in this region, which indicates that a change in the position of the methyl group on the chain causes no detectable change in the absorption curve, possibly on account of the size of the molecule. Even similar compounds of lower molecular weight previously studied show considerably smaller differences in this region than in the region 7900 to 8900 cm^{-1}.

The absorption curves of 3,4,5,5-tetramethylhexane and 3,5,5-trimethylheptane (fig. 5) have a complicated structure which has not yet been separated into the different components. Both curves resemble those of highly methylated structures (2,2,3-trimethylbutane and 2,2,4-trimethylpentane) in the earlier study [1].

(c) ABSORPTION FROM 5400 TO 6400 cm^{-1}

The presence of many maxima in close proximity, but which are attributed to structures quite different from one another renders this region less susceptible to analysis. There may be distinguished

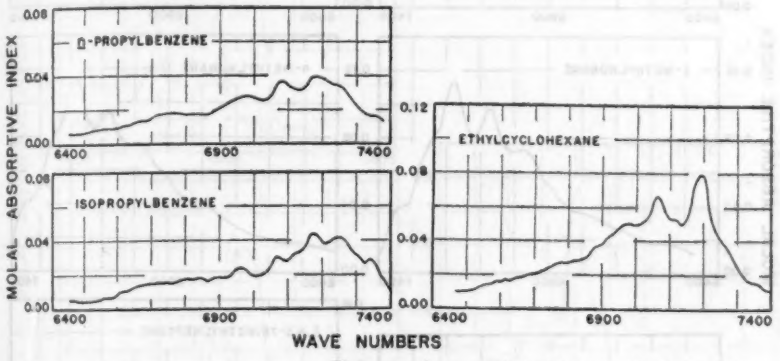

FIGURE 4.

absorption caused by secondary ($>CH_2$) linkages at 5700 cm^{-1} in the curve for *n*-propylbenzene (fig. 6). While the maximum at 5950 cm^{-1} is present and has nearly the same intensity in both *n*-propyl- and isopropylbenzene (fig. 6), the latter shows a higher peak at 5910 cm^{-1}, which is caused by the presence of more methyl groups. The remark made above concerning monosubstituted phenyl derivatives; i. e., that the maximum is more constant both as to magnitude and position than for the polysubstituted derivatives, can be repeated here, with the additional comment that less complexity is observed (in sharp contrast with hemimellitene, pseudocumene, and mesitylene, as previously reported).

Ethylcyclohexane (fig. 6) exhibits the characteristics of secondary aliphatic absorption in this region and little else.

As in the other regions, the absorption curves of the methylnonanes (fig. 7) are again alike in shape. Variation in intensity occurs, and it may be remarked that almost the same order is followed here as was shown in the absorption from 7900 to 8900 cm^{-1}. In general, the curves are typical of an aliphatic hydrocarbon containing a small number of methyl groups.

The 3,4,5,5-tetramethylhexane and the 3,5,5-trimethylheptane (fig. 7) have maxima indicative of methyl groups.

2. HYDROCARBONS OF HIGH MOLECULAR WEIGHT

(a) ABSORPTION FROM 7900 TO 8900 cm^{-1}

The absorption curve of *n*-nonacosane ($C_{29}H_{60}$) may be considered an excellent example of the absorption resulting from the presence of a

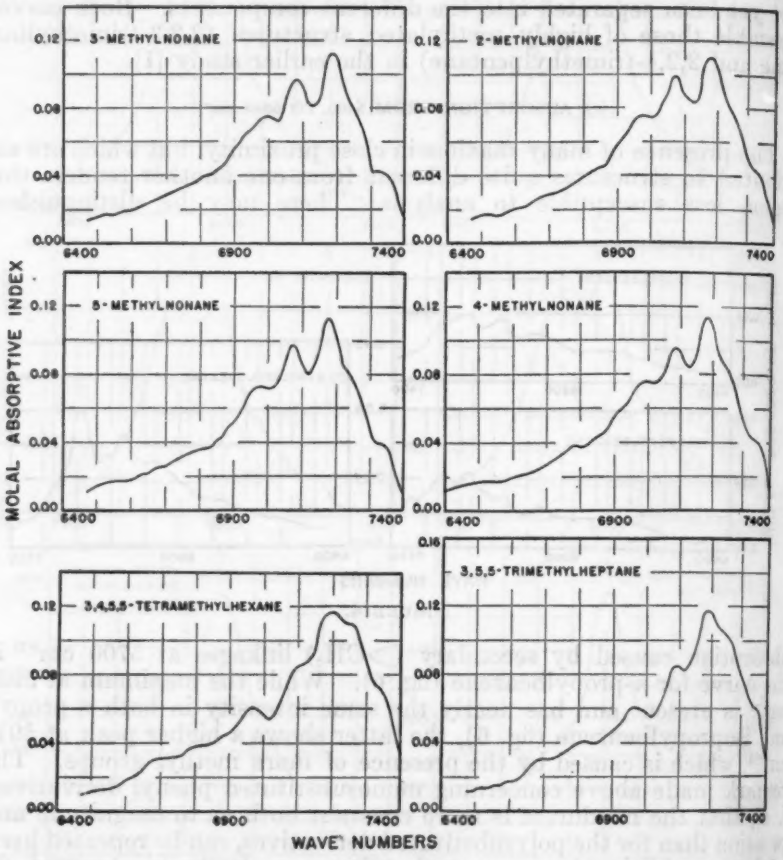

FIGURE 5.

number of average $>CH_2$ groups. In the molecule $R-(CH_2)_n-R'$, the absorption due to $>CH_2$ is modified where R and R′ are groups containing a small number of carbon atoms (methyl to propyl). In *n*-nonacosane (fig. 8) such disturbances are proportionally small. It may be observed that the secondary ($>CH_2$) group causes a single peak in this region (at 8250 cm^{-1}) which nicely confirms the earlier statement of Brackett [15]. Inasmuch as no maximum in the absorption curve of this compound occurs at 8680 cm^{-1} the peak found at this point in other compounds having a larger proportion of methyl groups may be allocated to primary ($-CH_3$) absorption. It is, however, a weak absorption best observed in highly methylated struc-

tures. Its use is minor in the detection of primary ($-CH_3$) groups, but is noted here to avoid possible ambiguities in the interpretation of the aromatic absorption at 8700 to 8800 cm^{-1}.

Since the compound 1-phenyl-*n*-octadecane (fig. 9) consists of 1 phenyl, 1 primary ($-CH_3$), and 17 secondary ($>CH_2$) aliphatic groups, maxima would be expected at 8750 and 8250 cm^{-1} (the effect of the single primary ($-CH_3$) group being concealed by the preponderance of the other structures). Not only does the curve follow the anticipated shape, but the value of the absorptive index at 8750 cm^{-1} (aromatic absorption) almost reproduces that found for the monosubstituted phenyl groups in *n*-propyl- and isopropylbenzene, where the side chains are considerably abbreviated. This statement may be

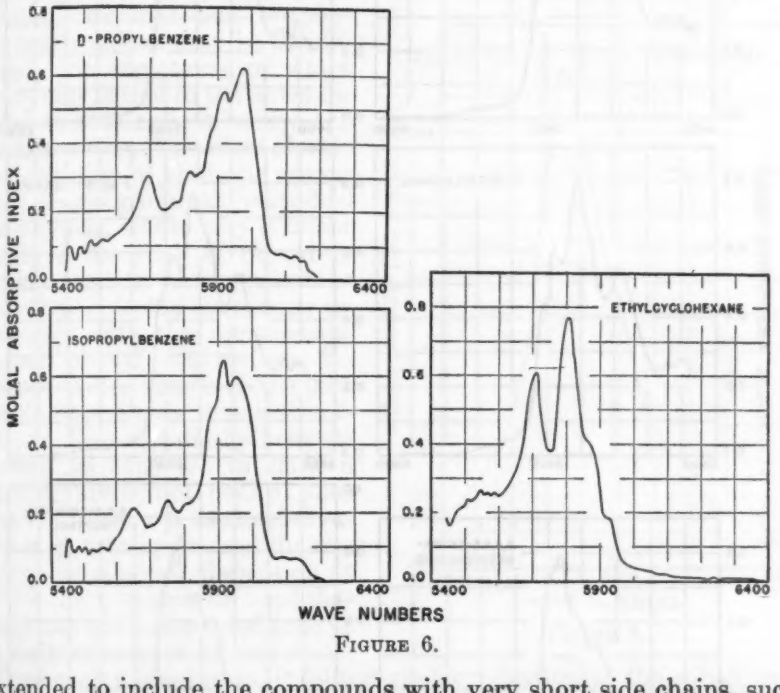

FIGURE 6.

extended to include the compounds with very short side chains, such as toluene and ethylbenzene. If to this structure a phenyl group is added, as in 1-(*p*-diphenyl)-*n*-octadecane (fig. 9), the difference in the absorption curves can be ascribed to the phenyl group introduced. The sole observed variation in the two curves is that in the latter the absorption is twice as intense at 8750 cm^{-1}. The absorption curve of the compound 5-(*p*-diphenyl)-*n*-docosene-5 (fig. 9) departs only slightly from that for 1-(*p*-diphenyl)-*n*-octadecane. The structure includes 2 phenyl group, 18 secondary ($>CH_2$), and 1 primary ($-CH_3$) linkages as well as 1 ethylenic bond. Although this and the previous study furnish no information concerning ethylenic bonds, the effect of unsaturation may be evaluated by the data of other workers. Thus Lecomte in the most recent treatise on infrared spectra [16] states, following the work of Freyman, that aliphatic compounds containing ethylenic bonds "possess, on the whole, all the principal

bands of the corresponding saturated hydrocarbons and a part of the secondary bands (but the latter have intensities singularly modified) and, in addition, new bands." Since only one carbon-hydrogen linkage is involved, the resulting alteration should be minor. It is, however, conceivable that the presence of this group would affect the

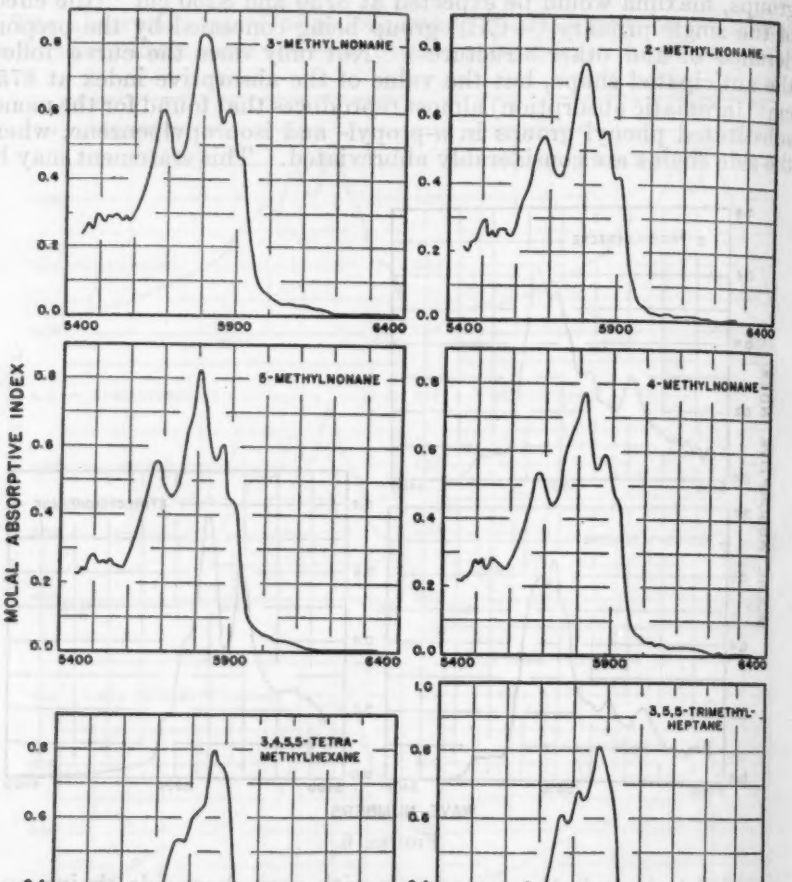

FIGURE 7.

remainder of the molecule sufficiently strongly to give rise to distinctly modified absorption. Such, however, is not the case; the absorption curve is indicative only of secondary aliphatic ($>CH_2$) and aromatic absorption in an amount to be predicted on the basis of the saturated groups present.

The naphthenic compounds, 1-cyclohexyl-*n*-octadecane (fig. 9) and 5-cyclohexyl-*n*-docosane (fig. 9), present similar absorption

curves, the latter logically having a greater value for the absorptive index at the maximum since the molecule possesses a larger number of secondary ($>CH_2$) linkages. The values of the absorptive indices for both substances are less than that for an equal number of secondary linkages ($>CH_2$) in a chain structure (a condition normally encountered in the saturated cyclics).

Curiously, the tetrahydronaphthyl derivatives (fig. 10) have no distinctive peak at the wave number (about 8750 cm^{-1}) associated with aromatic absorption. Further, the curves are indistinguishable from those for the corresponding cyclohexyl derivatives (fig. 9), except that for the former the region 8550 to 8800 cm^{-1} generally shows somewhat greater absorption. In an attempt to explain this discrepancy, the probable difference in the absorption curves of *o*-diethylbenzene and tetrahydronaphthalene may be considered, the structures of which vary only in that in the latter the aliphatic chains have been joined to form a ring. The effect of *ortho* substitution of aliphatic groups in a phenyl group can be studied in *o*-xylene, where only a minor shift of the peak in regard to either position or magnitude is observed. If one may judge by analogy with the monosubstituted phenyl derivatives, increase in the length of the side chain causes only minor alterations. Hence, *o*-diethylbenzene would be expected to show a distinct absorption peak at 8750 cm^{-1}. Inasmuch as the derivatives of tetrahydronaphthalene show no marked absorption at 8750 cm^{-1}, tetrahydronaphthalene may not be expected to have a distinctive peak at this point.

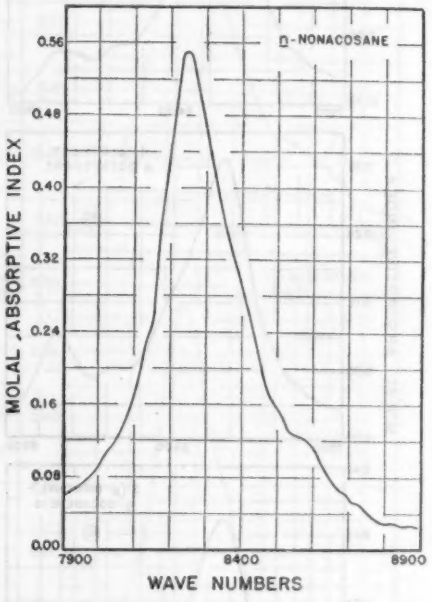

FIGURE 8.

From such a conclusion, it follows that cyclization of the substituent groups of a benzene ring exercises a profound effect on the form of the absorption curve. This effect is naturally absent in 5-(2-decahydronaphthyl)-*n*-docosane (fig. 10), which consists principally of secondary linkages ($>CH_2$). Both the tetrahydro- and decahydronaphthyl derivatives have the same value of the absorptive index at 8250 cm^{-1} as do the aliphatic compounds having the same number of secondary groups ($>CH_2$), in contrast with the cyclohexyl derivatives which consistently show lower values.

(b) ABSORPTION FROM 6400 TO 7400 cm^{-1}

The absorption curve of *n*-nonacosane (fig. 11) has the peaks assumed for secondary linkages ($>CH_2$) in the hydrocarbons of lower molecular weight but, because of the better separation of the peaks, now has maxima at 7065 and 7185 cm^{-1} (previously 7075 and 7175 cm^{-1}).

The remainder of the compounds (fig, 12, 13) have maxima at 7065 and 7185 cm^{-1}. This is logical since they all consist principally of

secondary linkages ($>CH_2$), with the exception of the three with aromatic rings. However, as stated above, aromatic rings have in this region a weak, multiple absorption that would manifest itself only by a minor increase in the values of the absorptive index over the entire curve. The presence of the ring might change the behavior of

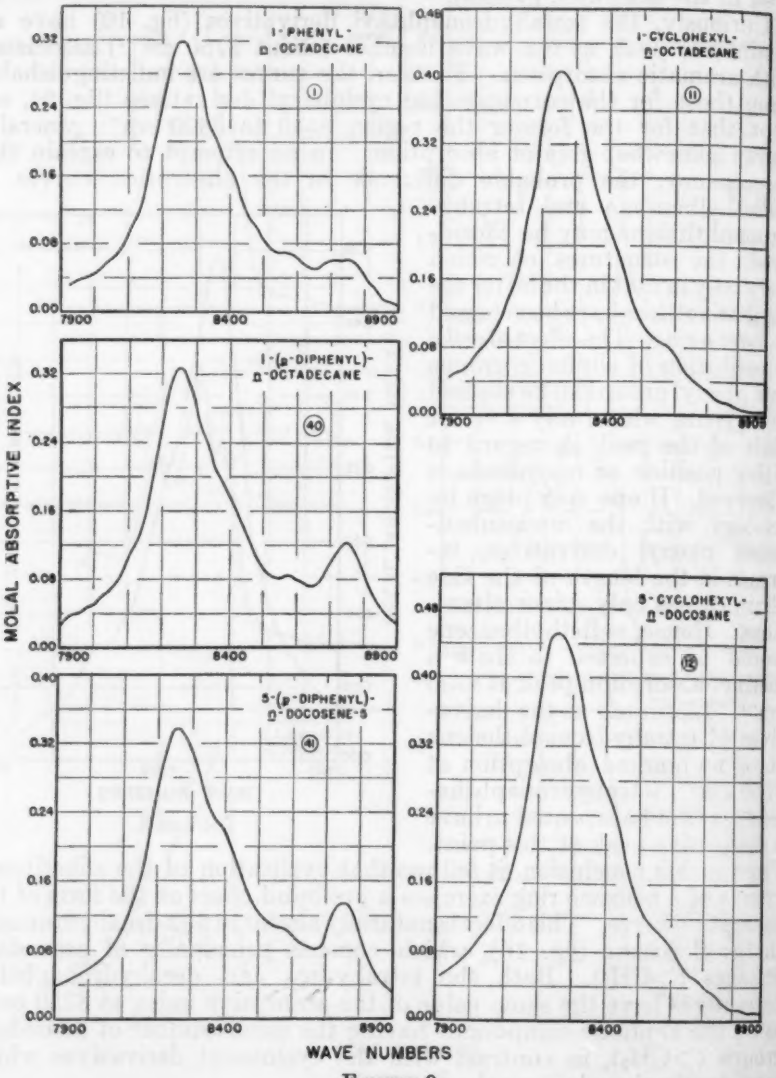

FIGURE 9.

the secondary linkages ($>CH_2$). Indeed, some such result is encountered, as may be seen from a consideration of the relative heights of the peaks. In 5-cyclohexyl-*n*-docosane (fig. 12) a complete reversal of the relative strengths of absorption at 7090 and 7190 cm^{-1} occurs. To a lesser extent, similar anomalies are evident in the majority of the compounds. Intensification and depressions of both maxima occur, although the peak at 7190 cm^{-1} is more often strongly affected. Any

attempt to follow the effect of a single structural variable results only in confusion, hence no correlation of the shape or magnitude of the curve with structure has been made.

(c) ABSORPTION FROM 5400 TO 6400 cm^{-1}

The absorption curve for *n*-nonacosane (fig. 11) substantiates the prior assignment of the maxima at 5670 and 5790 to secondary linkages ($>CH_2$).

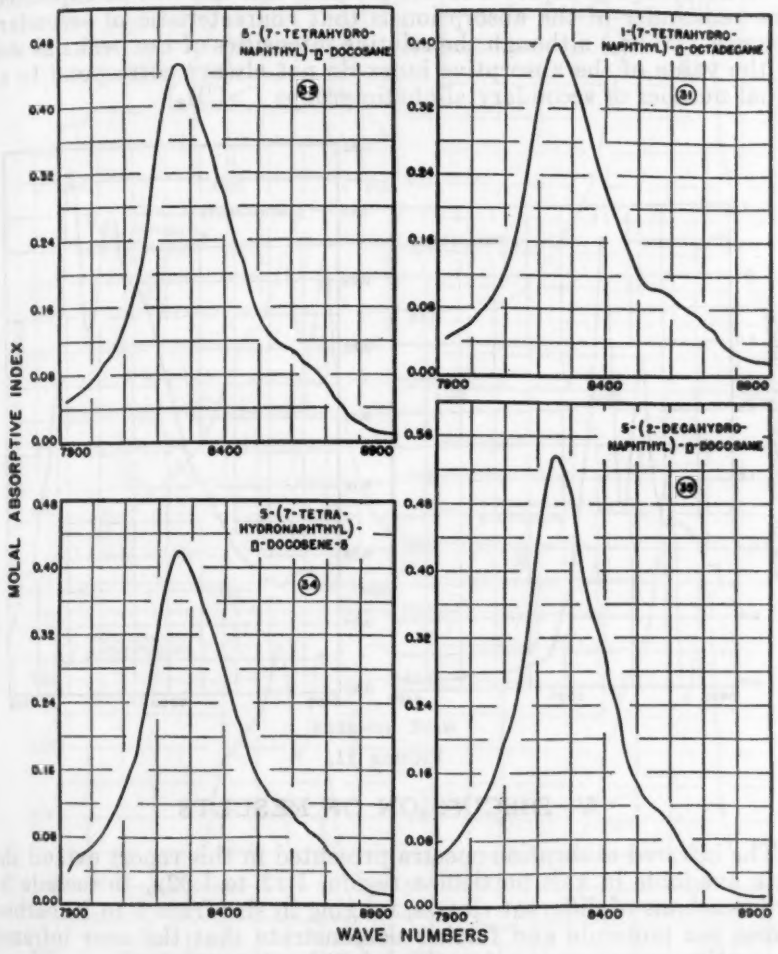

FIGURE 10.

The compounds, 1-phenyl-*n*-octadecane, 1-(*p*-diphenyl)-*n*-octadecane, and 5(*p*-diphenyl)-*n*-docosene-5 (fig. 14), all have maxima at or near 5990 cm^{-1}. All the structures contain aromatic rings in addition to the secondary linkages ($>CH_2$). The first and second compounds vary only in the number of rings and their curves vary only in the maxima at 5990 cm^{-1}. Hence absorption at this point may be attributed to the phenyl group. The third compound has additional absorption at 5900 cm^{-1} which may be related to greater proportion of

methyl groups. The remainder of the curves show normal characteristics of secondary aliphatic ($>CH_2$) absorption (compare with *n*-nonacosane (fig. 11)).

In agreement with the curves of the region from 7900 to 8900 cm^{-1}, the tetrahydronaphthyl derivatives (fig. 15), though only partially hydrogenated and still apparently possessing an "aromatic" ring, do not absorb in the interval, 5900 to 6000 cm^{-1}, significantly more than do the decahydronaphthyl and cyclohexyl derivatives which have no phenyl groups. For the present, this can not be explained. The remainder of the absorption is that characteristic of secondary linkages ($>CH_2$) although the relative intensities of the peaks as well as the value of the absorptive index do not always correspond to an equal number of secondary aliphatic groups ($>CH_2$).

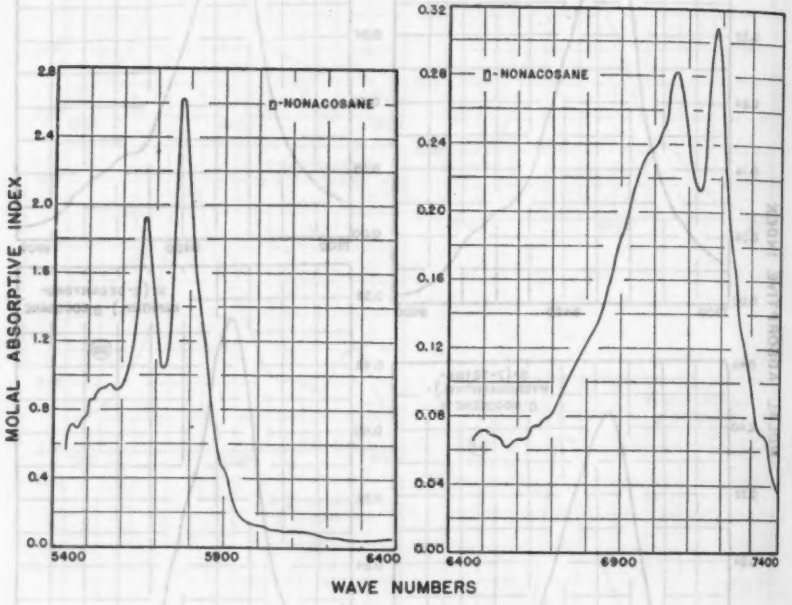

FIGURE 11.

V. DISCUSSION OF RESULTS

The infrared absorption spectra presented in this report extend the data available in this particular region, 1.12 to 1.82μ, to include 54 hydrocarbons of different classes, ranging in size from 5 to 32 carbon atoms per molecule and further demonstrate that the near infrared absorption spectrum is a function of molecular structure.

Heretofore, visual comparison of the individual curves has served to give some qualitative measure of the differences in molecular structure. It appears that these data can now be correlated quantitatively with respect to the structural units ($-CH^3$, $>CH^2$, $\gtrless CH$, and aromatic of hydrocarbon molecules. The results of a mathematical analysis of the near infrared absorption spectra of these 54 hydrocarbons follow in a subsequent report.

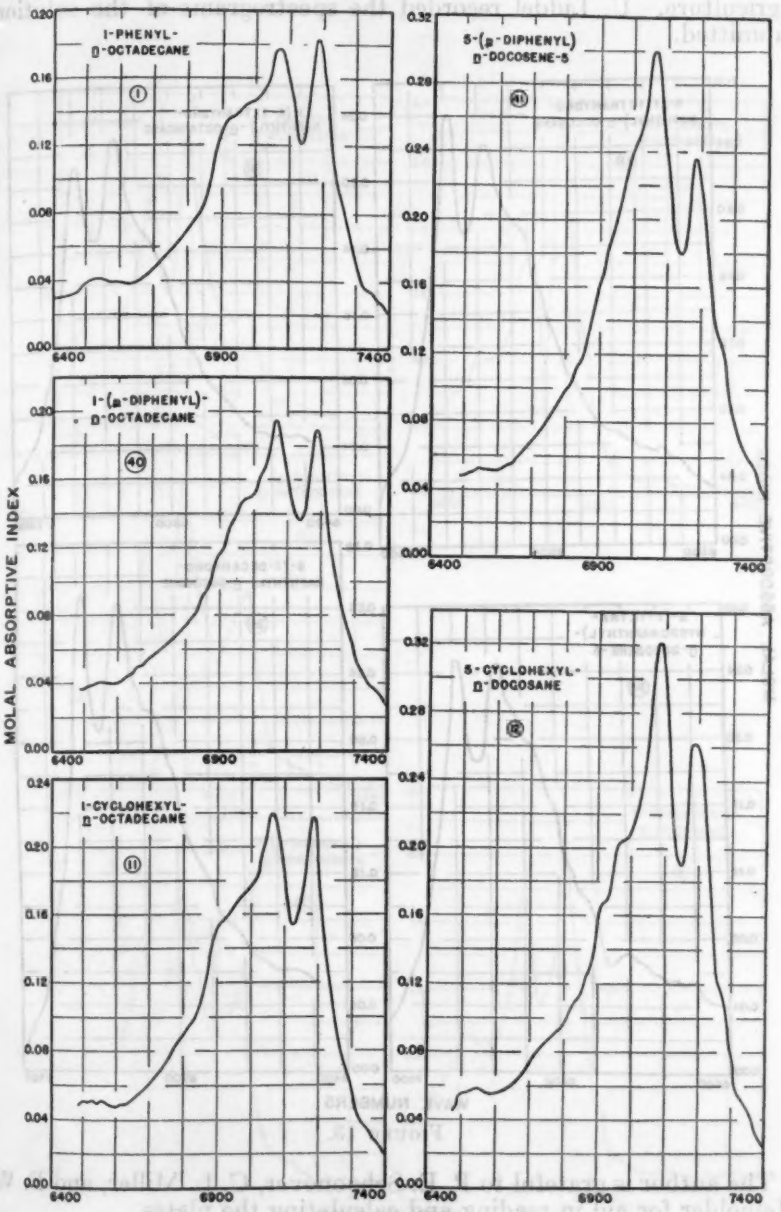
1-PHENYL-n-OCTADECANE
(1)
1-(p-DIPHENYL)-n-OCTADECANE
(40)
1-CYCLOHEXYL-n-OCTADECANE
(11)
5-(p-DIPHENYL) n-DOCOSENE-5
(41)
5-CYCLOHEXYL-n-DOCOSANE
(12)
MOLAL ABSORPTIVE INDEX
WAVE NUMBERS
6400
6900
7400

FIGURE 12.

This work was made possible by the courtesy and cooperation of O. R. Wulf, of the Bureau of Chemistry and Soils, Department of Agriculture. U. Liddel recorded the spectrograms of the solutions submitted.

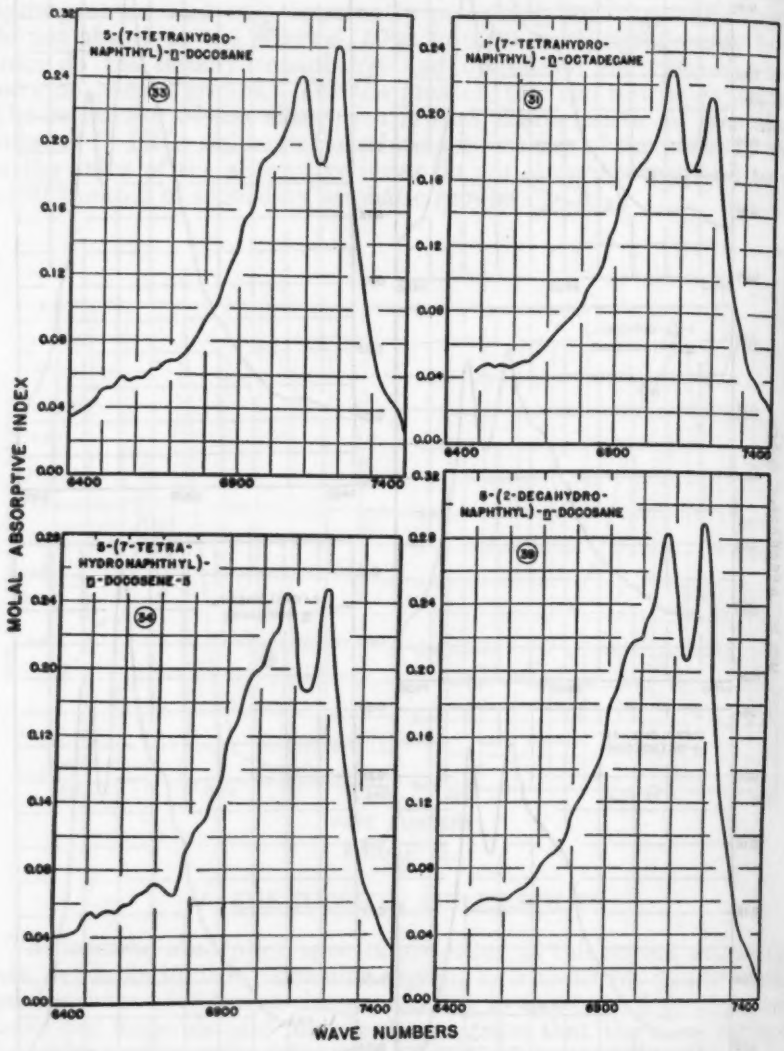

FIGURE 13.

The author is grateful to P. E. Schoonover, C. L. Miller, and F. W. Melpolder for aid in reading and calculating the plates.

The suggestions and guidance of O. R. Wulf, and of F. D. Rossini, director of this project, have materially aided the preparation of this report.

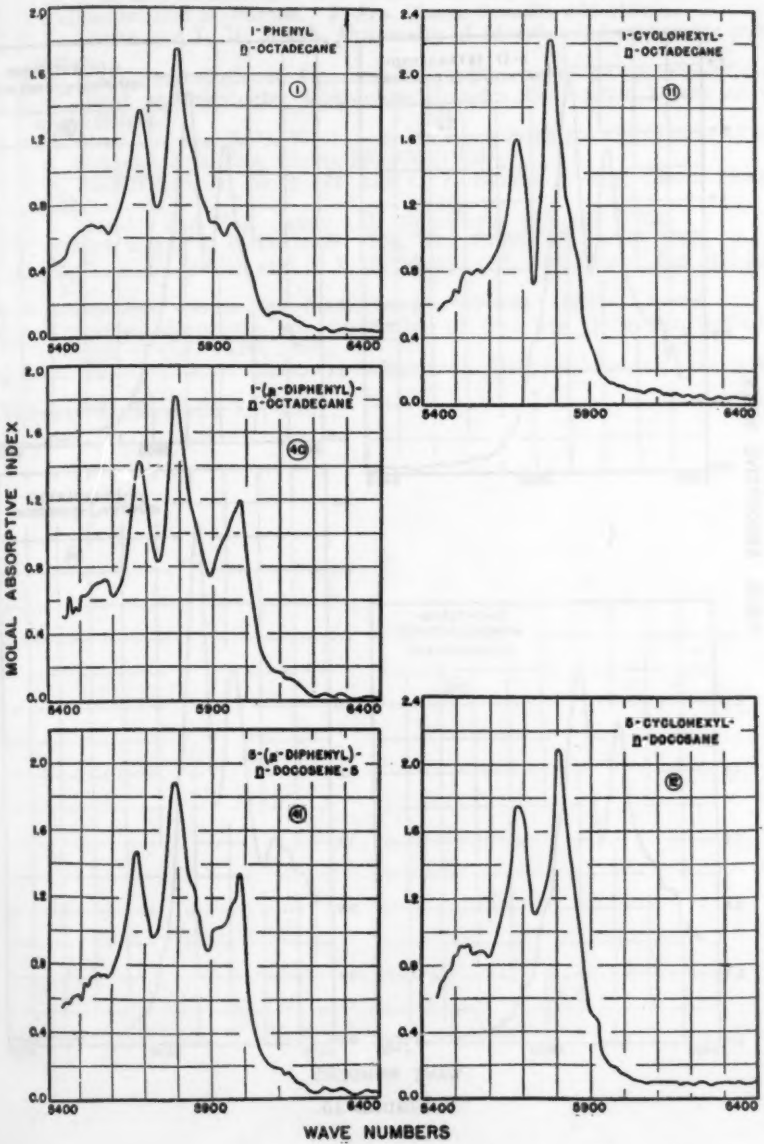
1-PHENYL
n-OCTADECANE
①
1-CYCLOHEXYL-
n-OCTADECANE
⑪
1-(p-DIPHENYL)-
n-OCTADECANE
⑭
5-(p-DIPHENYL)-
n-DOCOSENE-5
⑭
5-CYCLOHEXYL-
n-DOCOSANE
⑫
MOLAL ABSORPTIVE INDEX
WAVE NUMBERS
5400
5900
6400

FIGURE 14.

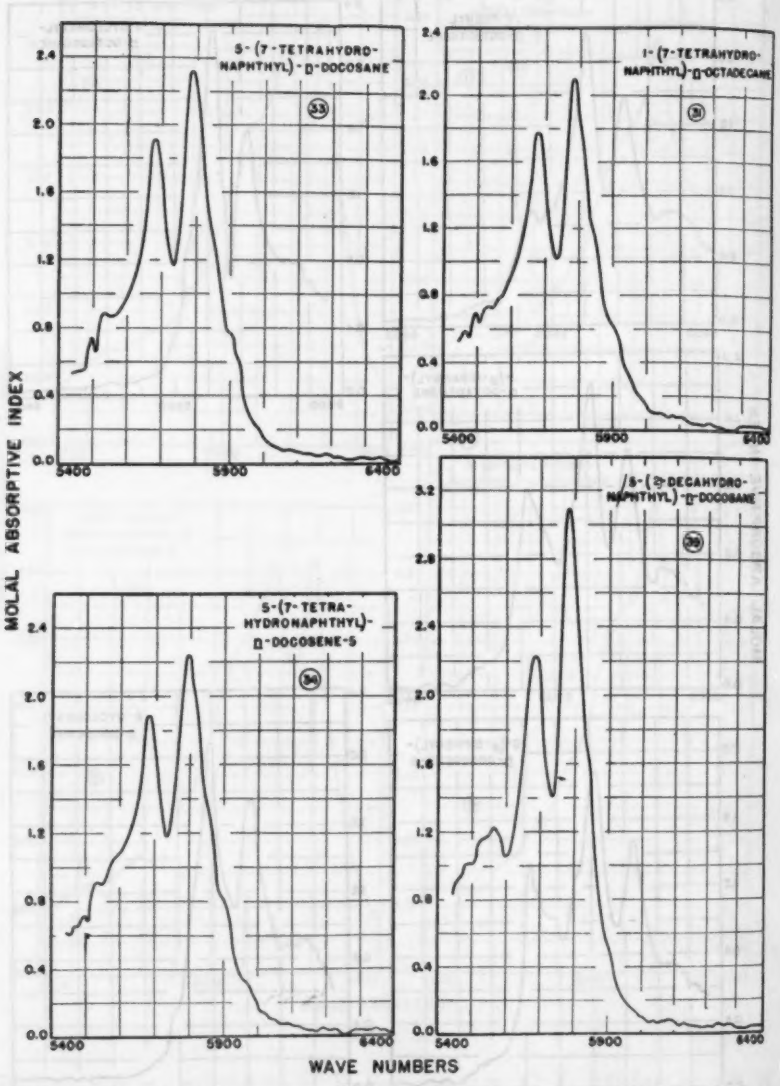
5-(7-TETRAHYDRO-NAPHTHYL)-n-DOCOSANE
(33)
1-(7-TETRAHYDRO-NAPHTHYL)-n-OCTADECANE
(31)
5-(7-TETRA-HYDRONAPHTHYL)-n-DOCOSENE-5
(34)
5-(2-DECAHYDRO-NAPHTHYL)-n-DOCOSANE
(29)
MOLAL ABSORPTIVE INDEX
WAVE NUMBERS
5400
5900
6400

FIGURE 15.

VI. REFERENCES

[1] U. Liddel and C. Kasper. BS J. Research **10**, 599–618 (1933) RP610.
[2] F. S. Brackett and U. Liddel. Smithsonian Misc. Coll. **85**, no. 5 (1931).
[3] U. Liddel and O. R. Wulf. J. Am. Chem. Soc. **55**, 3574 (1933).
[4] O. R. Wulf and U. Liddel, J. Am. Chem. Soc. **57**, 1464 (1935).
[5] G. Calingaert and H. Soroos. J. Am. Chem. Soc. **58**, 635 (1936).
[6] N. L. Drake and L. H. Welsh, University of Maryland; forthcoming publication.
[7] W. B. Holton and students, American University; report as yet unpublished.
[8] E. E. Reid and students, The Johns Hopkins University, report as yet unpublished.
[9] F. W. Rose, Jr., and J. D. White. J. Research NBS **15**, 151 (1935) RP817.
[10] L. A. Mikeska, Ind. Eng. Chem. **28**, 970 (1936).
[11] K. S. Markley, S. B. Hendricks, and C. E. Sando, J. Biol. Chem. **98**, 103 (1932).
[12] K. S. Markley and C. E. Sando. J. Biol. Chem. **101**, 431 (1933).
[13] B. J. Mair and S. T. Schicktanz. Ind. Eng. Chem. **28**, 1448 (1936).
[14] O. R. Wulf, U. Liddel, and S. B. Hendricks. J. Am. Chem. Soc. **58**, 2287 (1936).
[15] F. S. Brackett. Proc. Nat. Acad. Sci. **14**, 857–864 (1928).
[16] J. Lecomte. Structure des Molécules et Spectres dans l'Infra-Rouge. (Masson et Cie., Paris, 1936).
[17] J. D. White and F. W. Rose, Jr., J. Research NBS; forthcoming publication.

WASHINGTON, June 15, 1937.

U. S. Department of Commerce National Bureau of Standards

RESEARCH PAPER RP1018

Part of Journal of Research of the National Bureau of Standards, Volume 19, August 1937

TEMPERATURE AND HYSTERESIS ERRORS IN CALOMEL HALF-CELLS

By Baker Wingfield and S. F. Acree

ABSTRACT

Saturated and undersaturated KCl-calomel half-cells were subjected to temperature changes between 22.5 and 31.3° C and the difference in electromotive force (emf) between them and saturated calomel half-cells at 25° C was measured. During an 8° C change, maximum differences of 0.5 to 0.9 mv were found between the measured emf values and the equilibrium emf values corresponding to the temperature of the KCl solutions. Potentials within 0.2 to 0.3 mv of the equilibrium value were obtained in 2 to 3 hours after an 8° C change. Calomel half-cells protected with dewar flasks against small fluctuations in room temperature were more stable in potential than the unprotected cells. The saturated half-cell had a $\Delta E/\Delta T$ of 0.25 mv/°C and the undersaturated half-cell, 3.8 N, gave the value 0.47 mv/°.C One half-cell, saturated at 25° C. without an excess of KCl crystals, was measured and its $\Delta E/\Delta T$ was found to be erratic.

CONTENTS

		Page
I.	Introduction	163
II.	Experimental results	164
III.	Discussion	170
IV.	Conclusions	174

I. INTRODUCTION

Calomel reference half-cells are used extensively in both electrometric titrations and pH work. Their potentials and temperature coefficients have been studied previously by other workers [1, 2, 3, 4, 5, 6, 7, 8, 9, 10, 12, 13, 14].[1] The purpose of this report is to emphasize the errors which may be introduced into pH measurements by temperature changes affecting the potential of calomel half-cells.

Temperature changes of the calomel half-cell produce two effects on its potential: (a) the proportional increase in potential per degree rise in temperature, between two steady states, through the usual working range, 15 to 40° C; and (b) the lag or hysteresis in potential from values calculated from the temperature coefficient or potential change per degree, as previously reported by the authors and others [2, 3, 4, 7, 9, 11, 15]. It is preferred in this article to use the term change in potential per degree, $\Delta E/\Delta T$, rather than the temperature coefficient,[2] as it is simpler for general use. While temperature coefficients have long been recognized, there has been noticed in

[1] Figures in brackets refer to the bibliography at the end of this article.

[2] The relationship between the temperature coefficient and $\Delta E/\Delta T$ is given by the following:

$$a_t = \frac{\Delta E}{\Delta T} \times \frac{1}{E_t}$$

where a_t = temperature coefficient and E_t = potential of the half-cell at some reference temperature.

some cases, particularly by the users of pH equipment in plant and mill operation, entire disregard of temperature effects on the results of pH measurements performed under varying conditions.

These investigations are given here to show the errors which may be present in reported pH values when the measurements are made with calomel half-cells under various temperature conditions; to emphasize the need for maintaining the half-cells at constant temperature for several hours before measurements can be made to an accuracy of 0.01 pH unit; to indicate the approximate difference of the emf measured under changing temperature conditions from that under equilibrium conditions; and to investigate a simple method for reducing the temperature changes of the calomel half-cell by insulation.

II. EXPERIMENTAL RESULTS

The mercury used in the preparation of the half-cells employed in these experiments was electrolytically purified, washed with nitric acid, and distilled. The calomel, containing finely divided mercury, was an excellent electrolytic preparation; and the KCl was a good chemically pure grade. The half-cells illustrated in figure 1 were made up and designated by letters as follows: Half-cells *G*, *N*, and *X*,[3] which are referred to in the text as saturated half-cells, were prepared with a mercury layer, *L*, covering the platinum contact wire *M*, to a depth of 1 to 1.5 cm and having a surface area of approximately 4 cm^2, and a calomel layer *K*, of 1 to 2 mm depth, a layer of KCl crystals, *J*, of about 1.5 cm depth, and a water solution of KCl, *O*, saturated at 25.0° C. Preliminary saturation of the KCl solution with calomel would have no measurable effect on the results reported. These half-cells were installed in dewar flasks *I*. Half-cell *H*, which is referred to in the text as the 4.1 *N* half-cell, was prepared in the same way as the preceding ones with the exception that the layer of KCl crystals was omitted. Half-cells *B*, *E*, and *L*, which are referred to in the text as 3.8 *N* half-cells, were prepared in the same way as *H*, with the exception that a 3.8 *N* KCl solution, which is saturated at about 20° C, was substituted for the 4.1 *N* solution. Half-cell *B* was not jacketed with a dewar flask but was left exposed to the air. Each half-cell was provided with a thermometer, *D*, graduated in 0.2° C divisions, which was immersed in the KCl solution to within 2.5 cm of the calomel layer. Calibrations of the thermometers showed a maximum deviation of 0.06° C from the graduated scale, and the readings were estimated to the nearest 0.1° C. The experimental half-cells were exposed to various temperatures between 22.2 and 31.3° C in a small, independent air bath, *B*, installed in a large constant-temperature room, *A*, kept at 25° C. The air bath was capable of being held constant to ±0.2° C at any temperature used and its temperature could be changed at the rate of 4 to 5° C/hr. The reference half-cells, indicated in figure 1, were arranged in the constant-temperature room outside of the air bath. A manifold, *S*, into which a 1-mm-capillary glass tube, *U*, from each of the half-cells led, and which was filled with a 4.1 *N* KCl solution containing an excess of solid KCl, was located in the constant-temperature room between the reference half-cells and those in the air bath. Each capillary tube contained a stopcock, *T*, to isolate the half-cell and prevent diffusion

[3] These letters are specific for the half-cells in the text and have no reference to the schematic drawing, figure 1.

between measurements. Reservoirs in the air bath and in the constant-temperature room supplied KCl solutions through the glass tubes, *E*, for fresh junctions. Copper wires, *Q*, led from the mercury contacts, *N*, of each half-cell to mercury cups, *P*, into which the potentiometer leads, *R*, dipped.

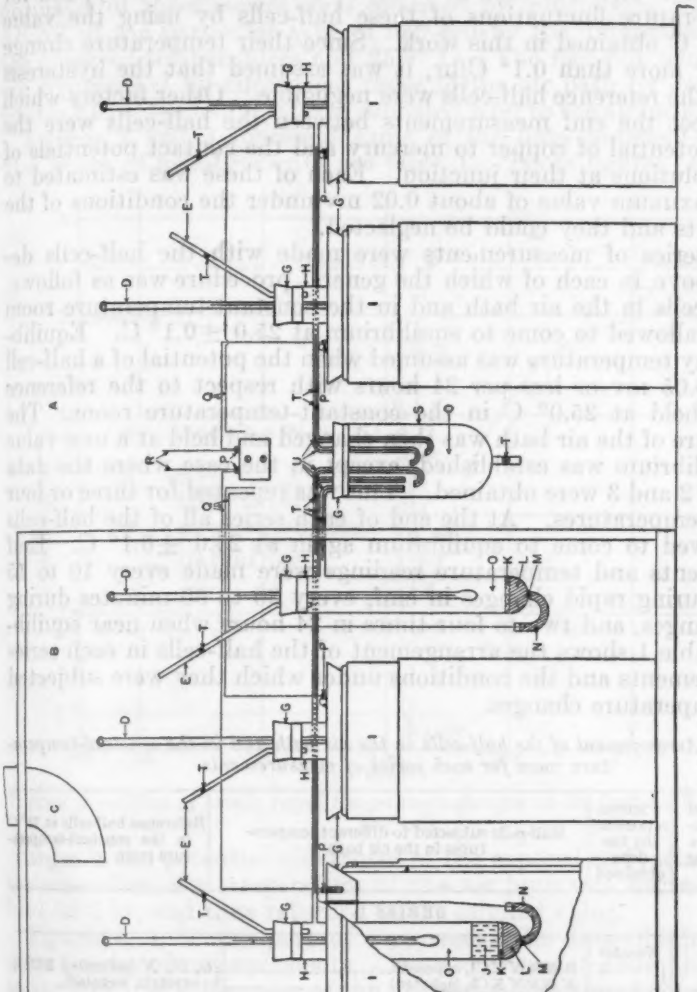

FIGURE 1.—*Details of the arrangement used in determining the effect of temperature on calomel half-cell potentials.*

A. Constant-temperature room.
B. Independent air bath.
C. Controlled air inlet.
D. Half-cell thermometers.
E. Leads to KCl reservoirs.
G. Rubber stoppers.
H. Half-cells.
I. Dewar flasks.
J. KCl crystals.
K. Calomel.
L. Half-cell mercury.
M. Sealed-in Pt wire.
N. Contact mercury.
O. KCl solution.
P. Mercury cups.
Q. Lead wires for half-cells.
R. Potentiometer leads.
S. Junction manifold.
T. Stopcocks.
U. Capillary salt bridges.

All values reported in figures 2 to 8 are the observed or calculated differences in potential, Δ mv, between the reference calomel half-cells at 25° C and the others placed in the air bath, and these values will be referred to throughout the text as the potential difference of the jacketed or exposed saturated system, 3.8 *N* system, etc. The emf was read to 0.001 mv with a Rubicon type *B* potentiometer and a reflecting type galvanometer with a sensitivity of 0.0005 μa/mm deflection at 1 m. The potentiometer readings were rounded off to the nearest 0.01 mv in the report. Although the room temperature was

25.0 ±0.1° C, the temperature of the reference half-cells varied from 24.7 to 25.2° C because of their proximity to the air bath and the radiation to and from it. As all of the observed potential differences, Δ mv, figures 2 to 8, of the half-cells subjected to temperature changes were expressed on the arbitrary basis that the average potential of the reference half-cells was zero at 25.0° C, corrections were applied for the temperature fluctuations of these half-cells by using the value 0.25 mv/° C obtained in this work. Since their temperature change was never more than 0.1° C/hr, it was assumed that the hysteresis effects in the reference half-cells were negligible. Other factors which might affect the emf measurements between the half-cells were the thermal potential of copper to mercury and the contact potentials of the salt solutions at their junction. Each of these was estimated to have a maximum value of about 0.02 mv under the conditions of the experiments and they could be neglected.

Three series of measurements were made with the half-cells described above, in each of which the general procedure was as follows: The half-cells in the air bath and in the constant-temperature room were first allowed to come to equilibrium at 25.0 ±0.1° C. Equilibrium at any temperature was assumed when the potential of a half-cell changed 0.05 mv or less per 24 hours with respect to the reference half-cells held at 25.0° C in the constant-temperature room. The temperature of the air bath was then changed and held at a new value until equilibrium was established, except in the case where the data for figures 2 and 3 were obtained. This was repeated for three or four different temperatures. At the end of each series all of the half-cells were allowed to come to equilibrium again at 25.0 ±0.1° C. Emf measurements and temperature readings were made every 10 to 15 minutes during rapid changes in emf, every 30 to 60 minutes during slower changes, and two to four times in 24 hours when near equilibrium. Table 1 shows the arrangement of the half-cells in each series of measurements and the conditions under which they were subjected to the temperature changes.

TABLE 1.—*Arrangement of the half-cells in the air bath and in the constant-temperature room for each series of measurements*

Maximum and minimum temperature of the air bath during each run	Figures representing the data obtained	Half-cells subjected to different temperatures in the air bath	Reference half-cells at 25° C in the constant-temperature room
SERIES 1			
°C	*Number*		
24 to 31	3	B (3.8 *N* KCl, exposed)	*G*, *N*, *X* (saturated KCl + crystals, jacketed).
	----	*E* (3.8 *N* KCl, jacketed)	
	2	*L* (3.8 *N* KCl, jacketed)	
SERIES 2			
22.2 to 31.5	5	*B* (3.8 *N* KCl, exposed)	*G*, *X* (saturated KCl + crystals, jacketed). *L* (3.8 *N* KCl, jacketed).
	4	*E* (3.8 *N* KCl, jacketed)	
	8	*H* (4.1 *N* KCl, jacketed)	
	6	*N* (saturated KCl + crystals, jacketed)	
SERIES 3			
25 to 31	----	*B* (3.8 *N* KCl, exposed)	*G* *X*, (saturated KCl + crystals, jacketed). *L* (3.8 *N* KCl, jacketed).
	----	*E* (3.8 *N* KCl, jacketed)	
	8	*H* (4.1 *N* KCl, exposed)	
	7	*N* (saturated KCl + crystals, exposed)	

The data obtained in the three series are represented graphically in figures 2 to 8. In each of these figures, the measured difference in potential, Δ mv, between a half-cell in the air bath and a reference half-cell at 25.0° C, are plotted against time in hours and represented by dots. For comparison, the temperatures of the KCl solution in the half-cell and of the air bath are plotted on the same scale. The ordinates of these curves were obtained by multiplying the average $\Delta E/\Delta T$ of the particular type of half-cell by the differences between the observed temperatures and 25.0° C. The half-cell temperatures are represented by circles and those of the air bath by crosses. In figures 2 to 8, the temperatures indicated refer to the air bath.

Figures 2 and 3 represent some of the data obtained from the first series of measurements, see table 1. These figures show the

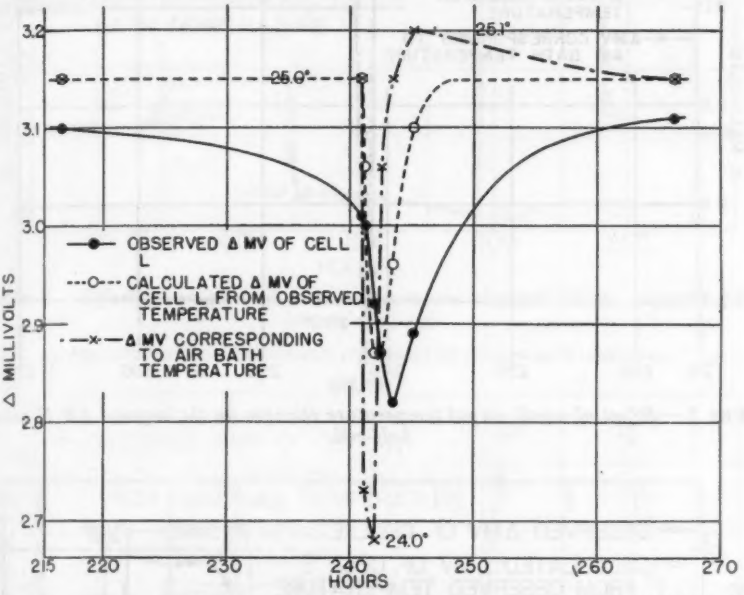

FIGURE 2.—*Effect of small, rapid temperature changes on the jacketed 3.8 N calomel half-cell.*

changes in the potential differences of the exposed and jacketed 3.8 *N* systems when the temperature of the air bath was decreased 1° C, held for 1 hr, and then returned to the original value.

Figures 4, 5, 6, and part of 8 represent the data obtained in the second series of measurements. Figures 4[4] and 5 show the changes in the potential differences of the exposed and jacketed 3.8 *N* systems during increasing and decreasing temperatures.

Figures 7 and part of 8 represent some of the data obtained in the third series of measurements. Figures 6 and 7 show the changes in the potential differences of the exposed and jacketed saturated systems with solid KCl present, and figure 8 shows those of the 4.1 *N* system at temperatures above and below its saturation point.

[4] Half-cell *E*, with values recorded in figure 4, was of different construction from the others. It was a 4-pocket, vertical cell, 4 half-cells in one container, with the mercury cups arranged in balconies one above the other and a common central opening extending the height of the cell and filled with the KCl solution. The Pt contact was near the surface of the Hg and the potentials of the individual half-cells varied when the container was handled. Half-cell L, similar in make-up to *E*, showed a temperature coefficient which was identical to that of the exposed type, but insufficient readings were made during the rise and fall of the temperature to determine the steep portion of the curve with any degree of accuracy.

In order to check the possibility that the temperature of the KCl solution and the mercury in a half-cell did not change at the same rate during an increase or decrease in the temperature of the air bath, a cell was arranged with two thermometers, one with its bulb completely

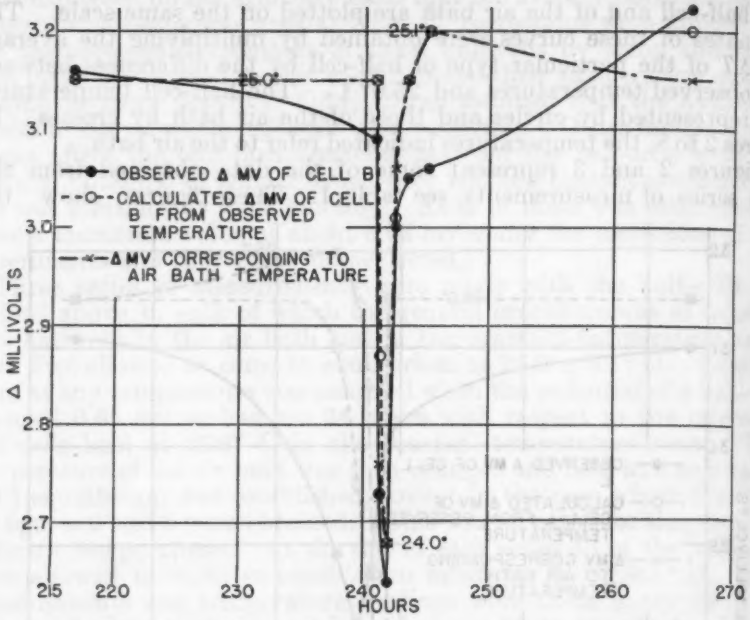

FIGURE 3.—*Effect of small, rapid temperature changes on the exposed 3.8 N calomel half-cell.*

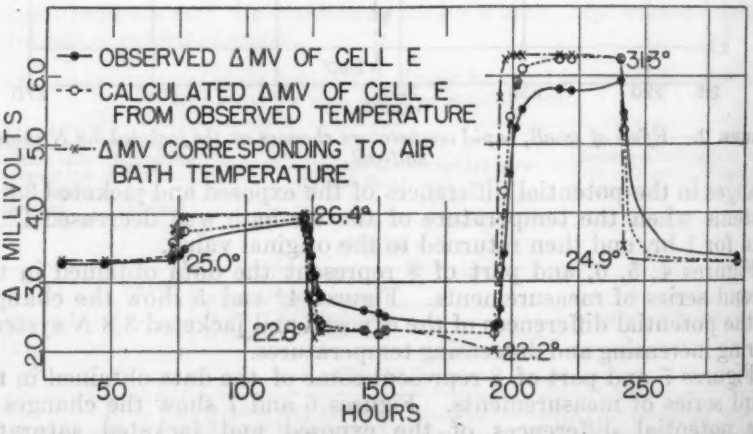

FIGURE 4.—*Effect of small and large temperature changes on the jacketed 3.8 N calomel half-cell.*

Approximate Hg temperatures are represented by triangles on the emf scale.

immersed in the mercury of the half-cell and the other extending to within 2.5 cm of the mercury and immersed in the KCl solution. The thermometer whose bulb was in the KCl solution corresponded to the

position of those in the half-cells used in obtaining the data for figures 2 to 8. The half-cell was subjected to changes in temperature in both the exposed and the jacketed state, which were comparable to those represented in figures 4 to 8, and the two thermometers were read at various time intervals so that the temperature-time relationships of the two liquids and the air bath could be correlated. The data obtained showed that during changes of temperature in the air bath

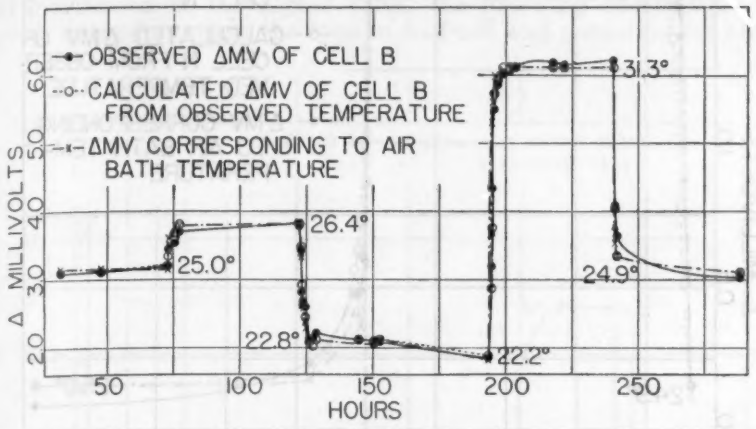

FIGURE 5.—*Effect of small and large temperature changes on the exposed 3.8 N calomel half-cell.*

Approximate Hg temperatures are represented by triangles on the emf scale.

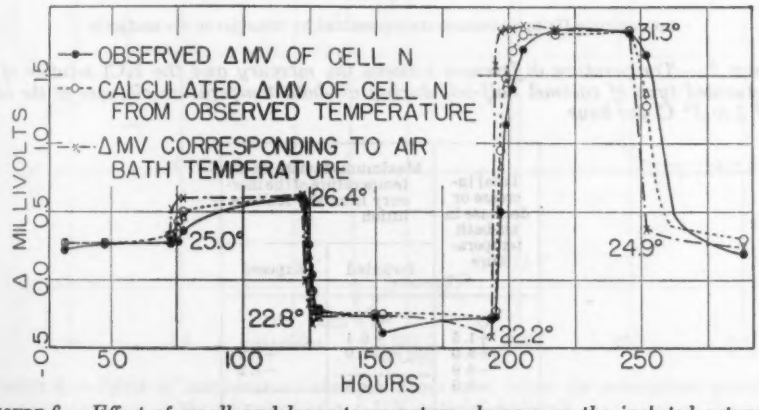

FIGURE 6.—*Effect of small and large temperature changes on the jacketed saturated calomel half-cell.*

Approximate Hg temperatures are represented by triangles on the emf scale.

there was a difference in temperature between the KCl solution and the mercury. This difference began with the first change in the temperature of the half-cell and increased rather rapidly during the first half of the total temperature increase or decrease, and then gradually decreased as the temperature of the two liquids approached that of the air bath. Table 2 shows the maximum differences between the temperatures of the mercury and the KCl solution for the saturated

type of half-cell. Similar effects were observed in the 3.8 *N* half-cell but with slight differences in magnitude. Some approximate points corresponding to the Hg temperatures are plotted in figures 4 to 7 and are indicated with triangles.

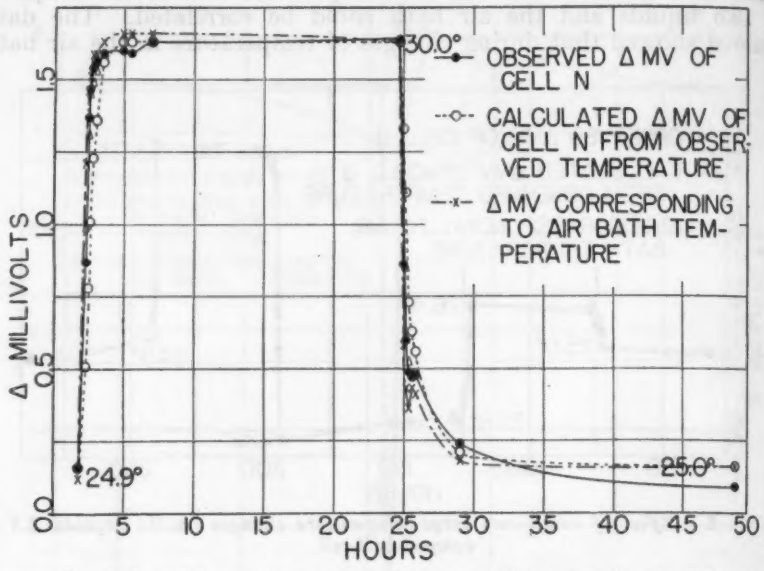

FIGURE 7.—*Effect of large temperature changes on the exposed saturated calomel half-cell.*

Approximate Hg temperatures are represented by triangles on the emf scale.

TABLE 2.—*Temperature differences between the mercury and the* KCl *solution of a saturated type of calomel half-cell during air-bath temperature changes at the rate of 4 to 5° C per hour*

Total increase or decrease in air-bath temperature	Maximum deviations in temperature of the mercury from the KCl solution	
	Jacketed	Exposed
°C	°C	°C
+1.5	−0.1	----------
+6.0	−.9	+2.2
−6.0	----------	−1.2
−8.0	+.3	----------

III. DISCUSSION

The dewar flasks surrounding the half-cells retarded the effect of changing external temperature on their temperatures and potentials. For small fluctuations in temperature, figures 2 and 3, the observed potential difference of the jacketed system was less and the potential difference of the exposed system was greater in amount than that calculated from the air bath temperature. Thus, for small changes above and below a uniform temperature, the potential difference of a

jacketed system was subject to smaller changes than the exposed type. For small temperature changes in one direction, in the first portion of the curves in figures 4, 5, and 6, there was a period of several hours in which the potential difference of the jacketed system did not change appreciably, while that of the exposed system followed the temperature almost immediately.

When the temperature of the air bath was increased 8° C in 2 hours and maintained at the higher value, the following effects were observed, depending upon the type of half-cell and persisting for about

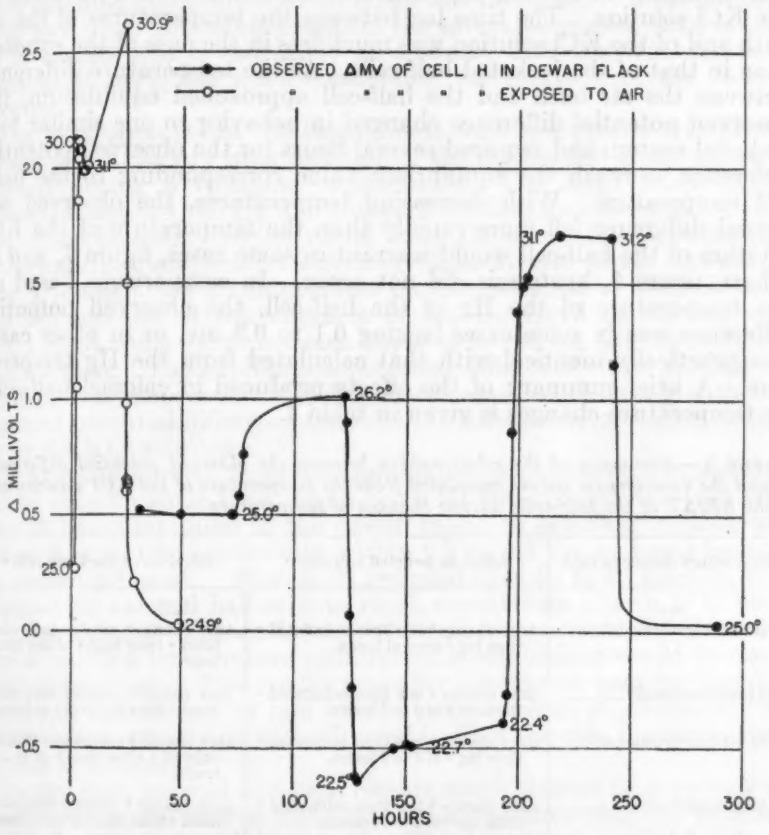

FIGURE 8.—*Effect of temperature changes above and below its saturation point on the potential of a 4.1 N calomel half-cell.*

60 to 80 percent of the rise. The potential differences of the jacketed systems lagged behind the equilibrium potential difference corresponding to the temperature of the KCl solution by 0.5 to 0.9 mv, 0.3 to 0.8 mv behind that corresponding to the Hg temperature, and 2 to 3 mv behind that corresponding to the air bath temperature; see figures 4 [5] and 6. These differences then gradually became smaller

[5] The behavior of this half-cell cannot be analyzed too closely, see footnote 4, and only its general concordance can be assumed.

until equilibrium was established. With a falling temperature, the hysteresis again occurred, but to a less extent. After the air-bath temperature began to increase, 1 to 2 hours elapsed before an appreciable temperature increase was observed in the half-cell temperature. This time lag slowly increased to 5 to 7 hours near the new temperature level. On the other hand, in the exposed half-cells, figures 5 and 7, the observed potential differences of these systems increased more rapidly than the equilibrium values corresponding to the temperatures of the KCl solution, but the reverse occurred if the equilibrium values corresponding to the Hg temperatures were substituted for those of the KCl solution. The time lag between the temperatures of the air bath and of the KCl solution was much less in the case of the exposed than in that of the jacketed half-cells. As the temperature difference between the air bath and the half-cell approached equilibrium, the observed potential difference changed in behavior to one similar to a jacketed system and required several hours for the observed potential difference to reach the equilibrium value corresponding to the half-cell temperature. With decreasing temperatures, the observed potential difference fell more rapidly than the temperature of the KCl solution of the half-cell would warrant in some cases, figure 7, and in others, figure 5, hysteresis did not occur. In comparisons based on the temperature of the Hg of the half-cell, the observed potential difference was in some cases lagging 0.1 to 0.3 mv, or in other cases was practically identical with that calculated from the Hg temperature. A brief summary of the effects produced in calomel half-cells by temperature changes is given in table 3.

TABLE 3.—*Summary of the relationships between the observed potential differences and the equilibrium values calculated from the temperature of the* KCl *solution and the* $\Delta E/\Delta T$ *of the half-cells during changes of temperature*

Temperature change in bath	Effect on jacketed half-cells [a]	Effect on exposed half-cells [a]
°C		
±1 (rapid fluctuations)	Δmv change [b] less than calculated [c] time lag [d] several hours.	Δmv change [b] greater than calculated [c] time lead [e] of less than 1 hour.
+1.5 (unidirectional) [f]	Δmv change [b] less than calculated [c] time lag [d] of 6 to 7 hours.	Δmv change [b] greater than calculated [c] time lead [e] of 1 to 2 hours.
−3 to −6 (unidirectional) [f]	Δmv change [b] less than calculated [c] time lag [d] of 1 to 7 hours.	Δmv change [b] =or greater than calculated [c] time lead [e] of ½ to 2 hours.
+8 (unidirectional) [f]	Δmv change [b] less than calculated [c] time lag [d] of 2 to 10 hours.	Δmv change [b] greater than calculated [c] time lead [e] of ½ to 2 hours.

[a] The magnitude of the differences between the observed and calculated potentials for the exposed and jacketed systems of the same type were of the same order but opposite in effect.
[b] Observed potential difference.
[c] Calculated from the temperature of the KCl solution and the $\Delta E/\Delta T$ of the half-cells.
[d] Time required for the observed potential differences to equal the values calculated from the temperatures of the KCl solution.
[e] Time required for the values calculated from the KCl solution temperatures to equal the observed potential differences.
[f] Temperature change between two steady states.

In comparing the behavior of the three types of half-cells, it will be noticed that while the $\Delta E/\Delta T$ of those saturated at all temperatures used and those undersaturated, 3.8 N, are different in magnitude, they behave in a similar and rather consistent manner.[6] On the other

[6] See footnotes 4 and 5.

hand, the half-cell saturated at 25.0° C and without an excess of solid KCl, showed an inconsistent $\Delta E/\Delta T$ as well as a variation of 0.4 to 0.5 mv in the equilibrium potential at 25.0° C. The variable $\Delta E/\Delta T$ was probably due to the half-cell acting first as a supersaturated half-cell and then as one saturated with an excess of crystals at temperatures below 25.0° C and as an undersaturated half-cell at temperatures above 25.0° C. In considering the potentials measured in the saturated system, it is possible that part of the value might be attributed to a concentration or diffusion potential of the KCl solution. It would then follow that the saturated system should show a long drift while reaching equilibrium or an overshoot in voltage. This did not occur to a more noticeable extent in the saturated system than in the 3.8 *N* system and it can safely be assumed that the concentration potential is negligible when considering the precision of the values reported.

The data obtained in the experiments were not precise enough to allow any satisfactory interpretation of the mechanism of the calomel half-cell during a changing temperature. The large temperature difference between the Hg and the KCl solution and the small thickness of the boundary region would make the accurate determination of the interface temperature extremely difficult, and would also introduce a temperature gradient effect on the potential of the half-cell. The temperature of the interface of the Hg–HgCl in the half-cell would be at some value between those observed for the Hg and the KCl solution. The equilibrium potential difference corresponding to the interface temperature would probably agree more closely with the observed potential difference than did the values corresponding to the Hg or the KCl solution.

The results showed, however, that stable conditions of temperature should exist for some time, 2 to 3 hours for the exposed half-cells and 7 to 10 hours for those in the dewar flasks, to establish equilibrium values that will be accurate to within 0.2 to 0.3 mv and satisfactory for precise pH work. Magoji [7] reported that 30 to 40 minutes was required for calomel half-cells to reach equilibrium after a 5° C temperature change. His work was performed in a water bath, where the rate at which a temperature equilibrium is established would be more rapid than in air. This would probably account in part for the difference in time found by him for the cells to reach equilibrium. In addition, the size of the half-cell would affect the rate at which equilibrium is attained.

In any case, calomel half-cells require much shorter time periods to reach equilibrium after a temperature change than they do to reach equilibrium when freshly prepared. This latter time period has been variously reported to be 2 days to 2 weeks [4, 7, 11]. The exposed half-cells would be more serviceable under conditions where large and rapid temperature changes, 3° C or more per hour, occur. For small fluctuations in temperature, the jacketed half-cell would be more serviceable, as the potential would be less variable and near a value corresponding to the mean temperature. There is apparently very little choice between the saturated and the undersaturated half-cells if only reproducibility and the time required to reach equilibrium at a new temperature are considered. However, the undersaturated half-cells have a larger $\Delta E/\Delta T$ than the saturated type and, furthermore, their potentials would have to be determined for the concentration of KCl solution used, unless standard buffers and a hydrogen electrode are

used in the calibration of a cell system. This, together with the difficulty of preventing evaporation and an accompanying change in the value of the half-cell, would indicate that the saturated type with an excess of crystals would be more serviceable for general use.

The $\Delta E/\Delta T$ of the saturated half-cell with an excess of solid KCl was found to be 0.25 mv/° C, and that of the 3.8 *N* KCl half-cell to be 0.47 mv/° C. Ewing [5] gives the saturated half-cell a $\Delta E/\Delta T$ of 0.20 mv/° C, and Bjerrum and Unmack [2] the value 0.22 mv/° C. The value obtained in this work agrees fairly well with the above results considering that only one half-cell was used in its determination. Taking the value 0.2 mv/° C as the $\Delta E/\Delta T$ of the calomel half-cell and the value −0.76 mv/° C [3] for the cell,

$$-\text{Pt, } H_2(1 \text{ atm}) \mid \text{HCl}(1\ N) \parallel \text{KCl(saturated)} \mid \text{HgCl, Hg}+,$$

then the $\Delta E/\Delta T$ of the hydrogen half-cell together with the liquid junction must be in the neighborhood of +1.0 mv/° C. This would indicate that the temperature of the hydrogen half-cell is the most important factor in the variation of the cell combination: saturated calomel–Pt−H_2. It has been customary, however, to assume the $\Delta E/\Delta T$ of the hydrogen half-cell to be zero and to throw the entire weight of the emf change on the companion reference half-cell. Under varying conditions encountered in commercial laboratories, as in the measurement of the pH of a solution having a temperature different from that of the reference half-cell, considerable error may be introduced when one half-cell is calculated to a value corresponding to the temperature of the companion half-cell by the use of the over-all $\Delta E/\Delta T$ of the cell. It should again be emphasized that for more precise and reproducible results the temperature of the cell system and the unknown solution, if possible, should be constant for several hours before measurements are made.

IV. CONCLUSIONS

The jacketing or insulating of calomel half-cells with dewar flasks does not eliminate the hysteresis, but in the case where small, fluctuating temperature changes are encountered the magnitude of the variation in potential is reduced.

Errors due to hysteresis in a jacketed half-cell during a temperature increase may amount to 0.5 to 0.9 mv, which is equivalent to 0.01 to 0.02 pH, depending on the type of half-cell, and 0.4 to 0.5 mv for exposed half-cells, when the temperature change is 6 to 8° C at a rate of 4 to 5° C/hr, and the temperature of the half-cell is taken as that of its KCl solution. Under similar conditions a drop in temperature of 6° C may give a hysteresis error of 0.5 mv.

Temperature differences were found between the Hg and the KCl solution of a half-cell during changes in temperature of the air bath. These varied from 0.1 to 2.2° C, depending on the magnitude of the change, at a uniform rate, in the temperature of the air bath. In the exposed half-cells, the Hg temperature was higher than that of the KCl solution during an increase and lower during a decrease in temperature of the air bath. The reverse occurred in the jacketed half-cell.

In determining the temperature of a half-cell for voltage corrections, it should be measured inside the half-cell and as close to the Hg interface as possible, rather than in the surrounding air.

The half-cell with an excess of solid KCl and hence saturated near the Hg interface at all temperatures used, had a $\Delta E/\Delta T$ of 0.25 mv/° C over the range 22.5 to 31.3° C. The 3.8 *N* half-cell, undersaturated at all temperatures used, had a $\Delta E/\Delta T$ of 0.47 mv/° C for the above range. The half-cell saturated at 25° C showed a variable and inconsistent $\Delta E/\Delta T$.

Care should be taken in the control and measurement of the temperature of a hydrogen half-cell during pH measurements as the apparent $\Delta E/\Delta T$ of this half-cell together with the liquid junction potential is in the neighborhood of 1.0 mv/° C and large errors could be introduced.

In pH measurements requiring an accuracy of 0.1 pH, temperature variations of 4 to 5° C could be tolerated without temperature corrections. For precision results to 0.01 to 0.02 pH, the measurements should be made in constant temperature air or liquid baths and after the temperature of the cell system has been uniform for several hours.

V. REFERENCES

[1] L. D. Bircher, and G. D. Howell. J. Am. Chem. Soc. **48,** 34 (1926).
[2] N. Bjerrum and A. Unmack. Mathem.-fysiske Medd. Danske Salsk. **9,** 23 (1929).
[3] W. M. Clark. *Determination of hydrogen ions.* Williams and Wilkins Co. Baltimore, Md. (1928).
[4] F. W. Clarke, C. N. Myers, and S. F. Acree. J. Phys. Chem. **20,** 256 (1916).
[5] W. W. Ewing. J. Am. Chem. Soc. **47,** 30 (1935).
[6] H. A. Fales and W. A. Mudge. J. Am. Chem. Soc. **42,** 2434 (1920).
[7] Hiraki Magoji. Acta Schol. Med. Univ. I, p. Kioto **14,** 300 (1932).
[8] G. N. Lewis and M. Randall. J. Am. Chem. Soc. **36,** 1969 (1914).
[9] N. E. Loomis and S. F. Acree. Am. Chem. J. **46,** 585 (1911).
[10] L. Michaelis. *Die Wasserstoffionen Konzentration,* Berlin (1925).
[11] C. N. Murray and S. F. Acree. BS J. Research **7,** 713 (1931) RP369.
[12] H. Riehm. Z. phys. Chem. **160,** 1–7 (1932).
[13] G. Scatchard. J. Am. Chem. Soc. **47,** 696 (1925).
[14] E. Vellinger. Arch. Phys. Biol. **5,** 119 (1926).
[15] B. Wingfield and S. F. Acree. J. Assn. Leather Chem. **31,** 403 (1936).

Washington, June 18, 1937.

U. S. Department of Commerce National Bureau of Standards

RESEARCH PAPER RP1019

Part of Journal of Research of the National Bureau of Standards, Volume 19, August 1937

DEVICE FOR TESTING HAEMACYTOMETERS AND OTHER PIPETTES OF SMALL CAPACITY

By Elmer L. Peffer

ABSTRACT

An instrument employing a volumetric method and used in the rapid and accurate testing of dilution pipettes is described. A double-walled evacuated cylinder is fitted with two metal plungers actuated by micrometer heads and a third opening is fitted with a rubber stopper having a hole to receive and hold without leakage of liquid the pipette to be tested. The test liquid is a 3 to 5 percent (by weight) solution of potassium dichromate in water. The plungers have cross-sectional areas in the ratio of 10:1 and have diameters designed to cover the range of all ordinary dilution pipettes.

The pipette, in the inverted position, is placed in the hole of the rubber stopper, and the large plunger, actuated by the micrometer head, is turned into the chamber until the liquid reaches the first graduation. The micrometer is then read. This micrometer is further advanced until the liquid fills the bulb and reaches the first graduation above the bulb. The micrometer is again read. The difference of these readings indicates the advancement of plunger in the test liquid. The same procedure is followed with the small plunger completing the calibration of the graduated capillary. The dilution ratios of the pipette are determined directly by the linear movement of the cylindrical plungers, as determined by the micrometer readings.

For many years it was customary practice at the National Bureau of Standards to use a weight method in the test of dilution pipettes, to determine the relative capacities, and thence the volume ratios, of the intervals tested.

In recent years, however, the great increase in the number of dilution pipettes submitted to the Bureau for test has made it necessary to develop a test method that would be more rapid than the weight method and at the same time sufficiently accurate for the purpose. With this end in view, the apparatus described herein was developed. It has been found entirely satisfactory with respect to both speed and accuracy. The apparatus is shown in figures 1 and 2.

The principle involved is that of displacing a volume of liquid by two cylindrical plungers of known relative areas of cross section, each plunger being actuated by a calibrated micrometer screw with a graduated indicating head. The cross-sectional areas of the plungers are in the ratio of 10:1, and the micrometer screws and graduated heads, which actuate the plungers and indicate their positions, are of equal pitch and are graduated in the same manner. Thus, when the two plungers are advanced the same distance as indicated by the graduated micrometer heads, the volume of liquid displaced by the larger plunger is 10 times that displaced by the smaller one. The micrometer heads are of the ordinary type used by machinists and instrument makers, having a screw of 40 threads to the inch, a rotatable thimble with 25 graduations around its circumference, and a range

of 1 inch. Thus, 1 division is equal to 0.001 inch, and readings are made to 0.0001 inch.

The large and the small cylindrical plungers have diameters of 0.3921 inch and 0.1240 inch, respectively. A movement of the full range of 1 inch, therefore, results in a liquid displacement of 0.1208 cubic inch for the larger cylinder, and 0.01208 cubic inch for the smaller. Expressed in milliliters, these volumes are approximately 2.0 and 0.2 ml, respectively. These volumes are adequate to cover the capacity range of all ordinary dilution pipettes.

Since the diameters of the cylindrical plungers are known, and the micrometer screws and graduated heads can be accurately calibrated, it would be possible to prepare a table for each plunger and micrometer showing the volumes of displaced liquid represented by various differences in micrometer readings. For use in the testing of dilution pipettes, however, such a table is unnecessary since all that is required in the testing of these pipettes is to determine the ratio of the volumes of the various intervals under test. These ratios are determined directly by the linear movement of the cylindrical plungers, as determined by the micrometer readings.

In the upper surface of the double-walled glass container is a third opening fitted with a rubber stopper having a hole of suitable size to receive and hold without leakage of liquid the pipette to be tested.

The test liquid employed is a 3 to 5 percent solution (by weight) of potassium dichromate in water. A suitable container for the test liquid is provided in the form of a double-walled evacuated glass cylinder with rounded ends, this container being mounted on a wooden base. In each end of the cylindrical container is an opening through which the micrometer plunger enters. The micrometer is sealed securely in place by a metal-in-glass ground joint.

The double-walled evacuated chamber for containing the test liquid was found necessary to prevent excessive volume changes of the test liquid as a result of temperature changes during test of a pipette.

The use of dichromate solution as the test liquid was found to have two advantages: first, this liquid served as a rust inhibitor, and second, the amber color of the liquid made possible quick and accurate setting of the liquid meniscus on the graduation lines.

In testing a dilution pipette the pipette is inverted and what is normally the upper end of the capillary tube is inserted in the hole in the rubber stopper which is in the opening in the upper surface of the double-walled glass chamber.

With the micrometer which actuates the smaller of the two cylindrical plungers set on zero, and the surface of the test liquid below the first graduation mark on the pipette, the micrometer which actuates the larger plunger is turned and the cylinder advanced into the chamber until the liquid surface in the capillary reaches the first, or lowest graduation mark. The micrometer is then read. The same micrometer is then further advanced and the test liquid forced into the pipette, filling the capillary below the mixing chamber, the mixing chamber, and the capillary up to the first graduation mark above the mixing chamber. The micrometer is then again read. The difference between the two readings of this micrometer indicates the amount the plunger has been advanced into the test liquid.

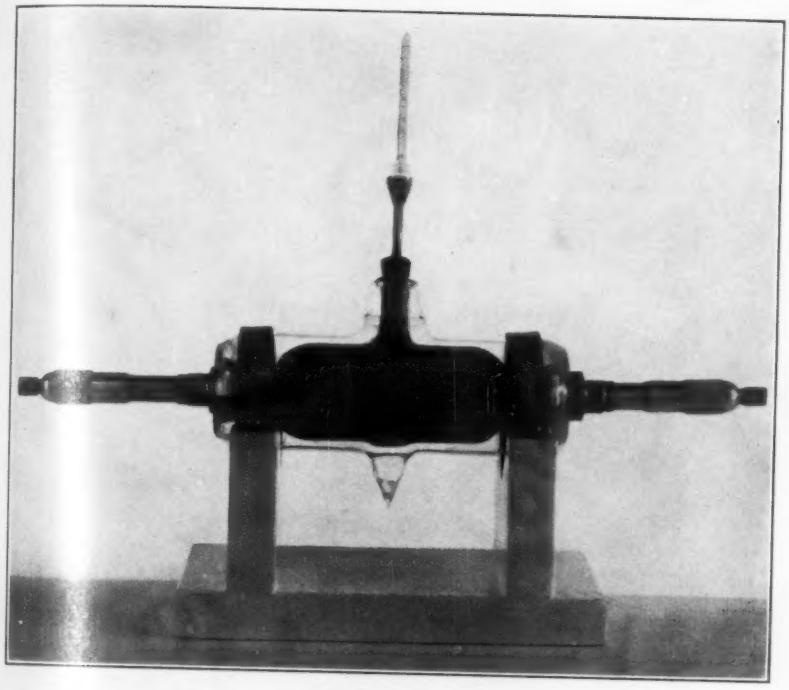

FIGURE 1.

UNIV. OF MICH.

The micrometer which actuates the smaller of the two plungers is then turned in such a direction as to advance this plunger into the test liquid, and the liquid is thus forced into the pipette until the liquid surface advances in the graduated capillary tube to the desired graduation. The micrometer is then read, and, since the areas of cross section of the plungers are as 10:1, the ratio of the intervals under test is 10 times the ratio of advance of the large plunger to the advance of the small plunger, as indicated by the micrometers.

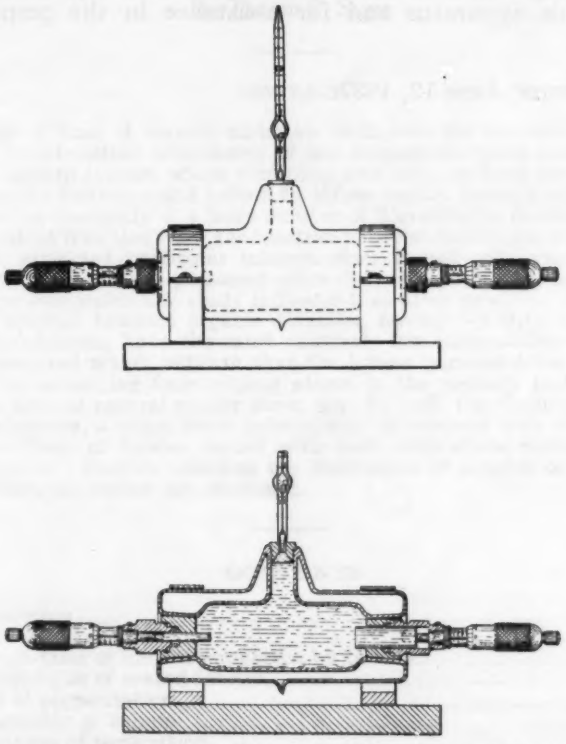

FIGURE 2.—*Sketch and cross section of dilution pipette testing apparatus.*

The ratio of the volumes of the two intervals on the pipette, as thus determined, is the "dilution ratio" of the pipette. It is customary to determine the "dilution ratio" for each pipette when using a full unit and when using a half unit of blood; for example, 100:1 and 200:1 for pipettes used in counting red corpuscles, and 10:1 and 20:1 for those used in counting white corpuscles.

The apparatus is checked from time to time by comparison of its results with those obtained by the weight method.

In general, the tolerances permitted on dilution pipettes are 5 percent for the pipette used in counting red corpuscles and 3.5 percent for the pipette used in counting white corpuscles. The apparatus and test method herein described yield results that are accurate to about one-fifth of the tolerance.

While the apparatus herein described was designed and is used primarily for the testing of dilution pipettes, it could readily be used for testing any other pipettes or similar apparatus within its capacity range, for the graduation and calibration of small measuring pipettes, for the filling of ampules, or for other purposes where the accurate delivery of small volumes or the testing of small capacities is desired.

Acknowledgment is due to H. W. Bearce for advice in the development of this apparatus and for assistance in the preparation of the paper.

WASHINGTON, June 12, 1937.

U. S. Department of Commerce National Bureau of Standards

RESEARCH PAPER RP1020

Part of Journal of Research of the National Bureau of Standards, Volume 19, August 1937

PERMEABILITY OF ORGANIC POLYSULPHIDE RESINS TO HYDROGEN[1]

By Theron P. Sager

ABSTRACT

The ability of films of organic materials to impede the passage of gases is of importance in connection with many of our modern products and particularly balloon and airship fabrics, where thin films and large surfaces are encountered. The tendency for hydrogen and helium to diffuse readily through rubber has been the incentive for the study of a large number of film-forming materials. Among these the product resulting from the reaction between dichloroethane and sodium polysulphide attracted particular interest since it not only exhibited a high impedance to hydrogen but possessed other desirable physical characteristics as well. A more comprehensive study indicates that other products, resulting from the general reaction between organic dihalides, having $-CH_2Cl$ terminals, and metallic polysulphides, have the same relatively low permeability to hydrogen. Data are presented which indicate that the lowest permeabilities are obtained with products containing four sulphur atoms in the primary molecule. Comparison with films of natural rubber show, that for both the disulphide and tetrasulphide derivatives, a much lower permeability is obtained with these products. The permeabilities of fabrics coated with both derivatives indicate the same relative behavior. Factors affecting the limitations of weights of coatings and the permeability to helium are discussed.

CONTENTS

		Page
I.	Introduction	181
II.	Experimental method	182
III.	Permeabilities of films unsupported by fabrics	183
IV.	Permeabilities of coated fabrics	184
V.	Effect of pigmentation	186
VI.	Permeability of helium	186
VII.	Mechanism of permeation	187
VIII.	References	187

I. INTRODUCTION

A characteristic of balloon and airship fabrics which is of prime importance is that they shall be gas-tight, or nearly so. The inherent tendency of hydrogen and of the more costly gas helium to diffuse through thin membranes of rubber provides the incentive for the study of the behavior of a large number of film-forming materials in a search for a more satisfactory material. Considering all of the requirements involved in this application, the permeability of the group of synthetic polymers which are characterized by elastic extensibility has been of particular interest.

[1] Presented as part of the Symposium on Organic Plastics before the Division of Paint and Varnish Chemistry at the 93rd Meeting of the American Chemical Society, Chapel Hill, N. C., April 12 to 15, 1937.

The general reaction between organic dihalides, having $-CH_2Cl$ terminals, and inorganic polysulphides has been shown to yield products which in many cases are characterized as rubber-like. Martin and Patrick [3, 4][2] have suggested that the structure of the polysulphide resins is that of long-chain polymers in which the radicals are connected through disulphide linkages and represented as: $-R-S-S-R-S-S-R-$. According to their hypothesis any additional sulphur in the material in excess of that required to provide the disulphide linkages is believed to be coordinately linked to the sulphur comprising the disulphide linkages. The structure is represented as

$$-R-\underset{\underset{S}{\|}}{S}-\underset{\underset{S}{\|}}{S}-R-\underset{\underset{S}{\|}}{S}-\underset{\underset{S}{\|}}{S}-R-$$

with the added possibility that the coordinately linked sulphur may be in a *trans* rather than a *cis* arrangement. It has been shown that the radical may be derived from ethylene or one of its homologs, or it may be obtained from a reactant containing an ether group, a sulphide group, or an unsaturated group. It is of interest particularly in connection with the present discussion that certain of these products exhibit elasticity, both when the amount of sulphur is confined to that representing the disulphide linkages and when the primary molecule contains sulphur in excess of these linkages.

What is often given as the specific example of the formation of this type of plastic is the product obtained when the reactants are dichloroethane and sodium polysulphide. Shortly after the addition of this material to the growing list of synthetic plastics, a compound containing this material was applied to a closely woven fabric by calendering. The weight of coating was 5.2 oz/yd^2 (176 g/m^2). The permeability to hydrogen of this fabric was found to be 0.014 ft^3/yd^2 (0.5 liter/m^2) per 24 hours. The low permeability of this material can be appreciated more fully when it is stated that a fabric coated with the same weight of a rubber compound would have a permeability of as much as 20 times this value.

There were, however, several objections to the use of the polyethylene polysulphide product for this purpose. This material cannot be dispersed in suitable solvents and does not therefore adapt itself easily to application in the form of a plurality of thin films to fabric. A somewhat less important objection is its distinctive and unpleasant odor, which made it undesirable for use on gas-cell fabric aboard an airship. With the extension of this general reaction to include other organic dihalides and the production of materials which are capable of being dispersed in solvents to form cements, their utility was greatly enhanced and their laboratory investigation rendered comparatively simple. The odor of these products is moreover much less offensive.

II. EXPERIMENTAL METHOD

The materials were prepared in a manner similar to the preparation of rubber cements; the resins were masticated on a differential speed mill and the compounding ingredients were added on the mill. The compounds contained ten parts of zinc oxide and one-tenth to two-tenths part of such accelerators as tetramethylthiuram disulphide and

[2] Numbers in brackets refer to the references at the end of this paper.

benzothiazyl disulphide. Thin cements were prepared by dispersing the compounds in beta-trichloroethane. In the preparation of films unsupported by fabric, the cements were applied to regenerated cellulose sheeting which had not been coated with any moisture-proofing composition [5]. After being cured in dry heat for 50 minutes at 130° C (268° F), the uncoated surface of the regenerated cellulose was moistened with water. The polysulphide films could then be removed without any appreciable deformation. In the preparation of coated fabrics, the cements were applied to closely woven balloon cloth by means of a small spreading machine. The curing conditions were the same as for the unsupported films.

The permeabilities were determined by means of a gas interferometer of the Rayleigh type. The apparatus and conditions of test have been previously described [1].

III. PERMEABILITIES OF FILMS UNSUPPORTED BY FABRIC

In table 1 are presented the permeabilities to hydrogen obtained with unsupported films of different thicknesses. The organic polysulphide products represent the disulphide and tetrasulphide derivatives obtained from the reaction between 2, 2′-dichloroethyl ether and sodium polysulphide. Values obtained with films of rubber of approximately corresponding thicknesses are included for comparison.

TABLE 1.—*Permeabilities to hydrogen of unsupported films*

Average thickness		Permeability		Specific permeability
cm	in.	l/m²/24 hr	ft³/yd²/24 hr	
DISULPHIDE DERIVATIVE				
0.030	0.012	0.6	0.018	12.5
.025	.010	.8	.024	13.8
.017	.007	1.4	.041	16.2
.015	.006	1.5	.044	14.6
.011	.004	2.2	.065	16.8
TETRASULPHIDE DERIVATIVE				
0.033	0.013	0.2	0.006	4.5
.024	.010	.4	.012	6.6
.019	.008	.6	.018	7.9
.016	.006	.8	.024	8.8
.009	.004	1.2	.036	7.5
RUBBER				
0.030	0.012	10.0	0.295	208
.025	.010	14.2	.419	246
.018	.007	20.0	.590	250

The results indicated sufficient uniformity to warrant the calculation of what may be called the specific permeability, or the volume of gas passing through a unit area of a material of unit thickness in unit time. This was calculated by means of the equation $P=Vd/At$, in which P is the specific permeability, V the volume of hydrogen in cubic centimeters, d the thickness in centimeters, A the area in square centimeters, and t the time in minutes.

The values for the specific permeability of rubber are in close agreement with those obtained by Kayser [2] and Edwards and Pickering [1]. The values obtained with both the disulphide and tetrasulphide derivatives are much lower than those with corresponding thicknesses of rubber, and those of the tetrasulphide product are consistently lower than those of the disulphide derivative.

While the specific permeabilities of the disulphide and tetrasulphide derivatives are of the same order of magnitude, they are not constant. This would appear to indicate that permeability in the case of these materials is not a linear function of the thickness. A possible explanation for this deviation is that the permeabilities were determined with a slight excess of pressure on the hydrogen side of the test specimen (30 mm of water), which, in the case of thin films, may have produced a small undeterminable reduction in thickness while under test.

IV. PERMEABILITIES OF COATED FABRICS

It has been previously observed that the permeability of a given weight of rubber of definite area is greatly decreased when it is spread on a corresponding area of cloth [1.] It has also been noted that the thread count of the cloth exerts an influence [6]. The permeabilities of fabrics of different thread counts, coated with the same weight of rubber, become lower as the thread count increases. The values given in figure 1 represent the permeabilities obtained on a fabric coated with different weights of the two polysulphide resins which were employed in the determinations of the permeabilities of unsupported films. The cloth employed was that designated as *HH* balloon cloth, a square-woven cotton fabric having a thread count of 120 in both directions, the average weight of a square yard being 2.05 oz.

The results indicate the same relative difference in the permeabilities of the two derivatives as was obtained in the examination of the unsupported films.

The effect of the supporting fabric upon the permeability is apparent when comparison is made with the values obtained for unsupported films given in table 1. For example, a film of the tetrasulphide derivative having a thickness of 0.009 cm (0.004 in.) weighs about 4.6 oz/yd^2. When unsupported by fabric, this film has a permeability of 0.035 ft^3/yd^2/24 hr. If this same weight of material is applied to fabric, the permeability of the coated fabric will be, according to figure 1, about 0.008 ft^3. Likewise, a film of the disulphide derivative 0.011 cm (0.004 in.) in thickness weighs about 4.2 oz/yd^2 and has a permeability, when unsupported, of 0.064 ft^3. When applied to fabric the permeability of the coated fabric is about 0.035 ft^3.

The specific gravity of the compound containing the disulphide derivative is 1.426 and that containing the tetrasulphide derivative is 1.547. The covering power of these compounds is not, therefore, as high as that of a corresponding compound of rubber, the specific gravity of which would be about 0.995. It is for this reason that, in the case of both derivatives, an abrupt increase in permeability occurs with decrease in weight of coating below about 2.6 oz. As the weight of material applied becomes less, it becomes increasingly difficult to cover the threads of the cloth uniformly with a continuous film. As the film becomes thinner it is probable that fibers of the fabric will protrude through the film, thus affording channels for leakage.

That the permeabilities become practically constant within the range shown in figure 1 would appear to be explainable on the basis of the difference in the permeabilities of films attached to fabric and those which are unsupported. Within the range shown in figure 1 the permeability of the impregnated fabric and the thin film overlying it, represented by a weight of coating of about 2.8 oz/yd², is apparently the controlling factor in the behavior of fabrics carrying higher weights of

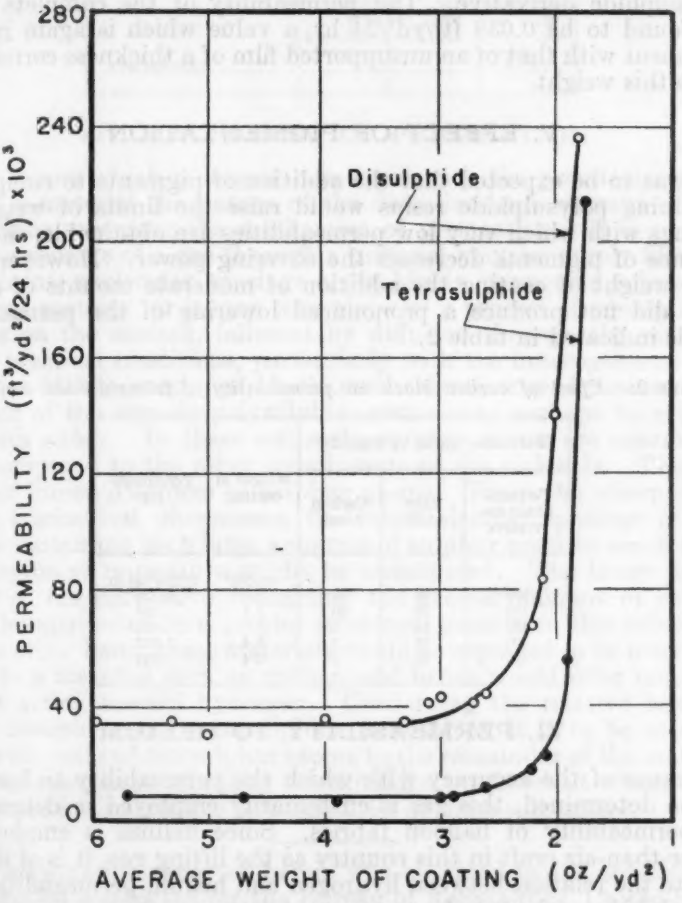

FIGURE 1.—*Permeabilities of coated fabrics.*

coatings. In accordance with this view the permeability of a coated fabric would be lowered further only when the thickness of the overlying film became sufficiently great as to have a permeability lower than that of the raw fabric, plus 2.8 oz of coating. A fabric was prepared on which the total weight of coating was the equivalent of 15.5 oz/yd². The permeability of this fabric proved to be 0.003 ft³/yd²/24 hr, a value considerably lower than those in the practically constant range in figure 1. The amount of overlying film in excess of the 2.8 oz/yd², representing the minimum constant value, was 12.7 oz, which corresponds approximately to a thickness of 0.029 cm. Comparison

of the permeability obtained with this fabric with that of an unsupported film of about this same thickness indicates fairly close agreement. The behavior of a resin film overlying a base fabric coated with rubber is also explainable on this basis. The weight of rubber applied to the raw fabric was about 0.6 oz/yd^2. The permeability of a fabric coated with this weight of rubber is so high as to be negligible in its impedance value. The rubberized fabric was now coated with 4.6 oz/yd^2 of the tetrasulphide derivative. The permeability of the complete fabric was found to be 0.038 ft^3/yd^2/24 hr, a value which is again in close agreement with that of an unsupported film of a thickness corresponding to this weight.

V. EFFECT OF PIGMENTATION

It was to be expected that the addition of pigments to compounds containing polysulphide resins would raise the limits of weights of coatings with which very low permeabilities are obtainable, since the presence of pigments decreases the covering power. However, for a given weight of coating the addition of moderate mounts of carbon black did not produce a pronounced lowering of the permeability. This is indicated in table 2.

TABLE 2.—*Effect of carbon black on permeability of tetrasulphide derivative*

Formulas (parts, by weight)			Weight of coating	Permeability
Tetrasulphide derivative	Zinc oxide	Carbon black		
			oz/yd^2	ft^3/yd^2/24 hr
100	10	15	3.2	0.029
100	10	10	3.4	.023
100	10	5	3.0	.021
100	10	2	3.4	.012
100	10	0	3.4	.010

VI. PERMEABILITY TO HELIUM

Because of the accuracy with which the permeability to hydrogen can be determined, this gas is customarily employed in determining the permeability of balloon fabrics. Since helium is employed in lighter-than-air craft in this country as the lifting gas, it is of interest to note the relation between hydrogen and helium permeabilities of a polysulphide resin. A few measurements made on fabrics coated with different weights of coatings on fabric are given in table 3. The average ratio is in close agreement with that found previously for rubber [1].

TABLE 3.—*Permeabilities of tetrasulphide derivative to hydrogen and helium*

	Permeability ($ft^3/yd^3/24$ hr)		
	Helium	Hydrogen	Ratio helium to hydrogen
	0.006	0.009	0.66
	.011	.017	.64
	.014	.023	.60
	.009	.013	.66
Average ratio			0.64

VII. MECHANISM OF PERMEATION

In a report which is largely concerned with the practical application of a material the nature of the data does not warrant definite conclusions regarding the mechanism of permeation. It is possible that the passage of a gas through a material may be simply filtration through intermolecular spacings or, in highly permeable substances, an actual porosity, or it may take place by a process of adsorption of the gas on the surface, followed by diffusion through the material. Under practical conditions, particularly with the heterogeneous compositions widely employed, both mechanisms may function. The behavior of the organic polysulphide resins may perhaps be explainable with either. In these resins the sulphur atoms are enormously large compared to the other constituents of the molecule. They are in effect linear polymers of sulphur atoms. From the viewpoint of simple mechanical phenomena the intermolecular spacings of substances containing such large amounts of sulphur must be small and a high degree of impedance might be anticipated. The lower permeability of the derivative containing the greater amount of sulphur might be attributed to a greater structural density in this substance. On the other hand, these materials would be expected to be inert compared to a material such as rubber, and hence would offer much less solvent action toward hydrogen. Concerning the relative behavior of the disulphide and tetrasulphide derivatives, it is to be expected that as the ratio of the sulphur atoms to the remainder of the molecule is altered changes in solubility relationships would result which would be reflected in the relative permeabilities of these substances.

The information reported herein was obtained in the course of an investigation conducted for the Bureau of Aeronautics, United States Navy Department. The interest of this organization and particularly that of Commander Garland Fulton is gratefully acknowledged.

VIII. REFERENCES

[1] J. D. Edwards and S. F. Pickering, BS Tech. Pap. **11** (1918) T113; BS Sci. Pap. **16**, 327–362 (1920), S387.
[2] H. Kayser, Wied. Ann. **43**, 544 (1891).
[3] S. M. Martin, Jr., and J. C. Patrick, Ind. Eng. Chem. 28, 1144–1149 (1936).
[4] J. C. Patrick, Trans. Faraday Soc. **32**, no. 177, pt. 1, 347–357 (1936); Rubber Chem. Tech. **9**, 373–382 (1936).
[5] T. P. Sager, Ind. Eng. Chem., Anal. Ed., **9**, 156 (1937).
[6] T. P. Sager, J. Research NBS, **13**, 879–885 (1934); RP750.

WASHINGTON, March 20, 1937.

U. S. DEPARTMENT OF COMMERCE NATIONAL BUREAU OF STANDARDS

RESEARCH PAPER RP1021

Part of Journal of Research of the National Bureau of Standards, Volume 19, August 1937

β-*d*-TALOSE AND *d*-TALOSE ACETATES AND ORTHOESTERS[1]

By William Ward Pigman and Horace S. Isbell

ABSTRACT

Mutarotation and oxidation measurements are given for the new sugar, β-*d*-talose. The difference between the molecular rotations of α- and β-*d*-talose, called by Hudson *2A*, is shown to be 9,870. This value is similar to that for *d*-mannose, which resembles talose in the configuration of carbons 2 and 3. Crystalline α-penta-acetyl talose, α-tetra-acetyl talose, 1-bromo-tetra-acetyl talose, and an orthoester derivative, triacetyl talose 1,2-orthomethylacetate, are reported. The conditions necessary for orthoester formation are discussed. A new crystalline monobenzoyl talose is described. This substance is produced in small yields along with the sugars when galactal is oxidized with perbenzoic acid. Evidence is presented which indicates that the monobenzoyl talose has an orthobenzoic acid structure and the properties of orthoester derivatives are contrasted with those to be expected of orthoacid derivatives.

CONTENTS

I. Introduction 189
II. α- and β-*d*-talose 190
III. Monobenzoyl talose and its relationship to the glycal synthesis 194
IV. Acetylated derivatives of *d*-talose 197
1. α-Penta-acetyl-*d*-talose and derivatives 197
2. Triacetyl-*d*-talose 1,2-orthomethylacetate 198
3. Reactions of acetyl sugar orthomethylacetates 199
4. Reactions of sugar orthoacids 202
V. Experimental procedure 203
1. Preparation of *d*-talose 203
(a) Preparation of galactal 204
(b) Preparation of perbenzoic acid 204
(c) Oxidation of galactal 204
(d) Separation of galactose and talose 205
2. β-*d*-Talose 205
3. Properties and identification of monobenzoyl-*d*-talose 206
4. α-Penta-acetyl-*d*-talose 209
5. 1-Bromo-tetra-acetyl-*d*-talose 210
6. Triacetyl-*d*-talose 1,2-orthomethylacetate 210
7. α-Tetra-acetyl-*d*-talose 211
8. Methyl talosides 212
VI. Summary 212
VII. References 212

I. INTRODUCTION

The elucidation of the chemistry and properties of talose and its derivatives is of particular importance since this sugar represents a fundamental pyranose type, concerning which very little has been

[1] A part of the material in this paper was presented as a thesis by William Ward Pigman, of this Bureau, in May 1936 to the Faculty of the Graduate School of the University of Maryland, represented by Dr. Nathan L. Drake, in partial fulfillment of the requirements for the degree of Doctor of Philosophy.

previously reported. Earlier workers have succeeded in preparing in the crystalline state only a few derivatives of *d*-talose, namely, talonic acid and its lactones [1, 2,],[2] several hydrazones [3, 4], and certain acetone derivatives [2]. The sugar was known only in an amorphous state until the relatively recent crystallization of *α*-*d*-talose by Levene and Tipson [4]. Shortly after this work was reported we succeeded independently in obtaining the crystalline *α*-*d*-talose, and later reported data showing that the mutarotation was complex in character and that solutions of talose contain at least three isomers in dynamic equilibrium [5, 6].

In this paper, crystalline *β*-*d*-talose, *α*-penta-acetyl-*d*-talose, tetra-acetyl-*d*-talose, 1-bromo-tetra-acetyl-*d*-talose, triacetyl-*d*-talose orthomethylacetate, and a monobenzoyl talose (obtained from the glycal synthesis and probably having an orthobenzoic acid structure) are reported. These new substances may be used for the separation and identification of talose, for the preparation of other derivatives, and for assistance in the correlation of the properties of the sugars with their configurations and structures.

II. *α*- AND *β*-*d*-TALOSE

Crystalline *β*-*d*-talose (I, p. 198) was prepared for the first time by crystallization from methyl alcoholic solution. It is difficult to obtain, since the alpha form under all of the conditions studied crystallizes the more readily when seed of both are present.

The mutarotation of *β*-*d*-talose is complex and, as with the alpha isomer, equations having two exponential terms are required to express the change of optical rotation. The equations developed for *β*-*d*-talose at 20° C and 0.1° C are

$$[\alpha]_D^{20} = -17.5\times10^{-.0282t} + 9.7\times10^{-.101t} + 21.0 \quad (1)$$

$$[\alpha]_D^{0.1} = -17.6\times10^{-.00339t} + 5.5\times10^{-.0241t} + 25.2 \quad (2)$$

The corresponding expressions for *α*-*d*-talose were given by Isbell and Pigman [5, 6] as

$$[\alpha]_D^{20} = 9.3\times10^{-.0263t} + 37.9\times10^{-.126t} + 20.8 \quad (3)$$

$$[\alpha]_D^{0.1} = 9.8\times10^{-.00362t} + 27.5\times10^{-.0255t} + 25.2 \quad (4)[3]$$

The data upon which equations 1 and 2 are based are given in tables 1 and 2 and are illustrated in figure 1. The curves constructed of alternate dots and dashes represent first-order reactions with reaction constants having the same value as those calculated for the latter part of the mutarotations. Since the mutarotation curve for *β*-*d*-talose exhibits a maximum value which cannot be explained by a simple beta-alpha interconversion, two or more reactions involving three or more substances must take place during the establishment of the equilibrium.

[2] Figures in brackets here and elsewhere in the text correspond to the numbered literature references at the end of this paper.

[3] On page 159 of reference [6], the exponent $-.00362t$ for *α*-*d*-talose at 0.1° C was printed incorrectly as $0.00652t$.

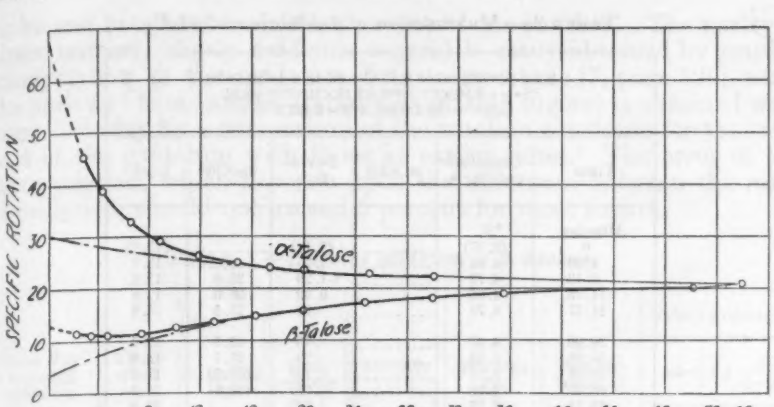

FIGURE 1.—*Mutarotation of α- and β-d-talose at 20° C.*

TABLE 1.—*Mutarotation of β-d-talose at 20° C.*

4.0 g per 100 ml at 20.0° C read in a 2-dm tube
$^{\circ}S^{a} = -4.04\times10^{-.0383t} + 2.25\times10^{-.101t} + 4.85$
$[\alpha]_D^{20} = (21.0/4.85)\times{}^{\circ}S = 4.330\times{}^{\circ}S$

Time [b]	Observed reading [b]	$m_1\times10^2$	Deviation	$m_2\times10^3$	$[\alpha]_D^{20}$
Minutes	°S				
0	(3.06)	----------	(2.25)	----------	(13.2)
2.27	2.66	----------	1.33	----------	11.5
3.52	2.58	----------	1.00	99	11.2
4.76	2.55	----------	0.73	105	11.0
7.43	2.64	----------	.37	108	11.4
10.20	2.89	----------	.22	99	12.5
13.13	3.14	----------	.12	96	13.6
16.31	3.40	----------	.06	96	14.7
19.99	3.64	----------	----------	----------	15.8
24.79	3.94	25.8	----------	----------	17.1
30.01	4.21	27.6	----------	----------	18.2
35.45	4.38	26.6	----------	----------	19.0
40.03	4.47	25.1	----------	----------	19.4
50.18	4.65	25.9	----------	----------	20.1
59.90	4.74	26.1	----------	----------	20.5
∞	4.85	----------	----------	----------	21.0
Average	----------	26.2	----------	101	----------

[a] The equations representing the optical rotations are calculated according to the method of T. M. Lowry and G. F. Smith, J. Phys. Chem. **33**, 9 (1929), as modified by H. S. Isbell and W. W. Pigman, J. Research NBS **18**, 156 (1937) RP969. The equations were developed for reactions of the type $x \rightleftarrows y \rightleftarrows z$, where one set of reactions is much more rapid than the other. As a first approximation, the sum of the velocity constants for the slow change may then be considered empirically to be m_1, while that for the rapid change may be considered to be m_2. The "deviation" represents the difference between the observed rotation and the rotation obtained by extrapolation of the slow mutarotation to the same time.

[b] Averages of consecutive readings.

TABLE 2.—*Mutarotation of β-d-talose at 0.1° C.*

3.4 g per 100 ml at 0.1° C read in a 4-dm tube
$°S_0 = -6.96 \times 10^{-.003304} + 2.18 \times 10^{-.03414} + 0.95$
$[\alpha]_D^{0.1} = (25.2/9.95) \times °S = 2.533 \times °S$

Time	Observed reading [b]	$m_1 \times 10^3$	Deviation	$m_2 \times 10^3$	$[\alpha]_D^{0.1}$
Minutes	°S				
0	(5.17)	----------	(2.14)	----------	(13.1)
4.00	4.95	----------	1.75	----------	12.5
9.12	4.75	----------	1.29	25.9	12.0
14.76	4.66	----------	0.92	26.0	11.8
21.17	4.74	----------	.69	23.5	12.0
29.90	4.87	----------	.43	23.5	12.3
39.91	5.14	----------	.29	21.7	13.0
49.58	5.41	----------	(.19)	(21.2)	13.7
60.27	5.68	----------	(.08)	(23.8)	14.4
76.31	6.15	----------	(.04)	----------	15.6
89.95	6.54	----------	(.04)	----------	16.6
119.96	7.22	----------	----------	----------	18.3
156.31	7.88	3.31	----------	----------	20.0
180.19	8.23	3.33	----------	----------	20.8
240.67	8.86	3.30	----------	----------	22.4
303.57	9.33	3.51	----------	----------	23.6
360.27	9.56	3.52	----------	----------	24.2
23.5 hr	9.95	----------	----------	----------	25.2
Average	----------	3.39	----------	24.1	----------

[a] See footnote b, table 1.
[b] Averages of 10 consecutive readings.

The initial rotations calculated from the equations representing the optical rotations are $[\alpha]_D^{20} = +13.2$ and $[\alpha]_D^{0.1} = 13.1$ for the β–*d*–talose, and $[\alpha]_D^{20} = +68.0$ and $[\alpha]_D^{0.1} = +62.5$ for the α–*d*–talose. The molecular-rotation difference (2*A*) is then (68.0—13.2) 180.1=9,870 at 20° C, and (62.5—13.1) 180.1=8,900 at 0.1° C. The corresponding value for *d*–glucose according to our measurements [6] is 16,840 and for *d*–mannose is 8,340 at 20° C. The value for *d*–talose (9,870) resembles that for *d*–mannose (8,340), as might be anticipated since the two sugars have the same configuration for the adjacent carbon atoms 2 and 3. The agreement of these values can be considered as evidence that the new modification of talose is the pure beta pyranose modification. Further evidence that the compound is pure was obtained by the oxidation of the sugar with bromine water according to the method described in previous publications [6, 7, 8], in which it is shown that the oxidation of a mixture of alpha and beta isomers of a sugar proceeds rapidly at first and then more slowly as the less readily oxidizable modification continues to be oxidized.

The oxidation data for β–*d*–talose are given in table 3. The reaction takes place at a rapid and uniform rate. When the oxidation is 92.1 percent complete, the velocity constant has a value (747×10^{-3}), which is close to the average of the values for the earlier times, and, therefore, the β–*d*–talose sample is essentially homogeneous. If the sample had contained appreciable quantities of the alpha isomer (5 percent or more), the reaction constants for the latter part of the oxidation would have had a much smaller value than that found. Heretofore there has not been any direct method for determining the homogenity of the alpha and beta forms of the sugars. The oxidation method, however, provides a direct means for the determination of

alpha and beta isomers in the presence of one another. The purity of alpha isomers (slowly oxidizble sugars) is easily obtained by graphic extrapolation of the oxidation data to zero time [7, page 529], while the purity of beta isomers (rapidly oxidizable sugars) is obtained with more difficulty by a comparison of the reaction constants for the later part of the oxidation with those at earlier times. The error of the determination, which depends upon the difference between the rates of oxidation, should not exceed 5 percent for most sugars.

TABLE 3.—*Bromine oxidation of β-d-talose*

Time after beginning oxidation	Unoxidized sugar	Oxidation	Temperature	Bromide (Br^-)	Bromine (Br_2)	Free bromine (a)	Velocity constants $ak=\frac{1}{t}\log\frac{A}{A-X}$	
							$ak\times10^3$	$k\times10^3$
Minutes	mg	*Percent*	°C	*Moles/liter*	*Moles/liter*	*Moles/liter*		
0	180.0	0	(+0.5)	(0.360)	(0.368)			
1.1	158.5	11.9		.367	.364	0.085	50.2	691
10.0	51.7	71.3		.403	.346	.070	54.2	774
25.0	14.2	92.1		.423	.323	.059	44.1	747
Average								704

Data have been previously given [6] for the bromine oxidation of α-*d*-talose. The velocity constant for the bromine oxidation of the beta form is approximately nine times that of the alpha. Thus the rates of oxidation for α- and β-*d*-talose are in accord with the generalization previously presented [6, 7] that the beta sugars, when named according to Isbell's nomenclature [9], are more rapidly oxidized by bromine water than the alpha isomers. The oxidation of a solution of *d*-talose in equilibrium at 0° revealed the presence of 56 percent of less reactive sugar (supposedly largely α-*d*-talose) and 44 percent of the more reactive modification (supposedly largely β-*d*-talose) [6].

A calculation of the relative amounts of the alpha and beta forms in the equilibrium solution, made by use of the optical rotations of the two isomers and of the equilibrium solution, and on the assumption that only two isomers exist in solution, gives 25 percent of alpha and 75 percent of beta. The discrepancy between the proportions calculated from the rotations and those derived from the oxidation data is probably due to the presence of more than two modifications in the equilibrium solution. This interpretation is also supported by the complex mutarotations of both α- and β-*d*-talose and by the changes in optical rotation which follow an alteration in the temperature [5, 6].

From the data given in tables 1 and 2 the heats of activation for the mutarotation reaction may be calculated by application of the Arrhenius equation. The values obtained are $Q_1=16{,}300$ calories for the slow reaction, and $Q_2=11{,}500$ calories for the rapid reaction; the corresponding values previously given for α-*d*-talose [6] are $Q_1=15{,}900$ and $Q_2=12{,}800$, while those for the averages of a number of sugars were given as $Q_1=16{,}900$, and $Q_2=13{,}200$. The temperature coefficient, which is the ratio of the rates of mutarotation at 35° C to that at 25° C, is 2.4 for the slow reaction and only 1.9 for the rapid reaction.

If the ring structure of the two crystalline isomeric taloses be assumed as pyranoid, it will be observed that these substances follow the lactone rule [10] since the ring lies to the right and the rotation of a solution containing equal proportions of the alpha and beta isomers [11] would be 1/2 (68.0+13.2)=+40.6.

III. MONOBENZOYL TALOSE AND ITS RELATIONSHIP TO THE GLYCAL SYNTHESIS

The talose needed for this investigation was prepared by the action of perbenzoic acid on galactal according to the method of Bergmann and Schotte [13] as applied to the preparation of talose by Levene and Tipson [4]. The glycal synthesis is of importance and is superior to the older methods for the preparation of certain rare sugars. However there are several problems connected with its application which hitherto have not been explained. Thus the rotation of anhydrous 4-glucosido-mannose, prepared by application of the glycal synthesis to cellobiose, is reported by Bergmann and Schotte [13] to be $[\alpha]_D^{16}=10.65$, and by Haworth, Hirst, Streight, Thomas, and Webb [14] to be $[\alpha]_D^{18}=12.5$ at equilibrium. On the other hand, Brauns [15] and Isbell [16], working with material prepared by the action of hydrogen fluoride on cellulose octa-acetate, reported the values $[\alpha]_D^{20}=+5.8$ and $[\alpha]_D^{20}=+5.88$, respectively, for the monohydrate. Also, Watters and Hudson [17] reported that a third substance of unknown composition was present with the lactose and 4-galactosido-mannose produced by the action of perbenzoic acid on lactal. We have now succeeded in separating from the products from the action of perbenzoic acid on 150 g of galactal, 5 g of a crystalline difficultly soluble substance which was identified as monobenzoyl talose. It seems probable that similar substances are responsible for the discrepancies in the rotations reported for 4-glucosido-mannose and for other sugars prepared by the glycal synthesis.

The crystalline compound obtained in the synthesis of talose gives a positive color test for benzoic acid only after acid hydrolysis, and, therefore, it is not a molecular compound of talose and benzoic acid. The method used for the preparation of monobenzoyl talose eliminates any position for the benzoyl residue other than carbons 1 and 2, but the properties of the monobenzoate are different from those which might be anticipated for a normal 1- or 2-monobenzoyl talose. Thus the β-1-monobenzoyl glucose of Zervas [18] is stable in hot methyl alcohol solution, does not mutarotate in water, and has a sharp melting point. In contradistinction to these properties, the monobenzoyl talose reacts with cold methyl alcohol, is decomposed by alkali (and even distilled water over a long period of time), and does not have a distinct melting point. The lack of mutarotation in acid solution does not correspond with properties to be expected of 2-monobenzoyl talose. These and other data which are presented in the next section are best explained by an orthoester structure and for the present the monobenzoyl talose is assigned the following formula:

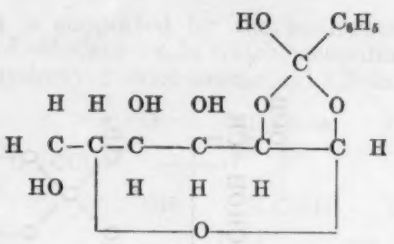

The monobenzoate probably is produced by the addition of benzoic acid to an intermediate ethylene oxide derivative [12] (formed by the action of perbenzoic acid on galactal) in a manner analogous to the formation of sugars and glycosides from glycals [13]. These reactions are illustrated as follows:

This mechanism is supported by the analogous reaction of trichloracetic acid and ethylene oxide which, according to Hibbert and Greig [20], give 2-hydroxy-2′-trichloromethyl 1,3-dioxolane (XI).

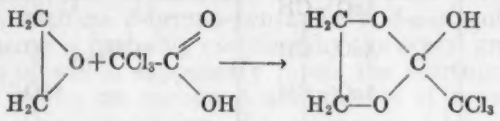

(XI)

In the glycal synthesis, however, the conditions are more complex because several competing reactions take place. Ordinarily water is present in large excess, and consequently the sugars are the principal products. When large quantities of benzoic acid are present, mixtures are obtained which contain benzoic acid but which do not yield crystalline products until after hydrolysis.

In contrast to the talose derivative, Levene and Tipson [4] obtained a 1-monobenzoyl-triacetyl galactose by the action of perbenzoic acid on an anhydrous solution of triacetyl galactal. The production of a galactose derivative in one case and a talose in the other is in harmony with their observation that the perbenzoic acid oxidation of triacetyl galactal gives principally galactose derivatives, while galactal gives talose predominantly [4]. Our monobenzoyl talose differs from the acetylated monobenzoyl galactose in that it is probably an orthoacid derivative.

In the next section the properties of the new monobenzoyl talose will be compared with the properties of other compounds which presumably have orthoacid structures.

IV. ACETYLATED DERIVATIVES OF *d*-TALOSE

1. α-PENTA-ACETYL-*d*-TALOSE AND DERIVATIVES

Upon acetylation with acetic anhydride at 0° C in the presence of pyridine, α-*d*-talose yields crystalline α-penta-acetyl-*d*-talose (II, p. 198) with $[\alpha]_D^{20} = +70.2$ in chloroform. β-*d*-talose under similar conditions gives a second penta-acetate which has not yet crystallized.

Crystalline α-1-bromo-tetra-acetyl-*d*-talose (III, p. 198), with $[\alpha]_D^{20} = 165.6$ in chloroform, is prepared by the action of glacial acetic acid solution of hydrogen bromide on α-penta-acetyl-*d*-talose.

Bromo-tetra-acetyl-*d*-talose reacts with moist silver salts to give crystalline tetra-acetyl-*d*-talose (IV, p. 198). This new substance mutarotates from a dextrorotation in pyridine solution at a rate corresponding to that for a first-order reaction ($k_1+k_2=0.0029$ at 20° C). The mutarotation reaction appears to be a simple reversible conversion of alpha and beta isomers because tetra-acetyl-*d*-talose may be recovered from the equilibrium solution. Since the optical rotation changes from a dextro to a less dextro rotation, the substance is called α-tetra-acetyl-*d*-talose. This classification is supported by the formation of α-penta-acetyl-*d*-talose when the tetra-acetate is acetylated at 0° C.

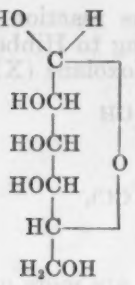

(I) β-*d*-talose.

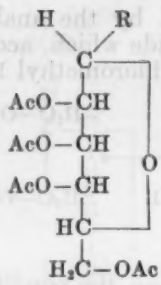

(II) α-Penta-acetyl-*d*-talose. R= CH_3-CO-O-.
(III) 1-Bromo-tetra-acetyl-*d*-talose. R=Br.
(IV) α-Tetra-acetyl-*d*-talose. R= OH.

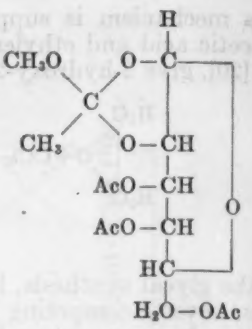

(V) Triacetyl-*d*-talose 1, 2 orthomethyl-acetate.

2. TRIACETYL-*d*-TALOSE 1,2-ORTHOMETHYLACETATE

The bromo-tetra-acetyl-*d*-talose reacts with methyl alcohol in the presence of silver carbonate to give a compound (V, p. 198) with the same empirical formula as a tetra-acetyl methyl taloside but which has only three acetyl groups which are hydrolyzable by alkali. The new substance is a derivative of orthoacetic acid similar to the so-called " 'γ'-triacetyl methyl rhamnoside" of Fischer, Bergmann, and Rabe [21].

Such substances have been variously described as orthoacetates, "γ"-glycosides, and α-methoxy-ethylidenes, etc. Since they are derivatives of orthoacetic acid [22, 23] and have unique reactions which may be associated with such a structure, it seems advisable when naming compounds of this type that the orthoacid nature be emphasized. Haworth, Hirst, and Stacey [24] have named their derivative of α-glucoheptose as tetra-acetyl-(α-glucoheptose) 1,2-orthomethylacetate. This method seems satisfactory as it may be applied to other known orthoacetates as well as to new types. The new talose derivative is then called triacetyl-*d*-talose 1,2-orthomethyl-acetate. Similarly the monobenzoyl-*d*-talose, which is probably a derivative of orthobenzoic acid with one acid hydroxyl not esterified, is named *d*-talose 1,2-orthobenzoic acid.

Previously orthomethylacetates have been reported for mannose [25], lyxose [26], rhamnose [21], 4-glucosido-mannose [28], ribose [27], *d*-α-glucoheptose [24], fructose [19], turanose [29], and maltose [30, 31], while in this paper the orthomethylacetate of talose is reported. The first four of these sugars have the mannose configuration, ribose has the talose configuration, and *d*-α-glucoheptose has the gulose configuration. Fructose and turanose are ketoses which have the galactose configuration, while maltose is a substituted glucose.

An exmaination of the configurations of the halogeno-acetyl sugars which have been converted to orthoesters reveals that many of these have the acetyl groups on carbons 2 and 3 in a *cis* position in a definite relation to the configuration of carbon 1. Thus when the two *cis*

acetyl residues are directed away from the ring-oxygen, orthomethylacetates are given by α-halogeno-acetyl sugars, as for example, by the mannose and talose derivatives. When these groups are directed toward the ring, the orthoesters are produced from β-halogeno-acetyl sugars, such as β-bromo-penta-acetyl-*d*-α-glucoheptose. The directing influence is probably exercised by the acetyl group on carbon 3, the oxygen of which supposedly repels the corresponding oxygen of the acetyl group on carbon 3 and directs it toward carbon 1. According to this conception the unknown β-bromo-tetra-acetyl derivatives of gulose and allose should yield orthomethylacetates.

Orthoacetate formation, however, is not limited to these favorable structures and other factors are responsible for the formation of this type of derivative by the halogeno-acetyl derivatives of fructose, turanose, and maltose. The position of the orthomethylacetate group for the fructose and turanose derivatives is not definitely established. The group is supposed to be attached to carbons 2 and 3 [19, 29], but since a 1,2 position is possible the interpretation of the formation of these derivatives must await a determination of the position of the orthomethylacetate group. In any case, the fructose structure must be considered as representing another favorable configuration. Three chloro-acetyl derivatives of maltose, supposedly the normal alpha and beta derivatives, and an orthoacetyl chloride are known. Since of the three only the hexa-acetyl maltose 1,2-orthoacetyl chloride will form the corresponding orthomethylacetate [44, 30], the formation of the maltose derivative is not comparable to that of mannose and talose. Probably orthomethylacetates could be prepared for all of the sugars if the corresponding orthoacetyl chloride derivatives were known.

Heretofore the importance of temperature on the reaction of the halogen acetyl derivatives with methyl alcohol to form orthoesters has not been emphasized sufficiently. Miss Harriet Frush and one of the authors (Isbell) found that good yields of triacetylmannose orthomethylacetate are obtained from bromo-acetyl mannose and silver carbonate in methyl alcohol when the reaction is conducted at low temperatures (0° C). At room temperatures and above only small quantities of the orthoester could be separated. The effect of temperature on this reaction may account for some of the conflicting results which have been obtained in this field.

3. REACTIONS OF ACETYL SUGAR ORTHOMETHYLACETATES

Since only a small quantity of the triacetyl-*d*-talose 1,2-orthomethylacetate (V, p. 198) has been prepared, the study of its reactions has not been completed. However, several reactions typical for the orthomethylacetates have been carried out. Thus hydroxyl ions hydrolyze only three of the four acetyl groups and give talose 1,2-orthomethylacetate (VI, p. 201), which was not isolated in the crystalline state. The presence of an acetyl group resistant to alkaline hydrolysis is characteristic of the orthomethylesters [21, 25]. Another typical reaction is the conversion of the orthomethylesters to normal chloro-acetyl sugars by hydrogen chloride in chloroform solution [28]. Triacetyl-*d*-talose orthomethylacetate under these conditions reacts so rapidly that the rate of change could not be measured polarimetrically. Thus the specific rotation of triacetyl-*d*-talose orthomethylacetate in purified chloroform is $[\alpha]_D^{20} = +3.7$, while in chloro-

form containing hydrogen chloride the specific rotation was $[\alpha]_D^{21} = +73$, 3 minutes after dissolution. After evaporation of the solution, crystals were obtained which are probably chloro-triacetyl talose (VII, p. 201). The triacetyl-*d*-talose orthomethylacetate was also found to be quite unstable since upon recrystallization from warm water the substance decomposed to give considerable quantities of tetra-acetyl talose (VIII, p. 201). This substance is also obtained by treating triacetyl-*d*-talose orthomethylacetate with aqueous alcoholic hydrogen chloride. Apparently triacetyl-*d*-talose orthomethylacetate is hydrolyzed more readily than hexa-acetyl-4-glucosido-mannose orthomethylacetate [28] and it resembles hexa-acetyl turanose orthomethylacetate, which hydrolyzes readily to give a normal hepta-acetate [29b].

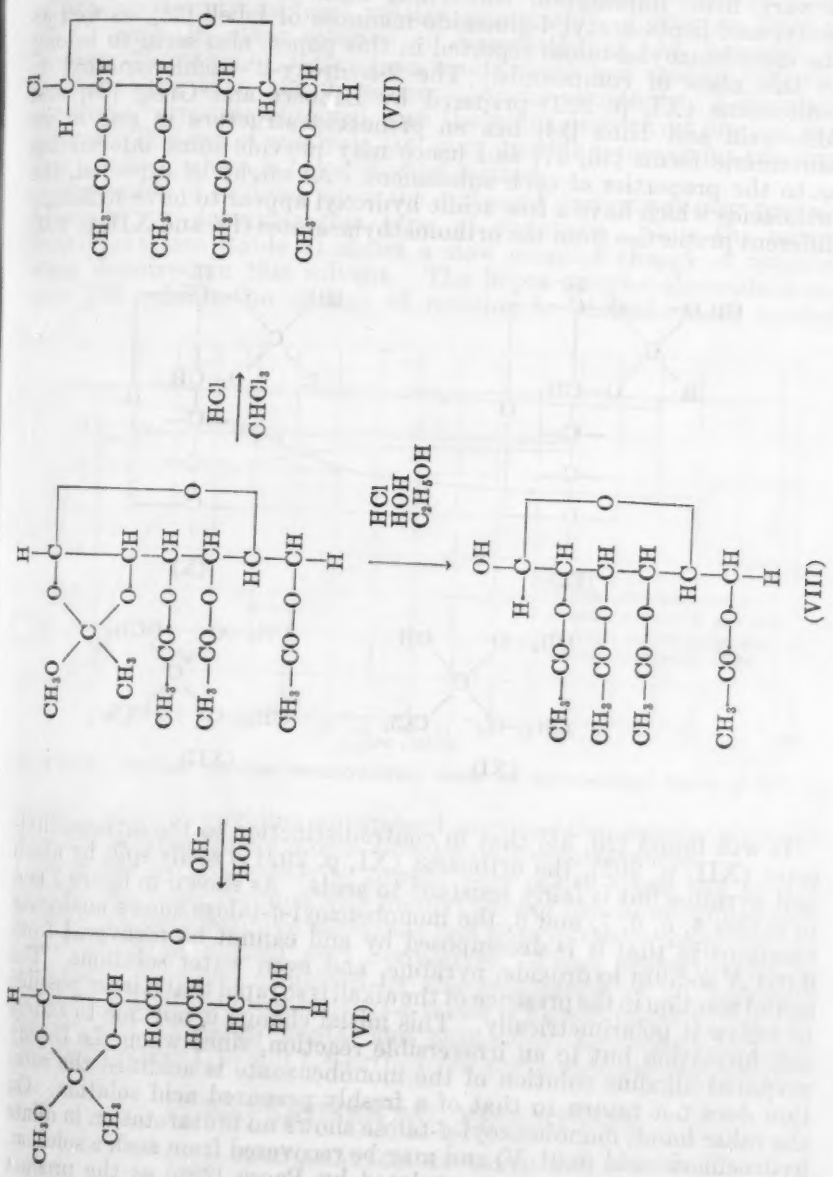
(VII)
HCl
CHCl3
HCl
HOH
C2H5OH
(VIII)
OH-
HOH
(VI)

4. REACTIONS OF SUGAR ORTHOACIDS

Several sugar derivatives have been postulated by Haworth, Hirst, and Teece [32], Pacsu [29], and Richtmeyer and Hudson [33] as having orthoacid structures (X, p. 202), but at the present time there is very little information concerning such structures. The hexa-acetyl and hepta-acetyl 4-glucosido-mannose of Isbell [28], as well as the monobenzoyl-*d*-talose reported in this paper, also seem to belong to this class of compounds. The 2-hydroxy-2′-trichloromethyl 1, 3-dioxolane (XI, p. 202) prepared by Hibbert and Greig [20] and Meerwein and Hinz [34] has an orthoacid structure in one of its tautomeric forms [36, 37] and hence may provide some information as to the properties of such substances. As might be expected, the orthoacids which have a free acidic hydroxyl appear to have strikingly different properties from the orthomethylacetates (IX and XII, p. 202)

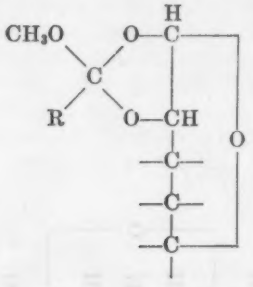

(IX)

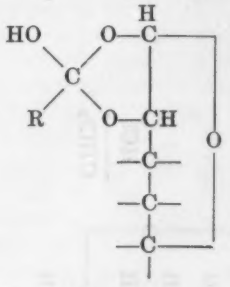

(X)

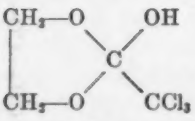

(XI)

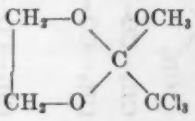

(XII)

It was found [20, 35] that in contradistinction to the orthomethyl-ester (XII, p. 202), the orthoacid (XI, p. 202) is easily split by alkali and pyridine but is fairly resistant to acids. As shown in figure 2 and in tables 4, 5, 6, 7, and 8, the monobenzoyl-*d*-talose shows analogous reactions in that it is decomposed by and cannot be recovered from 0.001 *N* sodium hydroxide, pyridine, and even water solutions. The initial reaction in the presence of the alkali is so rapid that it is not possible to follow it polarimetrically. This initial change is not due to simple salt formation but to an irreversible reaction, since when the freshly prepared alkaline solution of the monobenzoate is acidified the rotation does not return to that of a freshly prepared acid solution. On the other hand, monobenzoyl-*d*-talose shows no mutarotation in dilute hydrochloric acid (0.01 *N*) and may be recovered from such a solution. The monoacetyl turanose postulated by Pacsu [29b] as the product resulting from the action of acid upon turanose orthomethylacetate exhibits a similar stability to dilute acid and instability to dilute alkali.

Since, according to Meerwein, Hinz, and Sönke, the orthoacid reacts with diazomethane to give the methylester [34, 35, 36], it was hoped that this reaction might be used as a criterion for orthoacid structures. However, none of the compounds tried (monobenzoyl-*d*-talose, hexa-acetyl-4-glucosido-mannose, hepta-acetyl-4-glucosido-mannose, and chloro-hepta-acetyl-lactose) reacted appreciably, during an hour at 0° C, with an ether solution of diazomethane. As, however 2-hydroxy-2′-methyl-1, 3-dioxolane reacts much less readily [36] with diazomethane than the 2-hydroxy-2′-trichloromethyl-1, 3-dioxolane the negative results obtained with the sugar derivatives are not surprising. The use of catalysts [34] may provide a means for effecting this reaction, which is being studied further.

The action of pyridine upon the orthoacid derivatives may provide a means for detecting this type of structure. Thus the monobenzoyl-*d*-talose (table 8) shows a slow complex change of rotation when dissolved in this solvent. The hepta-acetyl-4-glucosido-mannose [28] exhibits no change of rotation in chloroform or methyl

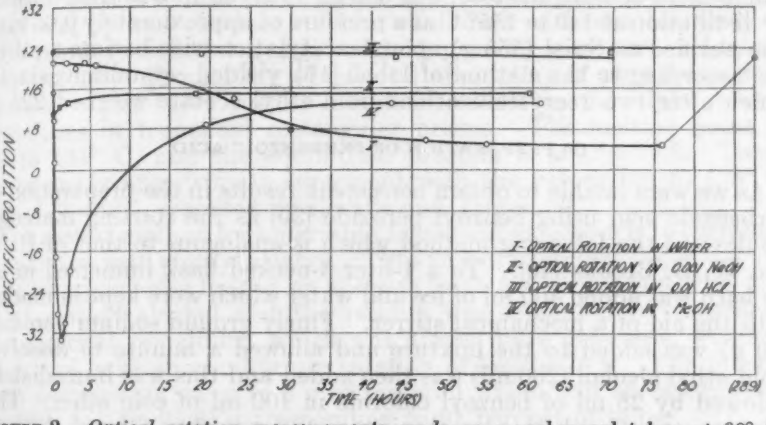

FIGURE 2.—*Optical rotation measurements made on monobenzoyl talose at 20° C.*

alcohol, while in pyridine an upward mutarotation occurs, although acetylation gives chiefly *a*-octa-acetyl-4-glucosido-mannose.

As shown by its sensitivity toward very dilute alkali and by the complex and rapid reaction with methyl alcohol (fig. 2), monobenzoyl-*d*-talose is a very reactive substance and does not have the properties characteristic of normal acyl derivatives. These properties are at the present time best explained by the postulation of an orthoacid structure and hence monobenzoyl-*d*-talose is named talose 1, 2-ortho-benzoic acid. Possibly hepta- and hexa-acetyl-4-glucosido-mannose may have similar 1, 2- and 1, 6-orthoacetic acid structures, respectively.

V. EXPERIMENTAL PROCEDURE

I. PREPARATION OF *d*-TALOSE

The *d*-talose used in this investigation was prepared by the oxidation of galactal with perbenzoic acid according to the general method used by Levene and Tipson [4] and T. Kumoda [38].

(a) PREPARATION OF GALACTAL

The galactal was prepared from bromo-tetra-acetyl galactose by reduction with zinc dust in 50-percent acetic acid solution according to the following procedure: To a 12-liter flask surrounded by an ice-salt bath there was added 1,000 ml of H_2O, 500 ml of glacial acetic acid, and 100 g of zinc dust which was kept in suspension by the aid of a mechanical stirrer. During a period of three hours ten 75-g portions of finely powdered bromo-tetra-acetyl galactose dissolved in 300 ml of warm glacial acetic acid were added. Water, in quantities to keep the composition at approximately 50-percent acid, and 600 g of zinc dust were also added at intervals during this period. The mixture, the temperature of which was allowed to rise slowly to room temperature over a period of 18 hours, was filtered and the filtered solution was extracted four times with a total of about 11 liters of benzene. The washed extracts were evaporated at a pressure of 14 mm to a thick sirup. The weight of the sirup, obtained by the combination of two such preparations from a total of 1,370 g of the bromo-tetra-acetyl galactose, was 685 g. This sirup was then purified by distillation at 140 to 155° C at a pressure of approximately 0.05 mm. The purified material (555 g) upon deacetylation with barium methylate, according to the method of Isbell [16], yielded crystalline galactal which after two recrystallizations from ethyl acetate weighed 225 g.

(b) PREPARATION OF PERBENZOIC ACID

As we were unable to obtain consistent results in the preparation of perbenzoic acid using benzoyl peroxide [39] as the starting material, we devised the following method which is analogous to that of B. T. and W. B. Brooks [40]. To a 1-liter 3-necked flask immersed in an ice bath was added 400 ml of ice and water which were kept in motion with the aid of a mechanical stirrer. Finely ground sodium peroxide (30 g) was added to the mixture and allowed a minute to dissolve. Cold ethyl alcohol (200 ml) was then added and this was immediately followed by 25 ml of benzoyl chloride in 100 ml of cold ether. The mixture was stirred for several minutes and was then filtered through a large Büchner funnel. The filtrate, after acidification with 700 ml of normal sulphuric acid, was extracted with four 150-ml portions of ether. The solutions were kept as cold as possible until after the final acidification. This procedure gives consistently about 20 g of perbenzoic acid.

(c) OXIDATION OF GALACTAL

The galactal was converted to a mixture of galactose, talose, and monobenzoyl talose in the following manner: An aqueous solution of galactal (50 g in 500 ml of water) was cooled to 0° C and then a cold solution of 58 g of perbenzoic acid in 305 ml of ether was added. The mixture was stirred at 0° C for 4 hours, and then stirred for an additional 14 hours, during which time the temperature rose slowly to 25° C. The aqueous phase was separated and extracted three times with ether and three times with chloroform. The resulting solution contained 53.4 g of reducing sugar (as galactose).

The oxidation mixture from 150 g of galactal was boiled down to about 60-percent sirup and allowed to stand overnight. A small crop of crystals appeared which were separated (weight 1.45 g). The solution was evaporated again to about a 70-percent solution and

allowed to crystallize. After five days 4.15 g of difficultly soluble crystals was separated. These crystals and the first crop proved to be talose monobenzoate.

(d) SEPARATION OF GALACTOSE AND TALOSE

The separation of the galactose and talose was accomplished in two ways, (1) fractional crystallization and (2) extraction of the mixture with methyl alcohol. Both methods will be described. The oxidation mixture from 100 g of galactal after removal of the monobenzoyl talose was evaporated to a thin sirup (about 70 percent) and diluted with an equal volume of methyl alcohol. Alpha talose seed was added and crystallization was allowed to take place for 24 hours. A crop weighing 37 g was separated, for which $[\alpha]_D^{20}=33.1$, at equilibrium. This corresponds to 79 percent of talose. The mother liquors upon evaporation and dilution with methyl alcohol in a similar manner gave, after seeding with galactose, 25 g of material, $[\alpha]_D^{20}=74.1$, at equilibrium (corresponding to 90 percent of galactose). Upon recrystallization of the crude talose ($[\alpha]_D^{20}=33.1$) 18.5 g of material ($[\alpha]_D^{20}=22.1$) was obtained. This, combined with another crop of crude talose (weight 9.7 g; $[\alpha]_D^{20}=23.6$), gave 23 g of pure α-*d*-talose ($[\alpha]_D^{20}=20.8$). From 100 g of galactal about 40 g of pure talose was obtained. The more readily obtained isomer is the alpha which crystallizes in truncated rectangular prisms. The melting point is 133 to 134° C, and the equilibrium rotation is $[\alpha]_D^{20}=20.8$. These values are in approximate agreement with the values 130 to 135° C and $[\alpha]_D^{27}=19.7$, reported by Levene and Tipson [4].

The easiest method for separating talose and galactose is to extract a dry mixture with methyl alcohol. Thus 25 g of a mixture ($[\alpha]_D^{20}=+40$, at equilibrium) was heated on a steam bath for 60 minutes with 200 ml of methyl alcohol and the residue was separated by filtration. The material remaining, which was almost pure galactose, weighed 5.5 g and gave an equilibrium rotation of $[\alpha]_D^{20}=79.8$. The filtrate upon evaporation gave 14.0 g of material which had an equilibrium rotation ($[\alpha]_D^{20}=25.9$) corresponding to 91 percent of talose.

The mother liquor from the oxidation of 100 g of galactal which remained after all of the galactose and talose which would crystallize had been separated, was hydrolyzed with 0.5 *N* sulphuric acid for 7 hours at the boiling point. When the solution had cooled, crystals appeared which were separated, recrystallized from petroleum ether, and identified by a melting-point determination as benzoic acid. The weight of the recrystallized benzoic acid was 1.0 g. The neutral filtered solution crystallized after evaporation and 4 g of sugar was separated. Since the equilibrium solution had a rotation of $[\alpha]_D^{20}=+64$, the sugar consisted of approximately 73 percent of galactose and 27 percent of talose. It is therefore apparent that benzoyl esters of both galactose and talose are produced in addition to the free sugars by the action of perbenzoic acid on galactal.

2. β-*d*-TALOSE

A number of small crops of crude β-*d*-talose were obtained by crystallization from methyl alcohol. Recrystallization was performed as follows: Finely ground sugar (6.3 g) was dissolved completely in 17 ml of ice-cold water and then induced to crystallize by the addition

of 24 ml of cold absolute ethyl alcohol. After 60 minutes the resulting crystals were separated, washed with alcohol, and dried in vacuo (weight 2.5 g). The crystals usually form hexagonal prisms which have the appearance of square plates. The melting point is 120 to 121° C and the mutarotation is given in tables 1 and 2.

The oxidation data given in table 3 were obtained by the bromine oxidation method previously reported [8] as modified for use with small amounts of sugar [7]. *Analysis.* Calculated for $C_6H_{12}O_6$: C, 39.98; H, 6.72. Found: C[5] (micro), 40.09; H, 6.83.

3. PROPERTIES AND IDENTIFICATION OF MONOBENZOYL-*d*-TALOSE

The 5.6 g of crystals, obtained by the oxidation of galactal with perbenzoic acid, as previously described, was recrystallized from hot water. The crystals separate as long slender needles. A description of some of the properties of this material and of the methods used for identifying it follows.

Solubility.—The bitter crystals are difficultly soluble in cold water, chloroform, benzene, ether, and alcohol. Pyridine, hot alcohol, and hot water dissolve them readily but the first two solvents cause decomposition. At 20° C the solubility in water is approximately 0.5 g per 100 ml. *Melting point.*—The material melts between 150 and 170° C, apparently with decomposition, to give a brown liquid. *Reducing power.*—A 20.3-mg sample after heating with Benedict's solution was equivalent to 10.25 ml of 0.04 *N* iodine solution. Under the same conditions glucose requires 18.44 ml of the iodine solution. Therefore the ratio of reducing power to that of glucose is 0.556. The corresponding ratio to that of galactose is 0.626. Since the ratio of the molecular weight of the hexose to that of a hexose monobenzoate is 0.634, the reducing value agrees with that to be expected of an easily hydrolyzable galactose or talose derivative. The reducing power after acid hydrolysis with 0.506 *N* HCl for 2¼ hours at 100° C was found to have decreased slightly so that the ratio to that of glucose was 0.502. *Identification of benzoic acid.*—After acid hydrolysis with 0.506 *N* hydrochloric acid for 2¼ hours at the boiling point, a positive color test for benzoic acid was obtained [41] and benzoic acid was isolated from the hydrolysate. *Optical rotatory power.*—The changes in optical rotatory power observed in distilled water, aqueous hydrochloric acid (0.01 *N*), aqueous sodium hydroxide (0.001 *N*), methyl alcohol, and pyridine solutions are shown in tables 4, 5, 6, 7, and 8. Each of the recorded values is the average of five or more consecutive readings.

[5] The microdeterminations of hydrogen and carbon reported in this paper were carried out by Dr. J. B. Spies and Dr. W. G. Rose, of the U. S. Department of Agriculture.

TABLE 4.—*Rotation of monobenzoyl talose in water at 20° C*

(0.1062 g made up to 25 ml and read in a 4-dm tube)

Time	Observed rotation	Specific rotation	Time	Observed rotation	Specific rotation
Hours	°S	$[\alpha]_D^{20}$	*Hours*	°S	$[\alpha]_D^{20}$
0.08	1.04	21.2	47	0.28	5.7
.49	1.03	21.0	54	.25	5.1
1.06	1.03	21.0	76	.24	4.9
1.9	1.04	21.2	143	.74	15.1
3.1	0.97	19.8	192	.93	18.9
4.2	1.04	21.2	241	1.04	21.2
5.7	1.01	20.6	289	1.09	22.2
23.	0.68	13.9	648	1.19	24.2
30.	.38	7.7			

TABLE 5.—*Rotation of monobenzoyl talose in 0.01 N* HCl *at 20° C*

(0.0498 g made up to 10 ml with 0.01 *N* HCl and read in a 2-dm tube)

Time	Observed rotation	Specific rotation
Hours	°S	$[\alpha]_D^{20}$
0.08	0.67	23.3
19.0	.65	22.6
43.0	.64	22.2
69.5[a]	.65	22.6

[a] After this reading the solution was evaporated and 0.045 g of monobenzoyl talose was recovered.

TABLE 6.—*Rotation of monobenzoyl talose in 0.001 N* NaOH *at 20° C*

(0.0508 g made up to 10 ml and read in a 2-dm tube)

Time	Observed rotation	Specific rotation
Hours	° S	$[\alpha]_D^{20}$
0.07	0.32	10.9
.83	.37	12.6
2.1	.39	13.3
19.5	.44	15.0
68.	.44	15.0
92.	.44	15.0

TABLE 7.—*Rotation of monobenzoyl talose in methyl alcohol at 19° C*

(0.0551 g made up to 10 ml and read in a 2-dm tube)

Time	Observed rotation	Specific rotation	Time	Observed rotation	Specific rotation
Minutes	° S	$[\alpha]_D^{19}$	*Minutes*	° S	$[\alpha]_D^{19}$
2.96	+0.49	+15.4	29.9	−0.67	−21.1
4.26	+.43	+13.5	40.0	−.90	−28.3
6.34	+.31	+9.7	50.8	−1.01	−31.7
8.52	+.27	+8.5	60.1	−1.06	−33.3
10.65	+.05	+1.6	91.0	−.96	−30.2
13.52	−.08	−2.5	144.9	−.63	−19.8
15.16	−.16	−5.0	1170.	+.28	+8.8
20.04	−.36	−11.3	2550.	+.35	+11.0
25.1	−.54	−17.0	3960.	+.35	+11.0

TABLE 8.—*Optical rotation of monobenzoyl talose in pyridine at 20° C*

(0.1932 g made up to 10 ml and read in a 2-dm tube)

Time	Observed rotation	Specific rotation	Time	Observed rotation	Specific rotation
Hours	°S	$[\alpha]_D^{20}$	*Hours*	°S	$[\alpha]_D^{20}$
0.1	+1.84	+16.5	166.7	−1.32	−11.8
.3	+1.81	+16.2	191.3	−1.39	−12.5
1.5	+1.74	+15.6	214.3	−1.32	−11.8
5.9	+1.59	+14.2	263.0	−1.04	−9.3
22.6	+1.09	+9.8	286.7	−0.85	−7.6
46.2	+0.42	+3.8	310.7	−.59	−5.3
94.2	−.53	−4.7	359.0	−.16	−1.4
118.3	−.88	−7.9	383.5	+.09	+0.8
143.0	−1.17	−10.5	430.5	+.54	+4.8

Proof that the monobenzoate is a derivative of d-talose.—A 0.1524-g sample of the crystals was made up to a volume of 25 ml with 0.050 *N* sulphuric acid and kept at 57 ± 2° C for 8 days. The optical rotation was measured at intervals as recorded in table 9. The resulting solution was extracted with ether and neutralized with barium carbonate. The precipitate of barium sulphate was removed by filtration and the salt-free solution evaporated in a vacuum desiccator to a thick sirup. Upon dilution with ethyl alcohol and seeding with a minute amount of talose, crystallization occurred. The crystals were of the truncated prism type characteristics of *α-d*-talose. The solvent was removed in a high vacuum and the sugar converted to the penta-acetate by cooling to 0° C, adding 2 ml of pyridine and 1 ml of acetic anhydride, and keeping at 0° for 3 days. After this time, the solution was poured into ice water and the whole extracted with chloroform. Upon evaporating the chloroform and taking up with ethyl alcohol, crystallization occurred spontaneously. These crystals had a melting point of 105 to 106° C and after recrystallization from ethyl alcohol melted at 106 to 107° C. A mixture of this material and known talose penta-acetate melted at 106.5 to 107° C, which is the same as that for the pure product.

TABLE 9.—*Hydrolysis of benzoyl talose at 57 ±2° C*

(0.1524 g made up to 25 ml with 0.05 *N* H_2SO_4 and read in a 2-dm tube)

	Observed rotation	Specific rotation		Observed rotation	Specific rotation
Minutes	°S[a]	$[\alpha]_D^{20}$	*Minutes*	°S[a]	$[\alpha]_D^{20}$
5.8	0.66	18.7	304.8	0.62	17.6
15.9	.62	17.6	1,620.	.29	8.2
30.0	.60	17.0	2,900.	.16	4.5
60.6	.60	17.0	[b] 10,290.	.19	5.4
124.5	.60	17.0			

[a] Averages of 10 readings.
[b] The temperature was raised to 80° C during the last 24 hours.

Analysis.—Calculated for $C_6H_{11}O_6$ (COC_6H_5): C, 54.90; H, 5.68; benzoyl, 8.05 ml of 0.02224 *N* NaOH per 51.2 mg. Found: C (micro), 54.76, 54.78; H (micro), 5.61, 5.57; benzoyl by alkaline saponification at 20° C for 24 hours, 7.84 ml. Under the conditions employed for

the molecular weight determination by the Rast method, the material decomposes.

Preparation of talose and galactose monobenzoates.—Attempts were made to combine galactal with perbenzoic acid in anhydrous solutions in order to increase the yield of talose monobenzoate. Using dioxane and ethyl formate as solvents small quantities of talose monobenzoate were prepared. The method used is illustrated in the following typical experiment.

A solution of 5 g of galactal in 150 ml of dioxane and 10 ml of acetone was prepared and cooled to 0° C. A solution of 6 g of perbenzoic acid in 10 ml of dioxane was added along with 4 g of benzoic acid and the mixture was left in a refrigerator for 3 days. The solution was then evaporated to a sirup which was extracted with ether and taken up with water. The aqueous solution after several ether extractions was evaporated and extracted with ethyl acetate. The ethyl acetate extractions after evaporation to a sirup were taken up with water and from the solution 0.13 g of talose monobenzoate crystallized. No other crystalline material was obtained from the preparation. When pyridine or acetic acid was used as the solvent instead of acetone-dioxane, crystalline material could be obtained only after acid hydrolysis, as described in the next paragraph.

The sirupy material from several such preparations (corresponding to 25 g of galactal) was combined and hydrolyzed with acid in a manner similar to that used for the talose mother liquors. After recrystallization from petroleum ether, the benzoic acid weighed 1.5 g. The sugar obtained weighed 4 g, had an equilibrium rotation of $[\alpha]_D^{20}=+34$, and hence consisted of 77 percent of talose and 23 percent of galactose.

4. α-PENTA-ACETYL-*d*-TALOSE

Five grams of powdered talose, dissolved in a cold mixture of 35 ml of pyridine and 23 ml of acetic anhydride, was allowed to remain in a refrigerator at 0° C for 3 days. The mixture was then poured into 125 ml of ice water and the resulting emulsion crystallized during the course of an hour of stirring. The crystals, which characteristically appear as truncated prisms, were separated by filtration and dried. They weighed 7 g, and 1 g additional was obtained by extraction of the filtrate with benzene, evaporation of the benzene solution, and crystallization. Several grams of sirupy material remained, probably consisting of isomeric penta-acetates, which could not be induced to crystallize. The penta-acetate upon recrystallization from hot ethyl alcohol had a melting point of 106 to 107° C. In chloroform (cp) the specific rotation was $[\alpha]_D^{20}=69.5$ (0.3541 g made up to a volume of 10 ml, read 14.21° S in a 2-dm tube). A second recrystallization from ethyl alcohol raised the melting point slightly to 106.5 to 107° C and the rotation to $[\alpha]_D^{20}=70.2$ (0.3617 g made up to 10 ml with chloroform (cp) read 14.67° S in a 2-dm tube.

The action of the acetic anhydride-sulphuric acid isomerizing agent [43] on the α-penta-acetate was studied and it was found that since 75 percent of the alpha form was recoverable, the equilibrium lies in favor of the alpha isomer. Crystalline β-penta-acetyl talose was obtained neither by this method nor by the action of the acetic anhydride and sodium acetate on alpha talose. *Analysis.*—Calculated for $C_6H_7O_6(COCH_3)_5$: C, 49.21; H, 5.68; acetyl, 12.81 ml

of 0.1 *N* Ba $(OH)_2$ per 100 mg. Found: C (micro), 49.64; H (micro), 5.77; acetyl (by alkaline saponification for 3 hours at 20° C), 13.13 ml.

5. 1-BROMO-TETRA-ACETYL-*d*-TALOSE

A mixture of 10 g of penta-acetyl talose, 50 ml of glacial acetic acid containing 38 percent of HBr, and 2 ml of acetic anhydride was prepared at 0° C. Solution took place in about an hour, after which the liquid was kept at room temperature for 2½ hours more. Chloroform (60 ml) was then added and the bromo-acetyl talose solution was poured into ice water and extracted with chloroform. The extracts (three in all with a total of 180 ml of solvent) were washed twice with ice water, twice with cold sodium bicarbonate solution, and once again with ice water. The chloroform solution, after being dried with anhydrous sodium sulphate, was evaporated to a thin sirup, and after dilution with toluene was evaporated again to remove the last of the chloroform. Upon taking up the residue with ether, crystallization commenced immediately. After several hours 7 g was separated and an additional 0.5 g was obtained from the mother liquors. The crystals appeared as poorly defined long rectangular prisms with one pointed end. The material, after one recrystallization from ether, had a melting point of 84 to 84.5° C, although a slight sintering occurred at 83° C. A preliminary optical rotation measurement showed that ordinary chemically pure chloroform causes decomposition. Thus 0.4499 g made up to 10 ml with chemically pure chloroform read 42.57° S in a 2-dm tube 5 minutes after solution, but at 180 minutes this had dropped to 38.02° S. Therefore, the chloroform was washed with water, dried, and distilled just before using. A measurement of the rotatory power in this purified chloroform gave $[\alpha]_D^{20} = 165.6$, (0.4058 g made up to 10 ml, read 38.82° S in a 2-dm tube). This value was not changed appreciably after 60 minutes. *Analysis.*—Calculated for $C_6H_7O_5Br(COCH_3)_4$: C, 40.87; H, 4.66; Br, 19.44; acetyl, 9.73 ml of 0.1 *N* NaOH per 100 mg. Found: C (micro), 40.76; H (micro), 4.78; Br [42], 19.51; acetyl [42], 9.82 ml.

6. TRIACETYL-*d*-TALOSE 1, 2 ORTHOMETHYLACETATE

A solution of 3.6 g of bromo-tetra-acetyl talose in 36 ml of dry methyl alcohol was shaken with 3.5 g of silver carbonate for 1¼ hours in an ice bath. The solution was treated with decolorizing carbon, filtered, evaporated, and diluted with water. Crystals appeared and after separation weighed 0.77 g. Ethyl alcohol and hot water were found to decompose the material. From the alcohol, however, the crystals appear as irregular hexagonal and pentagonal plates. Benzene was found to be the best medium for recrystallization.

After one recrystallization from benzene the melting point was 91.5 to 92.5° C and the values of the optical rotation as measured in chloroform are given in table 10.

TABLE 10.—*Optical rotation of triacetyl-d-talose 1,2-orthomethylacetate in chloroform*

Time	Observed rotation[a]	Specific rotation[b]
	°S[a]	$[\alpha]_D^{20}$
15.5 min	0.18	3.7
156. min	.11	2.2
19. hr	.11	2.2

[a] Average of 10 or more readings.
[b] 32.0 mg of material made up to a volume of 0.9321 ml and read in a 0.5-dm tube.

Acetyl analysis.—A 0.0323-g sample was hydrolyzed at 0° C with 20 ml of 0.025 *N* barium hydroxide solution during a period of 24 hours (blanks containing only barium hydroxide solution were run under the same conditions). The solution was then titrated with 0.0291 *N* hydrochloric acid (carbon dioxide-free). Found: Acetyl 9.12 ml of 0.0291 *N* $Ba(OH)_2$ per 32.3 mg. Calculated for three acetyl groups: 9.19 ml.
Analysis by microcombustion.—Calculated for $C_{15}H_{22}O_{10}$: C, 49.70; H, 6.12. Found: C (micro), 49.89; H (micro), 6.12.

7. α-TETRA-ACETYL-*d*-TALOSE

To 2.2 g of silver benzoate suspended in 25 ml of moist acetone and cooled to −4° C there was added 2 g of bromo-tetra-acetyl talose. After shaking for 1½ hours the suspension was filtered through charcoal. The filtrate which showed a negative Beilstein test for halogen was evaporated. The sirup was taken up with benzene and allowed to crystallize. A total of 0.8 g of crystalline material was obtained, which appeared as hexagonal prisms. From the mother liquors there was separated by extraction with hot petroleum ether 0.1 g of benzoic acid, mp 122° C.

After one recrystallization of the material from hot water, the melting point was 112 to 113° C and the initial rotation in purified chloroform (cp) was $[\alpha]_D^{20}=42.8$ (0.2016 g made up to 10 ml read 4.98° S in a 2-dm tube). The mutarotation in pyridine is given in table 11. This substance crystallizes very readily and was obtained

TABLE 11.—*Mutarotation of tetra-acetyl-d-talose in pyridine*

(0.1888 g made up to 10 ml and read in a 2-dm tube)

Time	Observed rotation	Specific rotation	k_1+k_2[a]
Minutes	°S[b]	$[\alpha]_D^{20}$	
4.8	7.16	65.6	
9.8	7.11	65.2	(0.0062)
30.6	7.06	64.7	.0025
61.4	6.91	63.4	.0032
88.4	6.84	62.7	.0030
239.7	6.60	60.5	.0027
319.5	6.52	59.8	(.0029)
∞	6.43	59.0	
Average			0.0029

[a] Calculated from the first-order equation:

$$k_1+k_2=\frac{1}{t}\log\frac{r_0-r_\infty}{r_t-r_\infty}$$

[b] Average of 5 or more readings.

in several other ways. It was separated (1) from mother liquors of bromo-tetra-acetyl talose which had decomposed; (2) from the products of reaction of silver acetate and bromo-tetra-acetyl talose in glacial acetic acid; and (3) from mother liquors of the triacetyl-*d*-talose 1,2-orthomethylacetate preparation and recrystallization. *Analysis.*—Calculated for $C_6H_8O_6(COCH_3)_4$: C, 48.25; H, 5.79; acetyl, 6.87 ml of 0.05 *N* NaOH per 29.9 mg. Found: C (micro), 48.15; H (micro), 5.79; acetyl (after hydrolysis with 0.05 *N* NaOH for 4½ hours at 20° C), 7.02 ml.

8. METHYL TALOSIDES

A solution of 5 g of talose in 75 ml of absolute methyl alcohol containing 1.52 percent of hydrogen chloride was refluxed for 8 hours. After the hydrogen chloride had been removed with the aid of silver carbonate, the solution was treated with Norit, filtered, and evaporated but it did not crystallize.

The mixture was than acetylated at 0° C with acetic anhydride in the presence of pyridine. The sirup was distilled in a high vacuum (about 0.01 mm); practically all of it volatilized at 100 to 115° C and appeared in the distillate. The colorless purified material did not crystallize.

VI. SUMMARY

The preparation and properties of the new crystalline sugar, β-*d*-talose, is reported. It is shown that *d*-talose resembles mannose in that the value of Hudson's *2A* is 9,870 and in that it forms orthoester derivatives. The mutarotation, however, is similar to that of galactose since β-*d*-talose mutarotates at a rate initially slower and α-*d*-talose initially faster than that for a first-order reaction. Bromine oxidation data show that β-*d*-talose is oxidized more rapidly than α-*d*-talose and that the new beta isomer is a homogeneous substance.

A crystalline monobenzoyl talose has been separated from the products obtained by the oxidation of galactal with perbenzoic acid. The unusual properties of this substance indicate that it may have an orthobenzoic acid structure.

Crystalline α-penta-acetyl-*d*-talose, tetra-acetyl-*d*-talose, and 1-bromo-tetra-acetyl-*d*-talose are reported. The 1-bromo-tetra-acetyl-*d*-talose reacts with methyl alcohol in the presence of silver carbonate to give an orthoester derivative, triacetyl-*d*-talose 1, 2-orthomethylacetate. The properties of this substance are compared with those of other orthoesters and the factors responsible for this type of isomerism are discussed.

VII. REFERENCES

The numbers in brackets are those given as literature citations throughout the text and tables of this paper.

[1] O. F. Hedenberg and L. H. Cretcher, J. Am. Chem. Soc. **49,** 478 (1927). L. H. Cretcher and A. G. Renfrew, J. Am. Chem. Soc. **54,** 1590 (1932).
[2] W. Bosshard, Helv. Chim. Acta **18,** 482 (1935).
[3] E. Fischer and H. Thierfelder, Ber. deut. chem. Ges. **27,** 2034 (1894). J. J. Blanksma and S. W. Van Ekenstein, Chem. Zentr. **1908,** II, 1584. J. v. Braun and O. Bayer, Ber. deut. chem. Ges. **58,** 2215 (1925).
[4] P. A. Levene and R. S. Tipson, J. Biol. Chem. **93,** 631 (1931).
[5] H. S. Isbell and W. W. Pigman, J. Research NBS **16,** 553 (1936) RP892.
[6] H. S. Isbell and W. W. Pigman, J. Research NBS **18,** 141 (1937) RP969; J. Org. Chem. **1,** 505 (1937).

[7] H. S. Isbell, J. Research NBS **18,** 505 (1937) RP990; J. Am. Chem. Soc. **54,** 1692 (1932).
[8] H. S. Isbell and W. W. Pigman, BS J. Research **10,** 337 (1933) RP534.
[9] H. S. Isbell, J. Chem. Education **12,** 96 (1935).
[10] C. S. Hudson, BS Sci. Pap. **21,** 280 (1926) S533.
[11] H. D. K. Drew and W. N. Haworth, J. Chem. Soc. **1926,** 2303.
[12] N. Prileschajew, Ber. deut. chem. Ges. **42,** 4811 (1909).
[13] M. Bergmann and H. Schotte, Ber. deut. chem. Ges. **54,** 440, 1564 (1921).
[14] W. N. Haworth, E. L. Hirst, H. R. L. Streight, H. A. Thomas, and J. I. Webb, J. Chem. Soc. **1930,** 2636.
[15] D. H. Brauns, J. Am. Chem. Soc. **48,** 2776 (1926).
[16] H. S. Isbell, BS J. Research **5,** 1179 (1930) RP 253.
[17] A. J. Watters and C. S. Hudson, J. Am. Chem. Soc. **52,** 3472 (1930).
[18] L. Zervas, Ber. deut. chem. Ges. **64,** 2289 (1931).
[19] E. Pacsu, J. Am. Chem. Soc. **57,** 745 (1935).
[20] H. Hibbert and M. E. Greig, Canadian J. Research **4,** 254 (1931).
[21] E. Fischer, M. Bergmann, and A. Rabe, Ber. deut. chem. Ges. **53,** 2362 (1920).
[22] H. G. Bott, W. N. Haworth, and E. L. Hirst, J. Chem. Soc. **1930,** 1395.
[23] K. Freudenberg and E. Braun, Naturwissenschaften **18,** 393 (1930). E. Braun, Ber. deut. chem. Ges. **63,** 1972 (1930).
[24] W. N. Haworth, E. L. Hirst, and M. Stacey, J. Chem. Soc. **1931,** 2864.
[25] J. K. Dale, J. Am. Chem. Soc. **46,** 1046 (1924).
[26] P. A. Levene and M. L. Wolfrom, J. Biol. Chem. **78,** 525 (1928).
[27] P. A. Levene and R. S. Tipson, J. Biol. Chem. **92,** 109 (1931).
[28] H. S. Isbell, BS J. Research **7,** 1115 (1931) RP392.
[29] (a) E. Pacsu, J. Am. Chem. Soc. **54,** 3649 (1932); [b] **55,** 2451 (1933). (c) F. B. Cramer and E. Pacsu, J. Am. Chem. Soc. **59,** 711 (1937).
[30] K. Freudenberg and H. Scholz, Ber. deut. chem. Ges. 63, 1969 (1930).
[31] E. Pacsu, J. Am. Chem. Soc. **57,** 537 (1935).
[32] W. N. Haworth, E. L. Hirst, and E. G. Teece, J. Chem. Soc. **1930,** 1408. B. Helferich and W. Klein, Liebigs Ann. Chem. **450,** 226 (1926); **455,** 177 (1927).
[33] N. K. Richtmeyer and C. S. Hudson, J. Am. Chem. Soc. **58,** 2534 (1936).
[34] H. Meerwein and G. Hinz, Liebigs Ann. Chem. **484,** 1 (1930).
[35] H. Meerwein and H. Sönke, Ber. deut. chem. Ges. **64,** 2375 (1931).
[36] H. Meerwein and H. Sönke, J. prakt. Chem. **245,** 295 (1933).
[37] J. S. Allen and H. Hibbert, J. Am. Chem. Soc. **56,** 1398 (1934).
[38] T. Kumoda, Bull. Chem. Soc. Japan **7,** 211 (1932).
[39] Organic Syntheses, XIII, p. 86. (John Wiley & Sons, Inc., 1933.)
[40] B. T. Brooks and W. B. Brooks, J. Am. Chem. Soc. **55,** 4309 (1933).
[41] H. C. Fuller, Chemistry and Analysis of Drugs and Medicines, p. 661 (John Wiley & Sons, Inc., New York, N. Y., 1920).
[42] D. H. Brauns, J. Am. Chem. Soc. **44,** 401 (1922).
[43] E. Montgomery and C. S. Hudson, J. Am. Chem. Soc. **56,** 2463 (1934).
[44] K. Freudenberg, H. v. Hochstetter, and H. Engels, Ber. deut. chem. Ges. **58,** 666 (1925).

Washington, June 11, 1937.

U. S. Department of Commerce National Bureau of Standards

RESEARCH PAPER RP1022

Part of Journal of Research of the National Bureau of Standards, Volume 19, August 1937

HYDRATION OF MAGNESIA IN DOLOMITIC HYDRATED LIMES AND PUTTIES

By Lansing S. Wells and Kenneth Taylor

ABSTRACT

Heat-of-solution and ignition-loss methods have been developed for determining the degree of hydration of magnesia in hydrated dolomitic limes and in hydrated dolomitic lime putties. The rate of hydration of magnesia in such limes has been studied when the limes were aged as putties at different temperatures, when subjected to steam hydration at various temperatures and pressures, and when exposed to different relative humidities. In the six commercial hydrates studied, 70 to 90 percent of the magnesia was still unhydrated after the customary 1 day of soaking. From 2 to 4 months were required to hydrate 95 percent of the magnesia when the limes were soaked at room temperature, but the rate of hydration was much more rapid at higher temperatures.

CONTENTS

	Page
I. Introduction	216
II. Methods of determining the degree of hydration of magnesia	216
III. Heats of solution of CaO, $Ca(OH)_2$, $CaCO_3$, MgO, and $Mg(OH)_2$	218
IV. Comparison of the observed and calculated heats of solution of hydrated dolomitic limes, and the degree of hydration of magnesia in these limes	220
V. Calculations involved in the determination of the degree of hydration of magnesia in dolomitic lime putties by the heat-of-solution method	223
VI. Rate of hydration of magnesia in dolomitic lime putties at room temperature	223
VII. Correlation of ignition-loss and heat-of-solution methods for determining the degree of hydration of magnesia in dolomitic limes	225
1. Calculations involved in the ignition-loss method	226
2. Correlation of heat-of-solution and ignition-loss methods in the case of aged putties	227
3. Correlation of heat-of-solution and ignition-loss methods in the case of steam hydration	228
VIII. Effect of temperature on the rate of hydration of magnesia in dolomitic limes	228
1. Hydration of putties at different temperatures	229
2. Hydration with steam at different temperatures	230
IX. Effect of moisture conditions on the rate of hydration of magnesia in dolomitic hydrated limes	231
X. Summary	235
XI. References	236

I. INTRODUCTION

Since plasters and mortars are continuously subjected to changing atmospheric conditions, expansions and contractions are constantly going on. These movements, except those caused by changes in temperature, may be ascribed almost wholly to the cementitious material.

A study of the durability of mortars or plasters therefore involves a consideration of the properties of the cementitious materials, especially those related to volume changes. Such changes are often the result of chemical reactions. The hydration of the constituents of limes is attended by marked expansion. If the hydration occurs prior to the setting and hardening of a plaster or mortar the danger of any subsequent expansion from this source is eliminated.

Calcium oxide, CaO, unless "dead burned", reacts so rapidly with water to form calcium hydroxide, $Ca(OH)_2$, that hydration is completed in a short time. Chemical analysis of high-calcium hydrated limes as commercially produced indicates that the combined water is almost sufficient for complete hydration. On the other hand, the magnesia, MgO, of dolomitic limes (which contain CaO and MgO in nearly equimolecular proportions) hydrates slowly. Chemical analysis of commercial dolomitic hydrated limes indicates that ordinarily only 55 to 65 percent of the water required for complete hydration is present. Some additional hydration occurs during the customary 1 day of soaking prior to their use, but just how much is not known. If the exposure conditions are such that no further hydration takes place in the hardened mortar or plaster, or if hydration is extremely slow, no damaging expansion is likely to result. However, the rates of hydration under various conditions are not known. In fact, but little work has been done on this subject, and no satisfactory method prior to this investigation had been developed for determining the extent of hydration of magnesia in dolomitic lime putties. The development of such a method is essential to the study not only of the rates of hydration of dolomitic limes but also to the possible correlation of the hydration with attending expansion. Furthermore, such a method would be useful in determining the time required to completely hydrate the limes either on the job or at the plant. It should prove useful for manufacturers in ascertaining the relationship of temperature and time of burning of limes to their rates of hydration.

An investigation was undertaken, therefore, with the primary objects of developing a satisfactory method of measuring the degree of hydration of magnesia in dolomitic hydrated limes and putties and of studying the rate of hydration under various conditions.

II. METHODS OF DETERMINING THE DEGREE OF HYDRATION OF MAGNESIA

In 1927 Richardson [1] [1] described a thermochemical method of analysis for determining the degree of hydration of magnesia and calcium oxide in commercially hydrated dolomitic limes. The method was based upon the fact that the two hydroxides have appreciably different dissociation temperatures. Thus the percentages of magnesia and calcium oxide hydrated could be calculated from the weight loss

[1] Figures in brackets here and elsewhere throughout the text refer to references at the end of this paper.

when the temperature was raised just high enough to decompose, first, the magnesium hydroxide and then the calcium hydroxide. By this method, Richardson analyzed 10 representative commercial dolomitic hydrates, and concluded that in such limes the calcium oxide is largely hydrated, while the magnesia is only slightly hydrated. He also determined the additional amount of magnesia hydrated when one of these limes was soaked (as putty) for 24 hours at room temperature. However, as the lime putty was oven-dried at 110° C, he could not be certain that a substantial amount of this hydration did not take place during the drying.

By a similar method, Fox and Mathers [2] determined the amount of hydrated magnesia in nine dolomitic hydrated limes, and also the additional magnesia hydrated upon soaking these limes at room temperature for 12 hours. The putties were oven-dried at 105° C, and here again it is probable that an appreciable hydration of magnesia took place during the drying period. The data given by Fox and Mathers showed that from 2.8 to 14.3 percent of the total magnesia was hydrated at the start and that from 9.1 to 18.1 percent of additional magnesia hydrated during the soaking and drying periods.

Campbell [3] used an ignition-loss method in determining the degree of hydration of magnesia (prepared from magnesite) soaked for various periods. Hydration was considered complete when the ignition loss (of the dried material) did not increase on further soaking. The results were expressed as percentage of total hydration, no distinction being made between the calcium oxide (about 4 percent on an ignited basis) and the magnesia. In his first experiments, the putties were dried for 1 day in a vacuum desiccator over concentrated sulphuric acid, and then oven-dried overnight at 102 to 105° C. He found, however, that the prolonged oven-drying decomposed some of the magnesium hydroxide, and so thereafter dried to constant weight in the desiccator. This usually required 7 or 8 days.

Since the determination of the degree of hydration of lime putties by the above methods involved uncertainties, as in drying, or required long drying periods, it seemed desirable to attack the problem in some other way. If, for example, the degree of hydration could be measured by determining the heats of solution of the putties in an acid, the accuracy of drying would not enter into the calculations. This method is possible since the hydration of a lime is attended by a decrease in its heat of solution. If the bulk of the unhydrated material is made up of one constituent, such as MgO, the problem of determining the extent of hydration by the heat-of-solution method is greatly simplified. Previous investigations have indicated that the unhydrated material is largely magnesia. The truth of this observation can be further tested by comparing observed heats of solution of dolomitic hydrated limes (or putties) with those calculated on the assumption that the lime, CaO, is completely hydrated to $Ca(OH)_2$ and that the magnesia is but partially hydrated. An agreement between the observed and calculated values would verify the assumption, provided there were a substantial difference in the heats of hydration of lime and magnesia.

In order to calculate the heat of solution of a hydrated dolomitic lime, it is necessary to know the heats of solution of the compounds which make up such a material. For practical calculations, these

may be considered as usually being calcium hydroxide, calcium oxide, calcium carbonate, magnesium hydroxide, and magnesium oxide. Iron and aluminum oxides and silica are also present, but usually in small amounts. If these are uncombined with the calcium or magnesium oxides, their heats of solution are very low; if combined, the heats of solution of the resulting compounds are roughly of the same order of magnitude as those of calcium and magnesium hydroxides, and are therefore largely compensated for. Disregarding these constituents does not, therefore, introduce any great error when their sum does not exceed 1 or 2 percent. Although some of the carbon dioxide may be combined with the magnesia, it seems probable that it is mainly combined with the calcium oxide, since the latter is much more active, and since calcium carbonate has a higher dissociation temperature than magnesium carbonate. At any rate, the carbonates have low heats of solution, and the error introduced by this assumption is necessarily small when there is not more than 2 or 3 percent of carbon dioxide present.

III. HEATS OF SOLUTION OF CaO, $Ca(OH)_2$, $CaCO_3$, MgO, AND $Mg(OH)_2$

Although the heats of solution of the above compounds had been determined by other investigators, it was necessary to redetermine these values. The heat of solution of a material in an acid varies with the concentration of the acid, the volume of acid per unit weight of material dissolved, the temperature at which the determination is made, and, in some instances, with the manner in which the sample has been prepared. Therefore, in comparing the observed heats of solution of limes with those calculated from the heats of solution of their constituents, it is important that the heats of solution of the limes and of the constituents be made under similar conditions.

The determinations of the heats of solution were made by means of an isothermal calorimeter [4] similar to the one used to test the Boulder Dam cements. The determinations were made at 25° C, using 640 g of 2 *N* hydrochloric acid and a sample of approximately 1.5 g.

The calcium carbonate used was of analytical reagent quality. An analysis showed that it was completely soluble in hydrochloric acid, free of chlorides, sulphates, and silicates, and contained only traces of iron and aluminum oxides. The ignition loss was 43.93 percent (theoretical, 43.97 percent).

The calcium oxide was prepared from the above calcium carbonate by igniting a sample for about 4 hours over a Meker burner just prior to each determination of the heat of solution. The ignition temperature was found to be 1,050 to 1,100° C, which roughly approximates the temperature at which dolomitic limes are burned.

The calcium hydroxide was also prepared from this sample of calcium carbonate. The carbonate was ignited for several hours in a muffle furnace at 950° C and then immediately hydrated in the autoclave for 2 hours at 125-lb/in.^{2} steam pressure. After the hydroxide had been oven-dried for 1 hour at 105° C, it had an ignition loss of 24.32 percent (theoretical, 24.32 percent).

The source of both the magnesium hydroxide and the magnesium oxide was a sample of magnesium oxide of analytical reagent quality. Before being used, this sample was extracted with water to remove

any water-soluble substances with which it might be contaminated. An analysis then showed that it was completely soluble in hydrochloric acid, free of chlorides and sulphates, and contained only traces of silica, iron oxide, and aluminum oxide.

In the preparation of the magnesium hydroxide the above oxide was ignited in a muffle furnace for several hours at 850° C and then hydrated and dried as in the preparation of calcium hydroxide. The ignition loss was 31.05 percent (theoretical, 30.88 percent).

The magnesium oxide used in determinations of the heat of solution was obtained by igniting a sample of the above prepared magnesium hydroxide for about 4 hours over a Meker burner just prior to each determination (ignition temperature, 1,050 to 1,100° C).

In determining the heat of solution of calcium carbonate, the carbonate was mixed with an equal weight of a hydrated dolomitic lime (heat of solution previously determined) and the mixture compressed into tablets. By this procedure, a too rapid effervescence of carbon dioxide was prevented. The heat of solution of the calcium carbonate was readily computed since the value for the dolomitic lime was known. In the case of calcium carbonate, determinations were made in 2 *N* hydrochloric acid, both saturated and unsaturated with carbon dioxide. With the other materials, the acid was not saturated with carbon dioxide. The results of determinations of the heats of solution of these various compounds are shown in table 1.

TABLE 1.—*Heats of solution (in 2 N hydrochloric acid at 25° C) of the principal compounds in hydrated dolomitic limes*

Determination	Heat of solution (cal/g)					
	CaO	$Ca(OH)_2$	MgO	$Mg(OH)_2$	[a] $CaCO_3$	[b] $CaCO_3$
1	833.4	556.4	890.5	666.5	59.5	104.6
2	834.9	557.5	891.2	667.5	58.8	105.4
3	833.3	557.2	889.8	667.8	----	----
4	----	----	891.3	666.6	----	----
Average	833.9	557.0	890.7	667.1	59.2	105.0
	Heat of solution (cal/mole)					
Average	46,760	31,230	35,910	26,900	3,320	5,780

[a] Acid saturated with CO_2.
[b] Acid not saturated with CO_2.

Table 1 shows that the heat of solution of calcium carbonate is less in the acid which has been saturated with carbon dioxide. In this case, substantially all of the carbon dioxide formed in the reaction escapes as a gas. When the acid has not been previously saturated, a part of the carbon dioxide formed goes into solution and the remainder escapes as a gas. The larger value, 105 cal/g, was used in all calculations since the heats of solution of the dolomitic limes were determined in acid not saturated with carbon dioxide. Obviously, the heat of solution of calcium carbonate in hydrochloric acid not saturated with carbon dioxide will vary, since if a small sample of calcium carbonate is taken, nearly all of the carbon dioxide formed may dissolve, while if a larger sample is taken, a smaller proportionate part may go into solution. However, since the limes tested contained

only small amounts of carbon dioxide, and the heat of solution of the carbonate is, in any case, low compared with that of the principal constituents, the error introduced by using the approximate value of 105 cal/g should not be appreciable.

The approximate heat of hydration may be obtained by subtracting the heat of solution of the hydrated from that of the unhydrated material. Table 1 shows that the molar heats of hydration of calcium oxide (approximately 15.53 Cal) and of magnesium oxide (approximately 9.01 Cal) differ markedly. (To obtain the exact heat of hydration from heat-of-solution data it is necessary to make several minor corrections which are not significant in this work.)

It should be understood that the data of table 1 apply only to materials prepared as described above. Giauque and Archibald [5] have reported an appreciably higher heat of hydration for magnesium oxide prepared by decomposing magnesium hydroxide at 300° C. It has been found in this laboratory that the heat of hydration of magnesium oxide varies appreciably with the temperature and time of ignition prior to a determination. However, the calcium oxide and magnesium oxide, for which data are given in this paper, were ignited at temperatures roughly approximating those at which dolomitic limes are burned in practice. It is planned to present, in a later paper, data showing the variation of the heat of hydration of magnesia with the ignition temperature, and also the corrected heat of hydration values for the calcium and magnesium oxides ignited as described above.

IV. COMPARISON OF THE OBSERVED AND CALCULATED HEATS OF SOLUTION OF HYDRATED DOLOMITIC LIMES, AND THE DEGREE OF HYDRATION OF MAGNESIA IN THESE LIMES

Having determined the heats of solution of the compounds in hydrated dolomitic limes, it was now possible to compare the calculated and observed heats of solution of several of these limes and thereby test the assumption that the calcium oxide was completely hydrated.

The limes, the analyses of which are given in table 2, were obtained from four different manufacturers. The first six were received as dry hydrates. Lime 7 was obtained as the ground limestone and burned in this laboratory. A comparison was made of the calculated and experimental heats of solution of these limes first, as they were received from the manufacturer, and second, after they had been hydrated in the autoclave for 2 hours at 120-lb/in.^{2} steam pressure. The limes were considered to be completely hydrated by this autoclave treatment. Lime 3, which was representative of the group, showed no further hydration, as measured by ignition loss, after 1 hour in the autoclave at this pressure.

TABLE 2.—*Chemical analyses of dolomitic limes*

(Lines 1 to 6, inclusive, hydrated limes; line 7, quicklime)

Constituent	Amount of constituents in limes						
	1	2	3	4	5	6	7
	Percent	*Percent*	*Percent*	*Percent*	*Percent*	*Percent*	*Percent*
CaO	48.1	46.3	47.8	48.1	47.2	48.1	54.6
MgO	33.9	32.4	33.3	33.6	33.0	33.7	38.7
SiO_2				0.2	0.2	1.2	4.7
R_2O_3				.4	.3	0.7	2.2
H_2O, extraneous *	0.2	0.4	0.1	.4	.3	.4	0.0
H_2O, combined	16.6	16.9	17.3	16.0	16.4	15.8	.0
CO_2	0.6	3.2	1.3	1.2	2.6	0.3	.1
Total	99.4	99.2	99.8	99.9	100.0	100.2	100.3

* Obtained as loss on drying 1 hour at 105° C.

The method used in calculating the heats of solution will be illustrated with lime 3. It is assumed that the calcium oxide is completely hydrated, provided of course that there is sufficient water available, and that only water present in excess of this amount goes to hydrate the magnesia. Also, it is assumed that all of the carbon dioxide is combined with the calcium oxide. The small amounts of iron and aluminum oxides and silica are ignored. The distribution of the compounds which enter into the calculation of the heat of solution of a gram of this lime is, therefore, as follows:

Calcium oxide in carbonate	0.016 g.
Calcium oxide in hydrate	.462 g.
Magnesium oxide in hydrate	.056 g.
Magnesium oxide	.277 g.

The heat of solution of each of these components is now calculated.

$$0.016 \times 105.0 \text{ cal} = 1.7 \text{ cal.}$$
$$.462 \times 557.0 \text{ cal} = 257.3 \text{ cal.}$$
$$.056 \times 667.1 \text{ cal} = 37.4 \text{ cal.}$$
$$.277 \times 890.7 \text{ cal} = 246.7 \text{ cal.}$$
$$\text{Total} = 543.1 \text{ cal.}$$

It is desirable to express the heat of solution, not in calories per gram but in calories per gram of ignited material. From the analysis (table 2) it is seen that 1 g of lime 3, upon ignition gives 0.813 g. Therefore, 543.1 is divided by 0.813, giving a heat of solution 668.0 cal/g of ignited material.

Calculations for the completely hydrated lime are made as follows. The heats of solution which were computed for the components of the lime at the start are again used, with the exception that the 0.277 g of free magnesia is now calculated as hydrated.

$$0.016 \times 105.0 \text{ cal} = 1.7 \text{ cal.}$$
$$.462 \times 557.0 \text{ cal} = 257.3 \text{ cal.}$$
$$.056 \times 667.1 \text{ cal} = 37.4 \text{ cal.}$$
$$.277 \times 667.1 \text{ cal} = 184.8 \text{ cal.}$$
$$\text{Total} = 481.2 \text{ cal.}$$

The hydration of 0.277 g of magnesia requires 0.124 g of water. As the lime at the start contained 0.1 percent of extraneous water, a gram of this lime upon complete hydration should produce 1+(.124−.001), or 1.123 g. Therefore, 481.2 cal is the heat of solution of 1.123 g of the completely hydrated lime. The heat of solution of 1 g is 481.2÷1.123, or 428.5 cal. Before the heat of solution can be expressed in calories per gram of ignited material, it is necessary to compute the ignition loss of the completely hydrated lime. The ignition loss at the start was 18.7 percent and 0.123 g of water was added to each gram of the lime upon complete hydration. The ignition loss therefore becomes 0.187+.123/1.123, or 27.6 percent. A gram of the completely hydrated lime should therefore produce 0.724 g of ignited material, and the heat of solution, on an ignited basis, should be 428.5÷.724, or 591.9 cal/g.

Similar calculations were made for all of these limes. The observed and calculated heats of solution are compared in table 3. The observed values are the average of two determinations which differed by a maximum of 2.1 cal/g.

An extremely close agreement between the observed and calculated values could not be expected, since besides the calorimetric work, there were several possible sources of slight error. Mainly, these were: uncertainty as to the distribution of the carbon dioxide, the chemical analysis, and the presence of iron and aluminum oxides and silica. In the case of the six hydrated limes, which contained relatively small amounts of impurities, it would seem that an agreement within 3 to 4 cal/g should be obtained. Deviations somewhat larger than this in the first two limes indicate the possibility of a small fraction of the calcium oxide being unhydrated. If it is assumed that the combined water is equally divided between the calcium oxide and magnesia, then the calculated heat of solution of lime 3, for example, becomes 695.6 cal. This is 26.9 cal higher than the observed value. At least for the practical purpose of following the hydration of magnesia, it would seem therefore, that one is justified in assuming the complete hydration of calcium oxide in such limes.

Table 4 shows the degree of hydration of magnesia in the six commercially hydrated dolomitic limes as received from the manufacturer. The values were calculated from the chemical analyses, the calcium oxide being considered as completely hydrated.

TABLE 3.—*Comparison of the observed and calculated heats of solution of dolomitic limes*

Condition		Heats of solution of limes						
		1	2	3	4	5	6	7
		cal/g	cal/g	cal/g	cal/g	cal/g	cal/g	cal/g
As received	observed	682.5	648.0	668.7	670.1	652.9	672.3	702.8
	calculated	677.1	643.4	668.0	673.4	657.4	673.1	797.5
	difference	−5.4	−4.6	−0.7	+3.3	+4.5	+0.8	+4.7
Completely hydrated	observed	593.6	570.6	590.2	587.8	576.4	587.7	567.4
	calculated	594.0	572.5	591.9	589.0	580.3	585.6	560.2
	difference	+0.4	+1.9	+1.7	+1.2	+3.9	−2.1	−7.2

TABLE 4.—*Degree of hydration of magnesia in hydrated dolomitic limes as receiv from the manufacturer*

Magnesian constituents	Amount of magnesian constituents in limes					
	1	2	3	4	5	6
	%	%	%	%	%	%
MgO, hydrated	3.1	7.4	5.6	2.5	5.1	1.1
MgO, unhydrated	30.8	25.0	27.7	31.1	27.9	32.4
Total MgO	33.9	32.4	33.3	33.6	33.0	33.5
$\frac{\text{MgO, hydrated}}{\text{Total MgO}} \times 100$	9.1	22.8	16.8	7.4	15.5	3.3

V. CALCULATIONS INVOLVED IN THE DETERMINATION OF THE DEGREE OF HYDRATION OF MAGNESIA IN DOLOMITIC LIME PUTTIES BY THE HEAT-OF-SOLUTION METHOD

Lime 3 will be used to illustrate the method of calculation. Table 4 shows that this lime, as received from the manufacturer, contained 33.3 percent of total magnesia and 5.6 percent of magnesia in the hydrated form. The percentage of the total magnesia which was hydrated was therefore 0.056÷.333, or 16.8. The experimental heat of solution of this lime as received was 668.7 cal/g and after complete hydration in the autoclave, 590.2 cal/g, a decrease of 78.5 cal/g. A change of 78.5 cal in the heat of solution is due to the hydration of 100.0—16.8, or 83.2 percent of the magnesia. Since the heat of solution is determined on an ignited basis, the change in the heat of solution is directly proportional to the percentage of magnesia hydrated. A decrease of 1 cal in the heat of solution therefore represents the hydration of 83.2÷78.5, or 1.06 percent of magnesia.

After this lime had been soaked for 1 day its heat of solution, as determined experimentally, was 661.1, a decrease of 7.6 cal. This number, 7.6, is multiplied by the factor 1.06 giving 8.1 percent of magnesia hydrated during the soaking period. As 16.8 percent of the magnesia was originally hydrated, the percentage of the total magnesia hydrated after 1 day of soaking is 24.9.

VI. RATE OF HYDRATION OF MAGNESIA IN DOLOMITIC LIME PUTTIES AT ROOM TEMPERATURE

The heat-of-solution method of determining the degree of hydration of magnesia in dolomitic limes was used to study the rate of hydration of the magnesia when the limes were soaked at room temperature. The limes, whose analyses were given in table 2, were made into putties of such consistency as to be readily workable, yet sufficiently stiff that water would not separate appreciably on standing. The putties were kept in sealed glass jars which had been coated on the inside with paraffin, and the heat of solution was determined from time to time. When a determination was to be made, a sample of the putty was taken from the jar, thoroughly mixed and placed in a weighing tube. This tube was about 0.5 in. in diameter and 3.5 in. in length. It was fitted with a plunger held in position by a stopper, and to one end was attached a small glass tube about 1 in. in length. By means of the plunger the desired amount of putty could be forced

from the tube. The weighings were made by difference. The end of the small glass tube was closed by means of a rubber cap to prevent loss by evaporation during weighing. A sample for determination of heat of solution and one for ignition loss were taken from the same filling of the weighing tube.

The putties had an ignition loss of from 50 to 60 percent, and samples of from 3 to 4.5 g were taken for determinations of heat of solution. In making the calculations of heat of solution, approximate corrections were made for the water in the putties in excess of that required for complete hydration.

It should be noted that the accuracy of drying is not involved in this method because the calorimetric data were obtained with the undried putty. The ignition loss, which was used to calculate the heat of solution from the calorimetric results, was that of the wet putty and not of the dried material.

TABLE 5.—*Relation between the time of soaking and the percentage of hydration of magnesia in dolomitic lime putties maintained at room temperature*

Soaking period	Total magnesia hydrated in putties						
	1	2	3	4	5	6	7
Days	*Percent*	*Percent*	*Percent*	*Percent*	*Percent*	*Percent*	*Percent*
0	9.1	22.8	16.8	7.4	15.5	3.3	0.0
1	17.4	27.6	24.9	11.8	22.1	10.7	61.7
3	22.9	36.3	31.0	.....	.....	.....	91.7
7	37.3	48.9	42.0	33.5	48.5	35.1	100.1
14	51.8	56.7	59.3	.....	65.2	.....	.....
21	69.9	68.5	.....	67.0	79.8	71.9	.....
28	82.2	75.6	80.0	.....	.....	.....	.....
35	.....	77.1	84.5	82.4	88.7	88.1	.....
42	89.1	81.3	.....	.....	.....	.....	.....
56	94.0	89.8	92.3	91.9	97.4	90.8	.....
77	98.2	93.6	93.2	.....	.....	.....	.....
98	.....	95.1	99.4	.....	.....	92.4	.....
119	.....	.....	.....	.....	.....	96.7	.....
140	.....	98.5	.....	96.8	.....	.....	.....

The results of the determinations are shown in table 5 and graphically in figure 1. Lime 7 was obtained from the manufacturer as ground limestone. It was burned in a muffle furnace for 7 hours at 950 to 980° C, and then immediately made into a putty. Since it was burned at a lower temperature than is customary in industry, its rapid hydration indicates that the temperature of burning has a marked effect on the rate of hydration. Campbell [3] obtained practically complete hydration of magnesia in 3 days when magnesite was burned at 800° C, but only about 70 percent of it had hydrated after 6 years when the temperature of burning was 1,450° C.

Figure 1 shows that the rate of hydration is not a linear function of the time, but that it becomes decidedly slower when about 80 percent of the magnesia has been hydrated. Roughly speaking, 80 percent of the magnesia in these limes is hydrated in from 20 to 40 days and 95 percent in from 2 to 4 months. It is also seen that the customary 1-day soaking leaves the bulk of the magnesia still unhydrated.

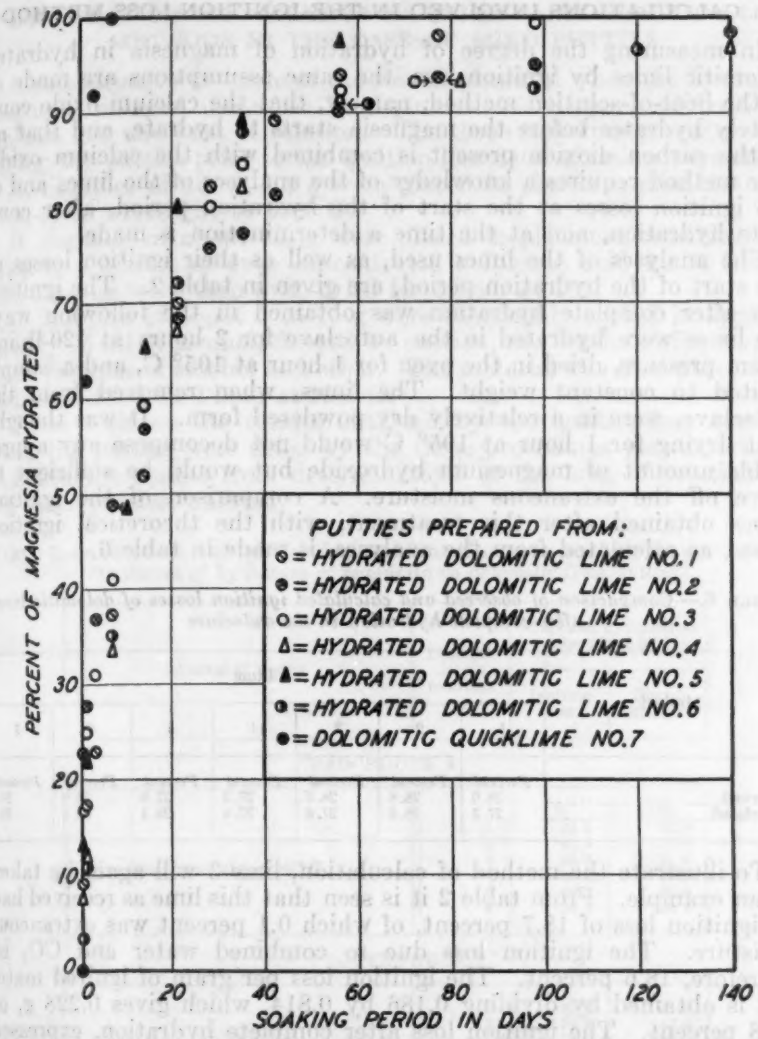

FIGURE 1.—*Rate of hydration of magnesia in dolomitic lime putties maintained at room temperature.*

VII. CORRELATION OF IGNITION-LOSS AND HEAT-OF-SOLUTION METHODS FOR DETERMINING THE DEGREE OF HYDRATION OF MAGNESIA IN DOLOMITIC LIMES

The determination of the degree of hydration by the heat-of-solution method appears to be theoretically sound and to give satisfactory results. However, for practical purposes a shorter and simpler procedure is desirable. It, therefore, seemed worth-while to make some measurements by loss on ignition and to compare the results with those obtained from determinations of heat of solution.

1. CALCULATIONS INVOLVED IN THE IGNITION-LOSS METHOD

In measuring the degree of hydration of magnesia in hydrated dolomitic limes by ignition loss, the same assumptions are made as in the heat-of-solution method, namely, that the calcium oxide completely hydrates before the magnesia starts to hydrate, and that all of the carbon dioxide present is combined with the calcium oxide. The method requires a knowledge of the analyses of the limes and of the ignition losses at the start of the hydration period, after complete hydration, and at the time a determination is made.

The analyses of the limes used, as well as their ignition losses at the start of the hydration period, are given in table 2. The ignition loss after complete hydration was obtained in the following way: the limes were hydrated in the autoclave for 2 hours at 120-lb/in.^{2} steam pressure, dried in the oven for 1 hour at 105° C, and a sample ignited to constant weight. The limes, when removed from the autoclave, were in a relatively dry powdered form. It was thought that drying for 1 hour at 105° C would not decompose any appreciable amount of magnesium hydroxide but would be sufficient to drive off the extraneous moisture. A comparison of the ignition losses obtained after this treatment, with the theoretical ignition losses, as calculated from the analyses, is made in table 6.

TABLE 6.—*Comparison of observed and calculated ignition losses of dolomitic limes after complete hydration in the autoclave*

Method	Lime						
	1	2	3	4	5	6	7
	Percent	*Percent*	*Percent*	*Percent*	*Percent*	*Percent*	*Percent*
Observed	28.0	28.8	28.0	27.3	27.9	26.9	26.2
Calculated	27.3	28.2	27.6	27.4	28.1	26.8	25.8

To illustrate the method of calculation, lime 3 will again be taken as an example. From table 2 it is seen that this lime as received had an ignition loss of 18.7 percent, of which 0.1 percent was extraneous moisture. The ignition loss due to combined water and CO_2 is, therefore, 18.6 percent. The ignition loss per gram of ignited material is obtained by dividing 0.186 by 0.814, which gives 0.228 g, or 22.8 percent. The ignition loss after complete hydration, expressed on an ignited basis, is 0.28÷0.72, or 38.9 percent.

It is seen in table 4 that 16.8 percent of the total magnesia in this lime is hydrated at the start. Therefore, the hydration of 83.2 percent of the magnesia is accompanied by a change in ignition loss of 16.1 percent. Since the ignition loss has been expressed on an ignited basis, its increase is directly proportional to the percentage of magnesia hydrated. That is, for each percent increase in ignition loss there is 83.2÷16.1, or 5.17 percent of magnesia hydrated. After lime 3 had been hydrated in the autoclave for 11 minutes at 120-lb/in.^{2} pressure, it had an ignition loss, on an ignited basis, of 34.4 percent, an increase of 11.6 percent. This increase is multiplied by the factor 5.17, giving 60.0 percent. As 16.8 percent of the magnesia was originally hydrated, the percentage of the total magnesia now hydrated is 76.8.

2. CORRELATION OF HEAT-OF-SOLUTION AND IGNITION-LOSS METHODS IN THE CASE OF AGED PUTTIES

A comparison was made of the results obtained when the hydrated magnesia in aged dolomitic lime putties was determined both by ignition loss and heat of solution. The three following procedures of drying the putties prior to the ignition loss determination were tried:

A. Samples of about 1.5 g were placed in platinum crucibles and oven-dried overnight at 105° C.

B. Samples of about 1.5 g were placed in platinum crucibles and dried in a desiccator over concentrated sulphuric acid for 20 hours. The samples were then oven-dried for 1 hour at 105° C.

C. Samples of about 5 to 10 g were thoroughly stirred in approximately 25 ml of alcohol, filtered by suction, and washed with several small portions of alcohol and ether. The material was then pulverized and oven-dried for 1 hour at 105° C.

Table 7 shows the results obtained by the ignition-loss method when the putties were dried by the three procedures just described, and also the results from determinations of the heat of solution on the same putties, undried.

TABLE 7.—*Comparison of ignition-loss and heat-of-solution methods for determining the degree of hydration of magnesia in dolomitic lime putties*

Method of drying	Determination numbers	Magnesia hydrated as determined by—	
		Ignition loss	Heat of solution
		%	%
PROCEDURE A			
Oven-dried overnight at 105° C.	1	38.3	22.9
	2	41.5	27.6
	3	49.3	31.0
	4	54.8	36.8
	5	46.6	36.8
	6	64.4	56.1
PROCEDURE B			
Dried in desiccator for 20 hours at 25° C. then oven-dried 1 hour at 105° C.	1	42.3	38.6
	2	39.5	42.0
	3	78.8	80.0
	4	75.8	81.3
	5	85.5	92.3
	6	95.5	93.2
	7	89.5	94.0
	8	94.0	98.2
PROCEDURE C			
Washed with alcohol and ether, then oven-dried 1 hour at 105° C.	1	14.0	11.8
	2	22.7	22.1
	3	45.5	48.5
	4	62.2	65.2
	5	74.6	67.0
	6	79.4	79.8
	7	88.4	82.4
	8	87.9	89.8
	9	85.4	92.3
	10	94.8	93.2
	11	96.0	98.2

The uniformly high results obtained by the ignition-loss method when the putties were entirely oven-dried were no doubt due to additional hydration during the drying period. An increase of 75 or 80 degrees in temperature greatly accelerates the rate of hydration, as will be shown later.

Although the results, when the putties were dried by procedures *B* and *C*, correlated only approximately with those of the heat-of-solution method, it is believed that such determinations are accurate enough to be of practical use in industry. By means of these methods, the manufacturer of aged lime putties can easily determine the approximate amount of unhydrated magnesia in the putty being aged. For such uses, the alcohol-ether-oven procedure of drying is probably preferable, for in this way a complete determination can be made in 4 or 5 hours.

3. CORRELATION OF HEAT-OF-SOLUTION AND IGNITION-LOSS METHODS IN THE CASE OF STEAM HYDRATION

Several samples of a dolomitic lime were hydrated with steam under pressure for various periods and were oven-dried for 1 hour at 105° C upon their removal from the autoclave. The percentages of hydrated magnesia in these samples were then determined by the ignition-loss and heat-of-solution methods. The results are shown in table 8.

TABLE 8.—*Comparison of ignition-loss and heat-of-solution methods for determining the degree of hydration of magnesia in dolomitic limes hydrated with steam*

Determination	Percentages of total magnesia hydrated	
	Ignition loss	Heat of solution
1	32.8	37.5
2	48.3	43.0
3	77.8	78.9
4	81.4	83.4
5	85.5	87.5
6	90.0	93.0
7	94.8	96.1

The samples were in a comparatively dry powdered form when removed from the autoclave, and it does not seem probable that appreciable hydration was caused by oven-drying, as was apparently the case when the putties were dried in this way. The fact that the results by the two methods correlate reasonably well indicates, on the other hand, that the drying was nearly complete, since underdrying would not affect the heat of solution perceptibly.

VIII. EFFECT OF TEMPERATURE ON THE RATE OF HYDRATION OF MAGNESIA IN DOLOMITIC LIMES

Section VI of this discussion reports that several months were required to completely hydrate the magnesia in the dolomitic lime putties which were soaked at room temperature.

The aging period may, however, be greatly shortened by soaking the putties at higher temperatures. Also a dry, completely hydrated dolomitic lime may readily be produced by steam hydration. The time

required for this process will vary markedly with the temperature (or pressure) of the steam. The following experiments were carried out, with the object of determining the approximate effect of temperature on the rate of hydration in such cases as those just mentioned.

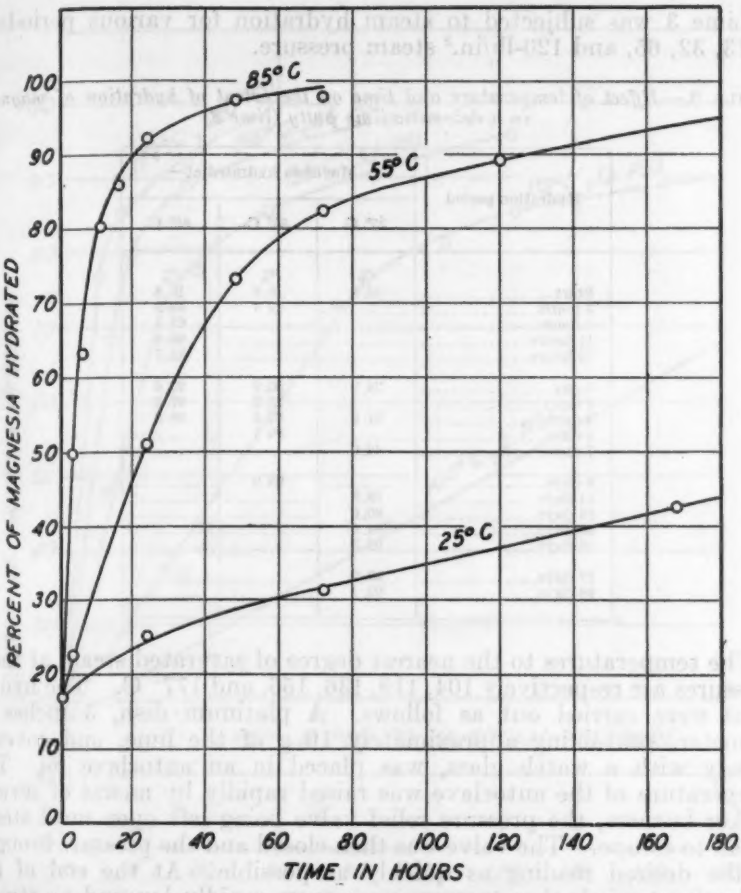

FIGURE 2.—*Effect of temperature on the rate of hydration of magnesia in lime 3 dolomitic lime putty.*

1. HYDRATION OF PUTTIES AT DIFFERENT TEMPERATURES

The results of the hydration of dolomitic lime putties at room temperature are shown in table 5 and figure 1. Lime 3 was also hydrated in the putty form at 55° C and 85° C. The putties were put into glass bottles of about 50-ml capacity, the bottles stoppered and placed in an electric oven maintained at the desired temperature. Samples were taken at various intervals and the percentage of the total magnesia which was hydrated was determined by the ignition-loss method. Prior to the ignition-loss determinations, the samples were washed with alcohol and ether and oven-dried for 1 hour at 105° C.

The results for the hydration of this putty at 25° C (room temperature), 55° C, and 85° C are shown in table 9 and figure 2. It is seen

that while it takes about 75 days to hydrate 95 percent of the magnesia at room temperature, the same results can be accomplished in 35 hours at 85° C.

2. HYDRATION WITH STEAM AT DIFFERENT TEMPERATURES

Lime 3 was subjected to steam hydration for various periods at 2, 13, 32, 65, and 120-lb/in.² steam pressure.

TABLE 9.—*Effect of temperature and time on the extent of hydration of magnesia in a dolomitic lime putty (lime 3)*

Hydration period	Magnesia hydrated at—		
	25° C	55° C	85° C
	%	%	%
Start	16.8	16.8	16.8
3 hours		22.4	49.9
6 hours			63.3
11 hours			80.4
16 hours			85.7
1 day	24.9	50.9	92.4
2 days		73.3	97.5
3 days	31.0	82.5	98.0
5 days		89.1	
7 days	42.0		
8 days		95.9	
14 days	59.3		
28 days	80.0		
35 days	84.5		
56 days	92.3		
77 days	93.2		
98 days	99.4		

The temperatures to the nearest degree of saturated steam at these pressures are respectively 104, 119, 136, 156, and 177° C. The hydrations were carried out as follows. A platinum dish, 3 inches in diameter, containing approximately 10 g of the lime, and covered loosely with a watch glass, was placed in an autoclave [6]. The temperature of the autoclave was raised rapidly by means of several Meker burners, the pressure relief valve being left open until steam began to escape. The valve was then closed and the pressure brought to the desired reading as quickly as possible. At the end of the hydration period, the steam pressure was rapidly lowered to atmospheric pressure by cooling the autoclave with water. The sample was then immediately removed, oven-dried for 1 hour at 105° C and the percentage of the total magnesia which was hydrated was determined by ignition loss.

Several minutes were required to raise the steam pressure of the autoclave to the desired reading and to cool to atmospheric pressure at the end of the experiment. This required a correction of the hydration period which was arbitrarily made as illustrated in the following example. In a hydration at 65 lb/in.² steam pressure, 13 minutes elapsed from the time the pressure relief valve was closed until the pressure-gage reading was 65. At the end of the experiment 3 minutes were required to cool to atmospheric pressure. The pressure was actually at 65 lb/in.² for 27 minutes. A correction of one-half the sum of the preheating and cooling periods, or 8 minutes, was added, making the total hydration period 35 minutes. The

corrections added varied from 1 minute at 2 lb/in.^{2} pressure to 9 or 10 minutes at 120 lb/in.^{2} pressure. The hydration periods are therefore approximations, since the exact time could not be determined with the autoclave available for this work. The results of the steam hydrations are shown in table 10 and figure 3.

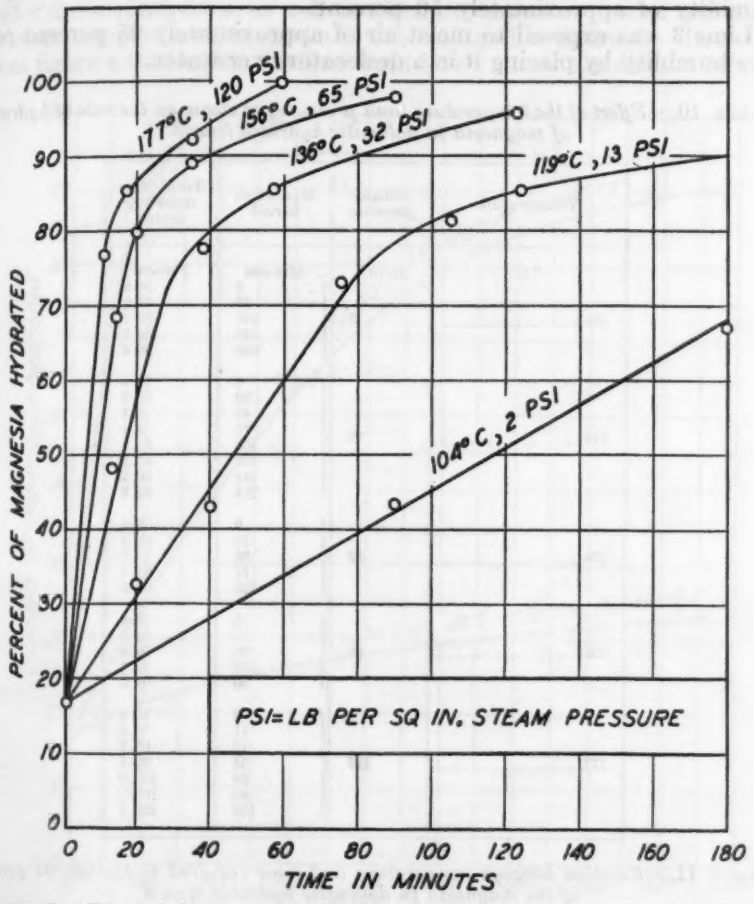

FIGURE 3.—*Effect of the temperature and pressure of steam on the rate of hydration of magnesia in hydrated dolomitic lime 3.*

Although the steam and putty hydrations are not strictly comparable, a rough idea of the effect of temperature on the rate of hydration of magnesia in this lime may be seen from table 11, which gives the approximate time required to hydrate 95 percent of the magnesia in lime 3 at the various temperatures.

IX. EFFECT OF MOISTURE CONDITIONS ON THE RATE OF HYDRATION OF MAGNESIA IN DOLOMITIC HYDRATED LIMES

It has been noted that when dolomitic limes are stored in paper bags, sufficient expansion occasionally takes place, in the course of a few months, to burst the containers. This indicates that appreciable

hydration is occurring. It further suggests that if hydration takes place under these conditions, it can also occur in plastered walls under certain atmospheric conditions. Some preliminary experiments were therefore made to determine the rate of hydration of magnesia when the dolomitic lime was exposed to moist air of approximately 95 percent relative humidity and to air kept at a relative humidity of approximately 50 percent.

Lime 3 was exposed to moist air of approximately 95 percent relative humidity by placing it in a desiccator over water.

TABLE 10.—*Effect of the temperature (and pressure) of steam on the rate of hydration of magnesia in dolomitic hydrated lime 3*

Temperature	Steam pressure	Hydration period	Total magnesia hydrated
°C	lb/in.²	*Minutes*	*Percent*
		0	16.8
		90	43.3
104	2	180	67.1
		340	90.3
		600	98.0
		0	16.8
		20	32.8
		40	43.1
119	13	75	73.1
		105	81.4
		124	85.5
		184	90.2
		244	94.8
		0	16.8
		13	48.3
136	32	38	77.8
		57	85.5
		123	96.0
		0	16.8
		14	68.5
156	65	20	79.8
		35	89.1
		90	98.0
		0	16.8
		11	76.8
		17	85.5
177	125	35	92.3
		59	100.0
		90	100.0
		120	100.0

TABLE 11.—*Relation between temperature and time required to hydrate 95 percent of the magnesia in dolomitic hydrated lime 3*

Temperature	Time
°C	*Hours*
25	1,800
55	180
85	35
104	7.7
119	4.1
136	1.9
156	1.1
177	0.7

The lime, which was in a layer about 1/16 in. in depth, was covered loosely with a watch glass to protect it from any drops of condensed water which might be formed. Also, samples of this lime, in layers of approximately the same depth, were placed in a desiccator over a 43.4-percent sulphuric acid solution to maintain a relative humidity approximating 50 percent [7]. The rate of hydration of magnesia under these conditions, as well as when the lime was soaked as a putty at room temperature, is shown in table 12 and in figure 4. It is seen from figure 4 that aging the lime from 3 to 4 months in air at a relative

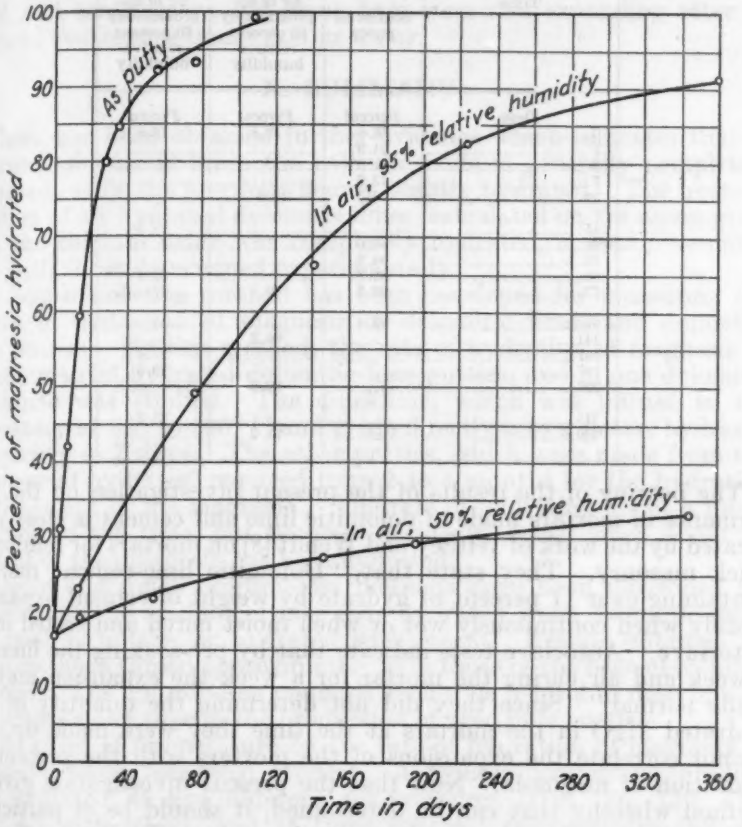

FIGURE 4.—*Effect of moisture on the rate of hydration of magnesia in hydrated dolomitic lime 3.*

humidity of approximately 50 percent is equivalent to aging it for 1 day as a putty. From a comparison of the rates of hydration, as indicated by the curves in figure 4, it is evident that at relative humidities lower than 50 percent the rates of hydration would be very slow. It is believed that these very slow rates may explain in part why there is not more damaging expansion of set plasters containing dolomitic limes, especially since the relative humidity of the air in buildings is usually considerably lower than 50 percent during those months that the buildings are heated. However, before definite conclusions can be drawn, it will be necessary to conduct a more com-

prehensive study of this phase of the subject, and, in particular, of the relation between the amount of free magnesia in such plasters and the expansions taking place under various conditions of moisture.

TABLE 12.—*Effect of moisture conditions at room temperature on the extent of hydration of magnesia in dolomitic hydrated lime S*

Time	Magnesia hydrated when—		
	Soaked as putty	Exposed to air of approximately 95 percent relative humidity	Exposed to air of approximately 50 percent relative humidity
Days	*Percent*	*Percent*	*Percent*
0	16.8	16.8	16.8
1	24.9		
3	31.0		
7	42.0		
14	59.3	23.0	
15			19.2
28	80.0		
35	84.5		
56	92.3		21.8
77	93.2	49.1	
98	99.4		
141		66.2	
147			27.4
197			29.3
223		82.5	
345			33.2
360		91.2	

The bearing of the results of the present investigation on the performance of mortars made of dolomitic lime and cement is clearly indicated by the work of Withey and Wendt [8] on mortars for reinforced brick masonry. They state that, "Dolomitic lime-cement mortars containing over 11 percent of hydrate by weight of cement expanded unduly when continuously wet or when moist cured and tested in an autoclave. Autoclave tests indicate that by pre-soaking the lime for a week and air curing the mortar for a week the expansion may be made normal." Since they did not determine the quantity of unhydrated MgO in the mortars at the time they were made up, one cannot correlate the expansions of the mortars with the percentage hydration of magnesia. Now that the present investigation gives a method whereby that can be determined, it should be of particular interest to carry out further investigations along the lines indicated by Withey and Wendt. That they were cognizant of the importance of the lineal changes in mortars is brought out in the following concluding sentence of their report. "The magnitude of the lineal changes of the lime-cement and clay-cement mortars in certain curing conditions necessitates determinations of the durability of the bond of these mortars to brick."

The question of the expansion of mortars containing magnesia is further complicated by the fact that the rate of hydration of magnesia, under any fixed condition of moisture, is markedly affected by the temperature at which the magnesia was burned. Although there appears to be considerable uniformity in the rates of hydration of the limes studied in the present investigation (which indicates that the

limes may have been burned under somewhat comparable conditions), yet there is no reason to believe that others may not be burned at considerably higher or lower temperatures. In some instances at least, it appears that prolonged exposure periods are necessary before an initial damaging expansion begins. This is more apt to be true if the magnesia is burned at a high temperature. White [9] made expansion measurements of bars of neat portland cement soaked in water, and containing known amounts of free magnesia. Marked abnormal expansions occurred in the bars containing 3 percent or more of free magnesia. The bulk of this expansion took place between the third and tenth years, but some bars were still expanding after 26 years of continuous immersion in water.

X. SUMMARY

There has been obtained further evidence which indicates that in hydrated dolomitic limes the calcium oxide is generally completely hydrated, while the magnesia is only slightly hydrated. The heats of solution of six hydrated dolomitic limes, calculated on the assumption that the calcium oxide was completely hydrated, agreed reasonably well with those determined experimentally.

A heat-of-solution method has been developed for measuring the degree of hydration of magnesia in dolomitic limes and dolomitic lime putties. By this method, the rate of hydration of magnesia in six commercial hydrated dolomitic lime putties, and in one dolomitic quicklime was studied. The quicklime, which was burned in the laboratory at 950 to 980° C and made directly into a putty, hydrated completely in 7 days. The other putties, which were made from the commercial hydrates, required from 2 to 4 months for the hydration of 95 percent of the magnesia. The rate of hydration is not a linear function of the time, but becomes decidedly slower when about 80 percent of the magnesia has been hydrated.

Simple and quick ignition-loss methods have been developed for determining the amount of magnesia hydrated when dolomitic limes are aged as putties or hydrated with steam. Results obtained by these methods agreed approximately with those of the heat-of-solution method. The ignition-loss methods should be helpful in determining the proper aging time in the production of aged lime putties.

The effect of temperature on the rate of hydration of magnesia in dolomitic limes has been studied. A typical commercial product was hydrated at five different temperatures (176, 156, 136, 119, 104° C) with steam, and at three different temperatures (85, 55, 25° C) in the putty form. By use of steam at 177° C (120-lb/in.^{2} pressure), 95 percent of the magnesia was hydrated in about 40 minutes; at 85° C, in the putty form, 95 percent was hydrated in 35 hours, while at approximately 25° C, a period of about 75 days was required for the same amount of hydration.

A preliminary study indicates that the magnesia in dolomitic limes may hydrate slowly but steadily in moist air. In air at a relative humidity of 50 percent, a lime having originally 16.8 percent of the total magnesia hydrated, had, after about 11.5 months, a total of 33.2 percent hydrated. At lower relative humidities the indications are that the rate would be very slow.

XI. REFERENCES

[1] Richardson, Ind. Eng. Chem. **19,** 625 (1927).
[2] Fox and Mathers, Indiana Acad. Sci. **43,** 113 (1934).
[3] Campbell, J. Ind. Eng. Chem. **1,** 665 (1909); **10,** 595 (1918).
[4] Described in Bureau of Reclamation Specification 566 for Boulder Dam cement, and referred to by Hornibrook, Kalousek, and Jumper, J. Research NBS **16,** 487 (1936) RP887.
[5] Giauque and Archibald, J. Am. Chem. Soc. **59,** 561 (1937).
[6] Described by Bishop in Rock Products **34,** 67 (1931).
[7] Wilson, J. Ind. Eng. Chem. **13,** 326 (1921).
[8] Withey and Wendt, Proc. Am. Soc. Testing Materials, **35,** part II, 426 (1935).
[9] White, Proc. Am. Soc. Testing Materials, **28,** II, 398 (1928).

WASHINGTON, May 19, 1937.

○